The Behavior of Bubble and Particle, Pulsatile and Peristaltic Flow

Stanislav Mingalev

Le Comportement de la bulle et des particules, l'écoulement pulsatile et le flux péristaltique

THESE EN COTUTELLE

Présentée pour l'obtention des titres de

Kandidat nauk de l'Université d'Etat de Perm

Docteur de l'Université de Lorraine

Spécialité: Géosciences

Par

Stanislav MINGALEV

Soutenue publiquement le 13 Dècembre 2013 à Perm (Russie) devant le jury constitué de:

Rapporteurs:	Vladimir SARANIN	Prof., Institut Pédagogique d'Etat de Glazov (Russie)
	Aleksej TCAPLIN	Chef du Département de Physique Générale, Université Polytechnique de Perm (Russie)
Examinateurs:	Vladimir MALANIN	Président de l'Université d'Etat de Perm (Russie)
	Bernard ROUX	Directeur de Recherche, Laboratoire de Mécanique, Modélisation & Procédés Propres (France)
	Oleg SKULSKY	Chercheur senior, Institute of continuous media. Russian Academy of Science. Ural Branch (Russie)
	Yuri BRATUHIN	Prof., Université d'Etat de Perm (Russie)
Directeur de thèse:	Lev FILIPPOV	Prof., Université de Lorraine (France)
Co-directeur de these:	Tatyana LYUBIMOVA	Chef du Département de Physique Théorique, Université d'Etat de Perm (Russie)

Résumé

Dans cette thèse on cherche à étudier le flux péristaltique des liquides dans un canal à onde de pression déterminée aux confins. Dans la plupart des recherches de systèmes de transportation péristaltiques la variation des coordonnées de la paroi est prédéfinie pour les raisons de commodité. Cependant les parois d'organes creux (comme œsophage intestin grêle, côlon urètre, vaisseaux lymphatiques) dont le fonctionnement consiste à transmettre des produits par la voie péristaltique, sont dotées de barorécepteurs – capteurs qui perçoivent la pression dans la couche limite de fluides et servent à réguler le calibre des vaisseaux. Pour créer le modèle du comportement des systèmes biologiques pareils il nous semble plus adéquat de prédéfinir l'onde de pression aux confins des vaisseaux. Cette approche réalisée dans notre thèse permet de découvrir et décrire des effets nouveaux, inexplorés auparavant.

Dans cette thèse nous étudions aussi l'influence des pulsations transversales des parois du canal sur la transmission du produit dues aux chutes de pression. Cet objectif est apparu lors de la détermination de la viscosité du liquide utilisant la méthode des canaux compressibles (squeezing flow viscometry). Des problèmes similaires sont assez répandus dans l'étude d'une variété des systèmes biologiques, en particulier, des mouvements de lubrification des articulations ou des micro-vaisseaux des muscles.

Nous avons aussi étudié l'influence du son sur l'interaction d'une particule solide tombante et d'une bulle de gaz montante dans le liquide. La pertinence de ce travail est liée à l'importance de recherche des solutions possibles pour augmenter l'efficacité de flottation, méthode d'enrichissement basée sur l'accrochage des particules minérales par des bulles de gaz.

Mots-clés: ecoulement de Poiseuille; écoulement pulsatile; péristaltisme; interaction des particules et de la bulle

Abstract

The thesis studies the peristaltic flow of fluid in a channel with the specified pressure wave at the boundary. The law of wall's coordinate variation isn't determined a priori. It is found from the initially definite law of pressure-variation on the wall. This way is based on the fact that some hollow organs change diameter under the signals of baroreceptors (sensors that detects the pressure). We studied the effects of various parameters on flow rate and structure of flow. Besides we studied the influence of vibration on the peristaltic flow under long wave approximation.

The paper also considers the influence of the wall transverse pulsation on the fluid transport under the pressure drop. This problem arises in defining the liquid viscosity by squeezing flow viscometry. The same problems occur in analyzing different biological systems, including the lubricant movement in joints or in the microvessels of working muscles.

The influence of sound on the interaction of a solid particle and a gas bubble in fluid is studied as well.

Keywords: Poiseuille flow; pulsating walls; squeezing flow; peristaltic flow; interaction of particle and bubble

Table of contents

1. Synthèse en Français

Le **premier chapitre** est consacré à l'étude du flux péristaltique à deux dimensions dans un canal à onde de pression déterminée aux confins. L'intérêt porté à ce problème est lié à l'étude de gestion de transportation des liquides pas des signaux des barorécepteurs. Ils analysent la pression et effectuent la régulation locale du courant de liquides biologiques. La façon la plus facile de modéliser ce type de régulation par force appliquée à la paroi, peut être une équation de type

$$F_x = -\kappa\left(p\big|_{x=\pm(h+\xi)} - \alpha\cos(ct/\lambda - y/\lambda)\right).$$

où h - distance entre les parois du canal, t - temps, y et x - coordonnées longitudinales et transversales, p - pression. Pour simplifier le problème on suppose que la régulation soit absolue et que le coefficient κ tend vers l'infini. Dans ce cas on peut négliger les forces outre la force F_x. Le résultat est une condition limitrophe de la pression dynamique:

$$x = \pm(h+\xi): p = \alpha\cos(ct/\lambda - y/\lambda),$$

qui est utilisée dans la thèse.

Ce même problème été étudié par D. Takagi[1] pour les petits nombres d'onde et vitesses de propagation des ondes. Les résultats, présentés dans le premier chapitre étendent ceux de la recherche de D. Takagi pour les vitesses arbitraires de propagation des ondes et pour les nombres d'onde arbitraires.

On résout le système des équations de Navier-Stokes:

$$\delta\left(\frac{\partial \mathrm{u}}{\partial t} + \mathrm{v}\frac{\partial \mathrm{u}}{\partial x} + \mathrm{u}\frac{\partial \mathrm{u}}{\partial y} + \frac{\partial \mathrm{p}}{\partial y}\right) - \frac{1}{C}\left(\frac{\partial^2 \mathrm{u}}{\partial x^2} + \delta^2\frac{\partial^2 \mathrm{u}}{\partial y^2}\right) = 0, \tag{1}$$

$$\delta^2\left(\frac{\partial \mathrm{v}}{\partial t} + \mathrm{v}\frac{\partial \mathrm{v}}{\partial x} + \mathrm{u}\frac{\partial \mathrm{v}}{\partial y}\right) + \frac{\partial \mathrm{p}}{\partial x} - \frac{\delta}{C}\left(\frac{\partial^2 \mathrm{v}}{\partial x^2} + \delta^2\frac{\partial^2 \mathrm{v}}{\partial y^2}\right) = 0, \quad \frac{\partial \mathrm{v}}{\partial x} + \frac{\partial \mathrm{u}}{\partial y} = 0; \tag{2}$$

Conditions aux limites:

$$x = \pm(1+\xi): \quad \mathrm{v} = \pm\frac{\partial \xi}{\partial t}, \quad \mathrm{u} = 0, \quad \mathrm{p} = A\cos\left(t - y\right). \tag{3}$$

Le problème (1)-(3) en forme adimentionnelle. Les unités de mesure choisies sont : pour la coordonnée transversale par rapport à l'axe du canal x - la moitié de la distance entre les parois de canal h, pour la coordonnée longitudinale y – le nombre d'onde inversé λ, pour la vitesse longitudinale u – la vitesse de propagation d'onde de pression sur la paroi c, pour le temps t – λ/c, pour la pression p – ρc^2 (où ρ - la densité du liquide), pour la vitesse transversale v – ch/λ, pour l'écart par rapport à la position moyenne du canal ξ – h.

Le problème est caractérisé par trois paramètres adimensionnels: la vitesse de propagation d'onde $C = hc/\nu$ (où ν - la viscosité kinématique), le nombre d'onde $\delta = h/\lambda$ et l'amplitude

[1] Takagi D. Nonlinear peristaltic waves: a bitter pill to swallow // GFD Proceedings Volume of WHOI. — 2009. — P. 2-25.

adimensionnelle des vibrations de pression sur la paroi $A = a/(\rho c^2)$ (où a - l'amplitude dimensionnelle des vibrations de pression). La solution du problème (1)-(3) était cherchée sous la forme d'une série selon le petit paramètre A. Au préalable, la transformation des coordonnées a été effectuée:

$$x \to x(1+\xi),\ y \to y,\ t \to t. \tag{4}$$

Dans le premier rang la solution du problème pour la pression est

$$p_1 = \mathrm{ch}(\delta x)\cos\tau / \mathrm{ch}\,\delta, \tag{5}$$

pour la vitesse longitudinale:

$$\begin{aligned} \mathrm{u}_1 = \cos\tau\,\mathrm{ch}(\delta x)/\mathrm{ch}\,\delta + \mathrm{sh}\,\chi_1 x \sin\omega_1 x\left[C_1\cos\tau - C_2\sin\tau\right] + \\ + \mathrm{ch}\,\chi_1 x\cos\omega_1 x\left[C_2\cos\tau + C_1\sin\tau\right], \end{aligned} \tag{6}$$

pour la vitesse transversale:

$$\begin{aligned} \mathrm{v}_1 = \mathrm{ch}(\chi_1 x)\sin(\omega_1 x)((\omega_1 C_1 - \chi_1 C_2)\cos\tau - (\omega_1 C_2 + \chi_1 C_1)\sin\tau)/(\chi_1^{\,2} + \omega_1^{\,2}) + \\ + \frac{\mathrm{sh}\,\chi_1 x\cos\omega_1 x}{\chi_1^{\,2} + \omega_1^{\,2}}((\chi_1 C_1 + \omega_1 C_2)\cos\tau - (\chi_1 C_2 - \omega_1 C_1)\sin\tau) - \frac{\mathrm{sh}\,\delta x}{\delta\,\mathrm{ch}\,\delta}\sin\tau, \end{aligned}$$

avec la notation suivante $\tau = t - y$ et

$$\chi_1 = \sqrt{\delta(\sqrt{\delta^2 + C^2} + \delta)/2},\ \omega_1 = \sqrt{\delta(\sqrt{\delta^2 + C^2} - \delta)/2},$$
$$C_1 = -\mathrm{sh}\,\chi_1 \sin\omega_1 / (\cos^2\omega_1 + \mathrm{sh}^2\,\chi_1),\ C_2 = -\mathrm{ch}\,\chi_1\cos\omega_1 / (\cos^2\omega_1 + \mathrm{sh}^2\,\chi_1).$$

La vitesse longitudinale moyenne dans le temps est déterminée par l'équation

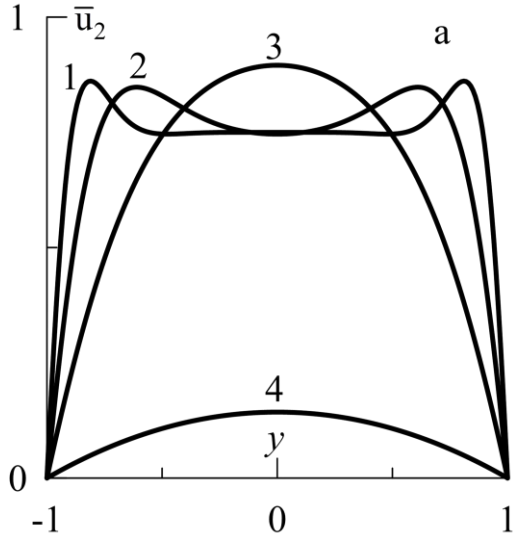

Figure 1. Dépendance de la vitesse longitudinale moyenne de la coordonnée transversale $x' = x(1+\xi)$

$$\bar{u}_2 = c_1 + c_2 x + \frac{C\delta}{2\pi}\iint_0^{2\pi}\Bigg(-x\frac{\partial\xi_1}{\partial y}\frac{\partial p_1}{\partial x} + \frac{x\delta}{C}\frac{\partial^2\xi_1}{\partial y^2}\frac{\partial u_1}{\partial x} + \frac{2\xi_1}{C\delta}\frac{\partial^2 u_1}{\partial x^2} + \frac{2x\delta}{C}\frac{\partial\xi_1}{\partial y}\frac{\partial^2 u_1}{\partial x\partial y} + v_1\frac{\partial u_1}{\partial x} + x\frac{\partial u_1}{\partial x}v_1\Big|_{x=-1}\Bigg)dtdxdx. \quad (7)$$

où les constantes c_1 et c_2 dans (7) sont déterminées via les conditions aux limites: $x = \pm 1 : \bar{u}_2 = 0.$

Le débit du liquide est calculé selon la formule

$$Q_2 = \int_{-1}^{1}(\bar{u}_2 + \frac{1}{2\pi}\int_0^{2\pi} u_1\xi_1 dt)dx.$$

La figure 1 présente le profil de la vitesse longitudinale moyenne dans le temps $\bar{u}_2$ pour le nombre d'onde $\delta = 0.01$. A petite vitesse de propagation d'onde C, le profil de la vitesse longitudinale avec la courbe en cloche avec le maximum dans le centre du canal (figure 1: courbe 4: $C = 1$ et courbe 3: $C = 100$). Avec augmentation de vitesse de propagation d'onde dans les parties centrales de courbes apparessent des segments applatis et des couches flimites près des parois (figure 1: courbe 2: $C = 2000$, courbe 1: $C = 20000$).

La figure 2 illustre la dépendance du débit du liquide à partir des paramètres du problème. Comme on peut le voir, la dépendance de débit à l'égard de nombre d'onde n'est pas monotone; il existe le débit maximal qu'on peut atteindre en modifiant les paramètres du problème. Il est à peu près 2.5, ce qui pour l'eau dans le canal d'un cm. de large correspond à la vitesse de l'ordre de 10^{-3} m/sec. Le débit de liquide est augmenté par l'augmentation de la vitesse de propagation d'onde et, avec des nombres importants de C il descend à l'asymptote horizontale ce qui

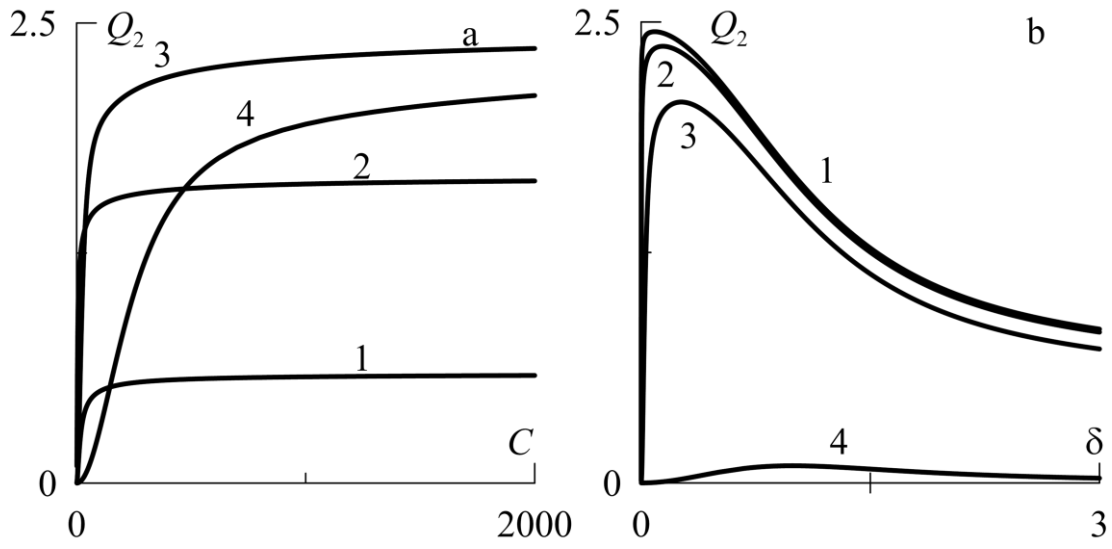

Figure.2. Dépendance de débit du liquide a) de la vitesse de propagation d'onde C pour $\delta = 0.01$ (1), $\delta = 0.1$ (2), $\delta = 1$ (3), $\delta = 10$ (4), b) du nombre d'onde δ pour $C = 20000$ (1), $C = 2000$ (2), $C = 100$ (3), $C = 1$ (4)

s'explique par la formation des couches limites.

Le **deuxième paragraphe du premier chapitre** est consacré à l'étude de l'influence des vibrations longitudinales à la transportations des produits par la voie péristaltique dans le canal bidimensionnel dans le cadre de l'approximation des ondes longues (petit δ). Pour le cas où les vibrations ne sont pas présentes, pour le débit de liquide on utilise la formule:

$$Q = \frac{A^2C^2\delta^2}{3} + \frac{A^2C^2\delta^4}{9}\left[\left(\frac{25}{12}A^2 - \frac{31}{63}C^2\right) - \frac{22}{5}\right] + O(\delta^6). \tag{8}$$

Dans le cas limite $\delta \to 0$ cette formule correspond à la formule précédente obtenue par D. Takagi pour ce cas limite (les différentes significations du coefficient sont dues à la différence de la géométrie des problèmes). Il faut souligner que D. Takagi avait étudié ce problème uniquement pour ce cas limite.

L'existence des vibrations longitudinales peut être simulée par la force d'inertie, comme quoi sans le problème (1)-(3) de flux péristaltique dans le canal à onde de pression déterminée aux confins la seule chose qui change c'est l'équation (1) qui prend la forme suivante:

$$\delta\left(\frac{\partial \mathrm{u}}{\partial t} + \mathrm{v}\frac{\partial \mathrm{u}}{\partial x} + \mathrm{u}\frac{\partial \mathrm{u}}{\partial y} + \frac{\partial \mathrm{p}}{\partial y}\right) - \frac{1}{C}\left(\frac{\partial^2 \mathrm{u}}{\partial x^2} + \delta^2\frac{\partial^2 \mathrm{u}}{\partial y^2}\right) = M\delta\cos wt. \tag{9}$$

Dans l'équation (9) deux nouveaux paramètres apparaissent: l'amplitude adimensionnelle des vibrations M et la fréquence adimensionnelle des vibrations w, ils sont liés à la fréquence dimensionnelle w et à l'amplitude m en corrélations suivantes

$$M = \lambda m / c^2, \quad w = \mathrm{w}\lambda / c. \tag{10}$$

La solution du problème (2), (9), (3) dans l'approximation d'ondes longues fait l'augmentation de débit de liquide grace aux vibrations de type:

$$\Delta Q = -\frac{5}{18}\frac{C^4\delta^4A^2M^2}{w^2 - 1} + \mathrm{O}(\delta^5). \tag{11}$$

Comme on peut voir dans l'équation (11), dans le cas des fréquences de vibrations plus hautes que la fréquence de l'onde de pression aux confins de paroi, les vibrations affectent négativement le transport péristaltique – le débit du liquide diminue. Dans le cas inverse – les vibrations entraînent l'augmentation du débit.

En cas de correspondance des fréquences de vibrations avec celles de l'onde de pression aux confins, la formule pour le débit de liquide (11) n'est plus efficace. Pour observer ce cas il faut étudier le comportement du système aux alentours de cette valeur, pour laquelle la fréquence serait $w = 1 + \gamma\delta^2$ ($\gamma\delta^2$ - valeur faible). Dans ce cas la méthode de petit paramètre ne permet pas de trouver la solution et il faut utiliser la méthode d'échelles multiples, dans le cadre de laquelle à côté du temps rapide t, on introduit aussi le temps lent $t_1 = \delta t$ et $t_2 = \delta^2 t$. Aux alentours $w = 1$ dans la décomposition de ξ il faut introduire le sommant ξ_0 d'ordre zéro de δ. Son équation est:

$$\left[\frac{AM}{6}(\xi_0 + 1)\sin z - \frac{5}{6}A\frac{\partial \xi_0}{\partial y}(A + M\cos z)\right](\xi_0 + 1)^4 C^2 = \frac{\partial \xi_0}{\partial t_2} \tag{12}$$

où $z = t + \gamma t_2$. L'équation différentielle peut (12) être réduite à une algébrique

$$(M\cos z + A)AC^2(\xi_0 + 1)^5 + 6\xi_0\gamma + \tilde{C} = 0, \tag{13}$$

où $\tilde{C}$ - la constante non-déterminée. Dans le cas de grands γ la solution de l'équation (13) a la forme suivante:

$$\xi_0 = -\frac{AC^2M}{6}\frac{\cos z}{\gamma} + \frac{5MC^4A^2(M\cos 2z + 2A\cos z)}{72\gamma^2} + O\left(\frac{1}{\gamma^3}\right). \tag{14}$$

Le débit de liquide dans ce cas sera

$$\Delta Q = \delta^2 C^2 A^2 \left[-\frac{5C^2M^2}{36\gamma} + \frac{5C^2A^2M^2}{18\gamma^2} \right] + \mathrm{O}\left(\frac{1}{\gamma^3}, \delta^3\right). \tag{15}$$

Si on prend $w = 1 + \gamma\delta^2$ dans la (11) et en la décomposant selon δ, nous aurons

$$\Delta Q = -\frac{5}{18}\frac{C^4\delta^4A^2M^2}{(1+\gamma\delta^2)^2 - 1} \approx -\frac{5C^4\delta^2A^2M^2}{36\gamma} + \mathrm{O}(\delta^3). \tag{16}$$

La comparaison de (11) et (15) nous prouve que loin du point $w = 1$ une solution passe en une autre. Dans le cas des relations faibles *M/A*<<1,

$$\xi_0 = -\frac{\cos z}{5+6\Gamma}\frac{M}{A} + 15\frac{\Gamma + 0.5}{(5+6\Gamma)^3}\left(\frac{M}{A}\right)^2 \cos 2z + O\left(\frac{M}{A}\right)^3, \tag{17}$$

où $\Gamma = \gamma / (A^2C^2)$. On peut déduire de (17) que dans l'ordre zéro de paramètre faible il y a une onde lente qui apparait ξ_0.

On a découvert que lorsque la valeur w tend vers 1, une onde lente dont la fréquence est égale à la différence des fréquences des deux effets se produit. Quand les valeurs des fréquences coïncident, cette onde dégénère en un modèle stationnaire.

Aux alentours de $w = 1$ au lieu de la formule (11) il faut utiliser:

$$\begin{aligned} \frac{Q}{A^2C^2\delta^2} &= \frac{1}{3} - \frac{5}{2}\frac{1+2\Gamma}{(5+6\Gamma)^2}\frac{M^2}{A^2} \\ &\quad - \frac{5\left[2916\Gamma^3 + 2025\Gamma + 325 + 4152\Gamma^2\right]}{4(6\Gamma+5)^6}\frac{M^4}{A^4} + \mathrm{O}\left(\delta^3, \left(\frac{M}{A}\right)^6\right), \end{aligned} \tag{18}$$

où $\Gamma = (w-1)/(\delta AC)^2$. Alors, vers le $w = 1$ l'influence des pulsations à la transportation des produits se transforme en effet de deuxième degrès, c'est à dire de même degès que l'effet transport des ondes péristaltiques. Comme conséquence, les pulsations puissent amener à l'augmentation du débit aussi bien qu'à la diminution du débit en fonction de changement de la valeur de Γ.

La formule (18) se diverge quand la différence des fréquences des effets correspond à la fréquence propre aux vibrations des parois du canal (en même temps $\Gamma = -5/6$). Dans ce cas

$$\xi_0 = y\sin(y - 5A^2C^2t_2/6)M/(5A) + O\left(M/A\right)^2. \tag{19}$$

De (19) on peut déduire que quand $\Gamma = -5/6$, l'approche utilisée n'est plus efficace parce que les parois du canal se percute.

Des liquides transportés par voie péristaltiques contiennent souvent des particules différentes. Dans certains cas, du à une collision de ces particules contre une paroi en phase de vibration quand la vitesse de paroi augmente, après la collision la paroi regagne la particule et une collision itérative se produit. En cas de plusieurs collisions itératives la particule termine par se retrouver sur la paroi et continue son mouvement avec elle.Pour définir une situation pareille on utilise le terme «l'adhésion» de particule.

Deuxième chapitre est consacré aux recherches de l'influence des pulsations transversalles sur transfert de matière sous action de chute de pression et force de gravité dans le canal dimétrique orthogonal vertical. Ce problème était étudié déjà par Weinberg S.L.[2], Longuet-Higgins M.S.[3], Shugan I.[4] et les autres. Ils ont découvrit, que les pulsations permettent d'augmenter le débit du liquide , surgeant à cause de la chute de pression aux bouts du canal. Cette théorie, édifiée dans ces travaux, décrit le comportement du système justement dans les cas des faibles fréquences des pulsations. Zwik K.J.[5] et les autres, ont étudié expérimentalement un problème analogue. Ils ont étudié le mouvement du liquide entre deux lames rondes, influencée par la force, consistant en composante oscillée (fréquence 73, 100, 200, 230, 246 Hz) et composante constante et ils n'ont pu pas découvrir l'augmentation de débit de liquide, surgeant à cause de la vibration des lames. C'est à dire, que l'effet d'augmentation du débit de liquide à cause des pulsations, découvert par Weinberg S.L., Longuet-Higgins M.S., Shugan I., doit disparaître aux hautes fréquences des pulsations. Dans le deuxième chapitre de la thèse, on a étudié théoriquement l'influence des pulsations transversales des parois sur le transfert de la matière sous action de chute de pression et force de gravité dans le canal dimétrique orthogonal vertical.

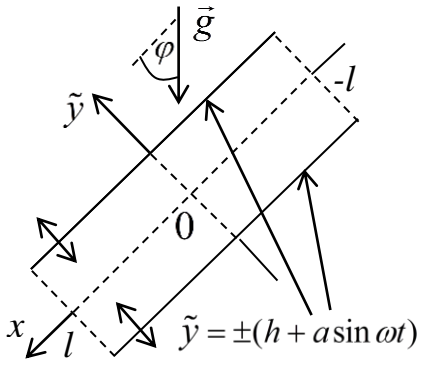

Fig. 3.

On résout le système des équations de Navier-Stokes (Fig. 3):

$$\rho\left(\frac{\partial \mathrm{U}}{\partial t} + \mathrm{U}\frac{\partial \mathrm{U}}{\partial x} + \mathrm{v}\frac{\partial \mathrm{U}}{\partial \tilde{y}}\right) = -\frac{\partial \tilde{p}}{\partial x} + \eta\left(\frac{\partial^2 \mathrm{U}}{\partial x^2} + \frac{\partial^2 \mathrm{U}}{\partial \tilde{y}^2}\right) + \rho \mathrm{g}\cos\varphi, \tag{20}$$

$$\rho\left(\frac{\partial \mathrm{v}}{\partial t} + \mathrm{U}\frac{\partial \mathrm{v}}{\partial x} + \mathrm{v}\frac{\partial \mathrm{v}}{\partial \tilde{y}}\right) = -\frac{\partial \tilde{p}}{\partial \tilde{y}} + \eta\left(\frac{\partial^2 \mathrm{v}}{\partial x^2} + \frac{\partial^2 \mathrm{v}}{\partial \tilde{y}^2}\right) - \rho g\sin\varphi\ , \tag{21}$$

[2] Weinberg S.L. Eckstein E.C., Shapiro A.H. Peristaltic pumping in circular tubes: A numerical study of fluid transport and its efficiency // J. Fluid Mech. — 1982. — Vol. 12, 2. — P. 439-465.

[3] Longuet-Higgins M.S. Peristaltic pumping in water waves // J. Fluid Mech. — 1983. — Vol. 137. — P. 393-407.

[4] Shugan I. Fluid mass transfer in a channel with vibrating elastic walls // Physics of Vibrations. — 1999. — Vol. 7, N.2. — P. 107-117.

[5] Zwick K.J. Ayyaswamy P.S. Cohen I.M. Oscillatory enhancement of the squeezing flow of yield stress fluids: A novel experimental result // J. Fluid Mech. — 1997. — Vol. 339. — P. 77-87.

$$\frac{\partial \mathrm{u}}{\partial x}+\frac{\partial \mathrm{v}}{\partial \tilde{y}}=0. \tag{22}$$

Conditions aux limites:

$$\tilde{y}=\pm(h+a\sin\omega t):\ \mathrm{u}=0,\ \mathrm{v}=\pm a\cos\omega t, \tag{23}$$

$$\tilde{p}\big|_{x=l}-\tilde{p}\big|_{x=-l}=2\Delta. \tag{24}$$

où $\tilde{y}$ – la coordonnée transversale par rapport à l'axe du canal x – la coordonnée longitudinale, t – le temps, p – la pression, U – la vitesse longitudinale, v – la vitesse transversale.

La transformation des coordonnées a été effectuée:

$$\tilde{p}\to p-\rho y g\sin\varphi+x\Delta/l, \tag{25}$$

$$\tilde{y}\to y\left(1+\frac{A}{h}\sin t\right). \tag{26}$$

En fonction des unités de mesure pour l'axe transversal du canal de la coordonné x et de la coordonné longitudinale y on a choisi la moitié de la distance entre parois *h*, pour le temps *t* - fréquence inverse des pulsations $1/\omega$, pour la pression $p-\eta\omega$ (où η - viscosité dynamique) pour les vitessees transversale v et longitudinale u - $h\omega$.

On résout le système des équations

$$\begin{aligned}(1+A\sin t)^2\left[\frac{\partial \mathrm{U}}{\partial t}+\mathrm{U}\frac{\partial \mathrm{U}}{\partial x}+\frac{\mathrm{v}-yA\cos t}{1+A\sin t}\frac{\partial \mathrm{U}}{\partial y}\right]=\\ =\frac{1}{2\mathrm{W}^2}\left[\left(-\frac{\partial p}{\partial x}+\frac{\partial^2 \mathrm{U}}{\partial x^2}\right)(1+A\sin t)^2+\frac{\partial^2 \mathrm{U}}{\partial y^2}\right]+(1+A\sin t)^2\mathrm{Ri},\end{aligned} \tag{27}$$

$$\frac{\partial \mathrm{v}}{\partial t}+\mathrm{U}\frac{\partial \mathrm{v}}{\partial x}+\frac{\mathrm{v}-yA\cos t}{1+A\sin t}\frac{\partial \mathrm{v}}{\partial y}=\frac{1}{2\mathrm{W}^2}\left(\frac{\partial^2 \mathrm{v}}{\partial x^2}+\frac{1}{(1+A\sin t)^2}\frac{\partial^2 \mathrm{v}}{\partial y^2}-\frac{\partial p}{\partial y}\right), \tag{28}$$

$$\frac{\partial \mathrm{U}}{\partial x}+\frac{1}{1+A\sin t}\frac{\partial \mathrm{v}}{\partial y}=0, \tag{29}$$

$$y=\pm 1:\ \mathrm{U}=0,\ \mathrm{v}=\pm A\cos t. \tag{30}$$

$$p\big|_{x=L}=p\big|_{x=-L}. \tag{31}$$

Ce problème est caractérisé par quatrième paramètres adimensionnels: nombre de Womersley W, nombre de Richardson Ri, longueur du canal L, amplitude de pulsation adimensionnelle *A*:

$$\mathrm{W}=h\sqrt{\frac{\rho\omega}{2\eta}},\ \mathrm{Ri}=\frac{g\cos\varphi-\Delta/(l\rho)}{\omega^2 h},\ A=\frac{a}{h},L=\frac{l}{h}.$$

La solution du problème a été obtenu sous une forme

$$\mathrm{U}=\mathrm{u}(y,t)-\frac{x}{1+A\sin t}\frac{\partial \mathrm{v}(y,t)}{\partial y}, \tag{32}$$

$$\mathrm{v}=\mathrm{v}(y,t),\ p=\phi(y,t)+x^2\gamma(t). \tag{33}$$

Le problème (27)-(31) résolvait à l'aide de décomposition selon amplitude des vibrations des parois A. A l'ordre zéro la solution est:

$$\mathrm{u}_0 = -\mathrm{Fr}\Omega\frac{y^2-1}{2},\ \mathrm{v}_0 = 0$$

Au premier ordre, la solution est

$$p_1 = p_{1s}(x,y)\sin t + p_{1c}(x,y)\cos t, \tag{34}$$

$$\mathrm{v}_1 = \mathrm{v}_{1s}(\mathrm{y})\sin t + \mathrm{v}_{1c}(\mathrm{y})\cos t, \tag{35}$$

$$\mathrm{u}_1 = \mathrm{u}_{1s}(\mathrm{y})\sin t + \mathrm{u}_{1c}(\mathrm{y})\cos t\,. \tag{36}$$

où

$$p_{1s} = (y^2-x^2)\mathrm{W}^2 f_1,$$

$$p_{1c} = -(y^2-x^2)\mathrm{W}^2 f_2,$$

où

$$f_1 = \mathrm{W}S\left[2\mathrm{W}(\cosh 2\mathrm{W}+\cos 2\mathrm{W}) - \sin 2\mathrm{W} - \sinh 2\mathrm{W}\right]. \tag{37}$$

$$f_2 = \mathrm{W}S\left[\sinh 2\mathrm{W} - \sin 2\mathrm{W}\right], \tag{38}$$

$$S = \left((2\mathrm{W}^2+1)\cosh 2\mathrm{W} + (2\mathrm{W}^2-1)\cos 2\mathrm{W} - 2\mathrm{W}(\sinh 2\mathrm{W}+\sin 2\mathrm{W})\right)^{-1}; \tag{39}$$

$$\mathrm{v}_{1s} = f_3 \sin \mathrm{W}y\cosh \mathrm{W}y + f_4 \cos \mathrm{W}y\sinh \mathrm{W}y + f_2 y, \tag{40}$$

$$\mathrm{v}_{1c} = f_4 \sin \mathrm{W}y\cosh \mathrm{W}y - f_3 \cos \mathrm{W}y\sinh \mathrm{W}y + f_1 y, \tag{41}$$

où

$$f_3 = 2S\left[\mathrm{W}\cos \mathrm{W}\cosh \mathrm{W} - (\cos \mathrm{W} + \mathrm{W}\sin \mathrm{W})\sinh \mathrm{W}\right], \tag{42}$$

$$f_4 = -2S\left[(\mathrm{W}\cos \mathrm{W} - \sin \mathrm{W})\cosh \mathrm{W} + \mathrm{W}\sinh \mathrm{W}\sin \mathrm{W}\right]; \tag{43}$$

$$\mathrm{u}_{1s} = \mathrm{Ri}\Big(\Big[(f_6 + f_7(y^2-1))y\cos \mathrm{W}y + (f_8 + f_9(y^2-1))\sin \mathrm{W}y\Big]\sinh \mathrm{W}y + f_{14} +$$
$$+\Big[(f_{10}(y^2-1)+f_{11})\cos \mathrm{W}y + (f_{12} + f_{13}(y^2-1))y\sin \mathrm{W}y\Big]\cosh \mathrm{W}y + f_5(y^2-1)\Big),$$

$$\mathrm{u}_{1c} = \mathrm{Ri}\Big(\Big[(f_{11} + f_{10}(y^2-1))\sin \mathrm{W}y - (f_{12} + f_{13}(y^2-1))y\cos \mathrm{W}y\Big]\sinh \mathrm{W}y - f_1 +$$
$$+\Big[(f_6 + f_7(y^2-1))y\sin \mathrm{W}y - (f_9(y^2-1)+f_8)\cos \mathrm{W}y\Big]\cosh \mathrm{W}y - f_2\mathrm{W}^2(y^2+1)\Big),$$

où

$$f_5 = \mathrm{W}^2(f_1-2),\ f_6 = -\frac{2}{3}\left(\frac{9}{8}f_3 + \mathrm{W}^2 f_4\right)\mathrm{W}^2,\ f_7 = \mathrm{W}^4 f_4/3,\ f_9 = -3\mathrm{W}^3(f_4+f_3)/4,$$

$$f_{10} = 3(f_3-f_4)\mathrm{W}^3/4,\ f_{12} = -2\mathrm{W}^2(f_3\mathrm{W}^2 - 9f_4/8)/3,\ f_{13} = f_3\mathrm{W}^4/3,\ f_{14} = 2(f_1-1)\mathrm{W}^2 - f_2,$$

$$f_8 = \frac{-f_{12}\sinh 2\mathrm{W} + f_6 \sin 2\mathrm{W} - 2(2f_2\mathrm{W}^2 + f_1)\cosh \mathrm{W}\cos W - 2f_{14}\sin \mathrm{W}\sinh \mathrm{W}}{\cos 2\mathrm{W} + \cosh 2\mathrm{W}},$$

$$f_{11} = \frac{-f_6\sinh 2\mathrm{W} - f_{12}\sin 2\mathrm{W} + 2(2f_2\mathrm{W}^2 + f_1)\sin \mathrm{W}\sinh \mathrm{W} - 2f_{14}\cos \mathrm{W}\cosh \mathrm{W}}{\cos 2\mathrm{W} + \cosh 2\mathrm{W}}.$$

La soultion trouvée permet d'obtenir les caractéristiques moyennes du courant avec la précision jusqu'à deuxième degré de petitesse. Aux ces conditions le débit du liquide peut être présenter comme suit:

$$\bar{Q} = Q_0 + \bar{Q}_1 A + \bar{Q}_2 A^2 + O(A^3), \tag{44}$$

où

$$Q_0 = \frac{4}{3}\mathrm{W}^2\mathrm{Ri}\,, \tag{45}$$

$$\bar{Q}_1 = 0, \tag{46}$$

$$\bar{Q}_2 = \int_{-1}^{1}\left(\frac{\mathrm{u}_{1s}}{2} + \bar{\mathrm{u}}_2\right)dy\,. \tag{47}$$

Sur la fig. 4 est représentée la dépendance, qui apparaisse à cause de pulsation d'addition Q_2 envers le débit du liquide et de paramètres du problème. Quand $W \to 0$ cette addition est positive et égale à:

$$\bar{Q}_2 \approx 2\mathrm{W}^2\mathrm{Ri}\,, \tag{48}$$

cela coïncide avec la formule de Liakhov G.V. et Chougan I.V.[6] pour ce cas extrême

En cas des grandes valeurs du nombre de Womersley l'addition du débit du liquide, surgeant à cause des pulsations, est négative et approximativement égal à:

$$Q_2 \approx -\frac{\mathrm{RiW}^3}{3}\,. \tag{49}$$

Caractère de l'addition Q_2 se change quand $W = 7.5$, et pour l'eau dans le canal en épaisseur 1 sm coïncide à la fréquence des pulsation 1 Hz. En conséquent, dans la plupart des cas, les pulsations doivent mener à la diminution de débit de liquide, et pas à l'augmentation, comme cela a été obtenu dans les recherches de Chougan I.V., qui avait étudié seulement les cas des fréquences basses des pulsations.

Dans la **deuxième partie du deuxième chapitre**, on a étudié l'influence des pulsations transversales des parois sur le transfert du liquide sous influence de la force de gravité dans le canal dimétrique orthogonal vertical, en comptant le liquide compressible.

Le comportement du liquide peut être décrit par un système d'équitations, qui sous la forme adimensionnelle est

$$\rho\left(\frac{\partial \mathrm{u}}{\partial t} + \mathrm{u}\frac{\partial \mathrm{u}}{\partial y} + \mathrm{v}\frac{\partial \mathrm{u}}{\partial x}\right) = \frac{1}{\Omega}\left[\frac{\partial^2 \mathrm{u}}{\partial x^2} + \frac{\partial^2 \mathrm{u}}{\partial y^2} - \frac{\partial \mathrm{p}}{\partial y}\right] + \frac{1}{\Omega_2}\frac{\partial}{\partial y}\left[\frac{\partial \mathrm{v}}{\partial x} + \frac{\partial \mathrm{u}}{\partial y}\right] + \rho\mathrm{Fr}, \tag{50}$$

$$\rho\left(\frac{\partial \mathrm{v}}{\partial t} + \mathrm{u}\frac{\partial \mathrm{v}}{\partial y} + \mathrm{v}\frac{\partial \mathrm{v}}{\partial x}\right) = -\frac{1}{\Omega}\frac{\partial \mathrm{p}}{\partial x} + \frac{1}{\Omega}\left[\frac{\partial^2 \mathrm{v}}{\partial y^2} + \frac{\partial^2 \mathrm{v}}{\partial x^2}\right] + \frac{1}{\Omega_2}\frac{\partial}{\partial x}\left[\frac{\partial \mathrm{v}}{\partial x} + \frac{\partial \mathrm{u}}{\partial y}\right], \tag{51}$$

$$\frac{\partial \rho}{\partial t} + \frac{\partial \mathrm{u}\rho}{\partial y} + \frac{\partial \mathrm{v}\rho}{\partial x} = 0,\ \ \mathrm{p} = c^2(\rho - 1) \tag{52}$$

et les conditions aux limites:

$$x = \pm(1 + A\sin t):\ \mathrm{v} = \pm A\cos t\,,\ \mathrm{u} = 0\,. \tag{53}$$

[6] Liakhov G.V., Chougan I.V. The energy efficiency of the acceleration mechanism of mass transfer fluid in the channel // JETP Letters. — 2002. — V. 28, №7. — pp. 57-61.

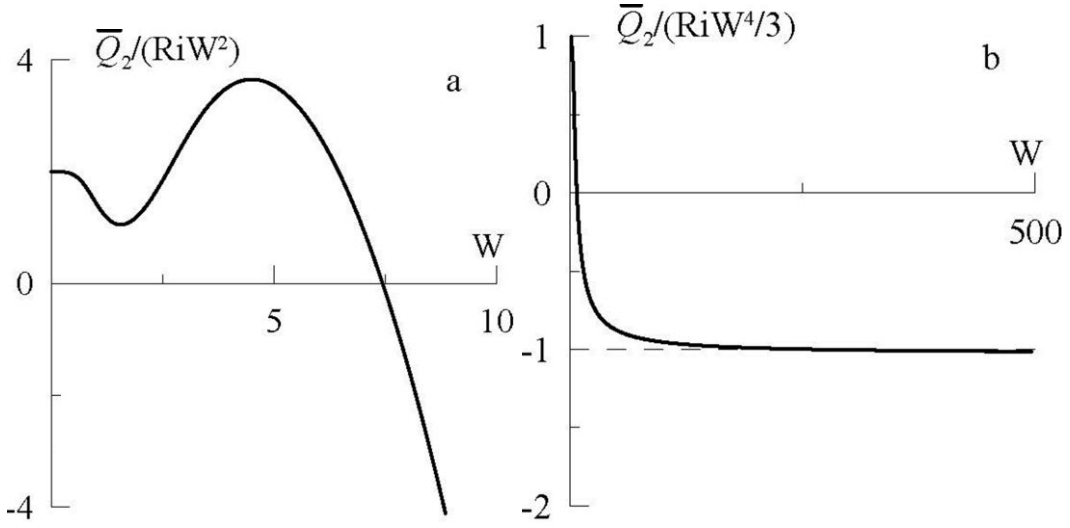

Fig. 4. Dépendance, surgeant à cause des pulsations d'addition à débit du liquide vis à vis du nombre de Womersley

L'incorporation des unités de mesure est faite comme dans le chapitre précédent, la densité est mesurée en densités équipondérantées ρ_i.

Les paramètres adimensionnels du problème sont les fréquences des pulsations Ω et Ω_2, nombre de Froude Fr, amplitude des pulsations *A* et la vitesse du son *c,* qui sont définis par les rapports:

$$\Omega = \frac{\omega h^2 \rho_i}{\eta};\ \Omega_2 = \frac{3\omega h^2 \rho_i}{3\varsigma + \eta};\ \mathrm{Fr} = \frac{-g}{h\omega^2};\ A = \frac{\alpha}{h};\ c = C_s\sqrt{\frac{\rho_i}{\eta\omega}}, \tag{54}$$

où C_s - vitesse du son au dimension, ς - viscosité de volume.

Une solution analytique du problème (50)-(53) a été trouvé à l'approximation des amplitudes basses des pulsations des parois. En ordre zéro selon le petit paramètre, la solution est

$$\mathrm{u}_0 = -\frac{y^2-1}{2}\Omega\mathrm{Fr},\ \mathrm{p}_0 = 0,\ \rho_0 = 1,\ \mathrm{v}_0 = 0.$$

En premier ordre la solution c'est la vitesse longitudinale:

$$\begin{aligned}\mathrm{u}_1 = {} & C_s^+ e^{\Omega' x}\sin(t+\Omega' x) + C_s^- e^{-\Omega' x}\sin(t-\Omega' x) + C_c^+ e^{\Omega' x}\cos(t+\Omega' x) + \\ & + C_c^- e^{-\Omega' x}\cos(t-\Omega' x) + U_s^- e^{-\delta x}\sin(t-yk) + U_c^- e^{-\delta x}\cos(t-xk) + \\ & + U_s^+ e^{\delta x}\sin(t+xk) + U_c^+ e^{\delta x}\cos(t+xk) + y\left[U_{ys}^- e^{-\delta y}\sin(t-xk) + \right. \\ & \left. + U_{yc}^- e^{-\delta x}\cos(t-yk) + U_{ys}^+ e^{\delta x}\sin(t+xk) + U_{yc}^+ e^{\delta y}\cos(t+xk)\right] \\ & - y^2\Omega\mathrm{Fr}\sin t,\end{aligned}$$

la vitesse transversale s'écrit

$$\begin{aligned}\mathrm{v}_1 = {} & V_{1s}^- e^{-\delta x}\sin(t-xk) + V_{1c}^- e^{-\delta x}\cos(t-xk) \\ & + V_{1s}^+ e^{\delta x}\sin(t+xk) + V_{1c}^+ e^{\delta x}\cos(t+xk),\end{aligned}$$

et la densité est définie comme suit

$$\rho_1 = R_{1s}^- e^{-\delta x}\sin(t-xk) + R_{1c}^- e^{-\delta x}\cos(t-xk)$$
$$+ R_{1s}^+ e^{\delta x}\sin(t+xk) + R_{1c}^+ e^{\delta x}\cos(t+xk),$$

où on a fait des dénomination

$$k = \sqrt{\frac{\Omega\Omega_2}{2}\frac{\sqrt{\Omega_2^2 c^4 + (\Omega_2+\Omega)^2} + \Omega_2 c^2}{c^4\Omega_2^2 + (\Omega_2+\Omega)^2}},\ \delta = \sqrt{\frac{\Omega\Omega_2}{2}\frac{\sqrt{\Omega_2^2 c^4 + (\Omega_2+\Omega)^2} - \Omega_2 c^2}{c^4\Omega_2^2 + (\Omega_2+\Omega)^2}},$$

$$\Omega' = \sqrt{\frac{\Omega}{2}}$$

et $C_{s,c}^{\pm}$, $U_{s,c}^{\pm}$, $U_{ys,yc}^{\pm}$, $V_{s,c}^{\pm}$, $R_{s,c}^{\pm}$ sont des constantes, dépendantes des paramètres du problème. On a trouvé la solution, qui permet d'obtenir les caractèristiques moyennes de courant (débit du

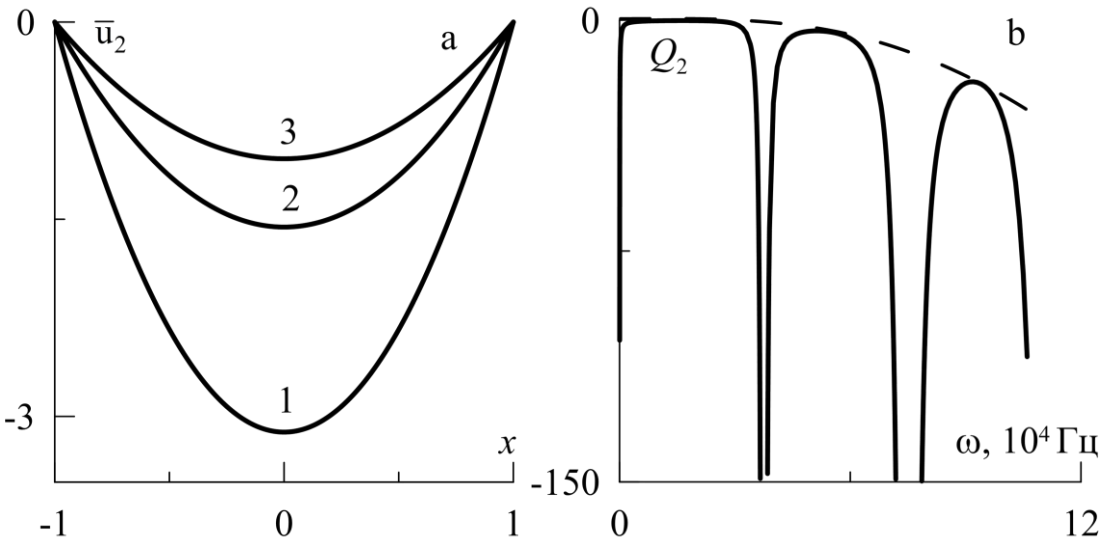

Fig. 5. a) l'addition moyenne par rapport à la vitesse longitudinal pour la fréquence des pulsations des parois 500 Hz(1) , 1000 Hz(2), 1500 Hz (3) ; dépendance de l'addition adimensionnele par rapport à la consomation du liquide de la fréquence $\rho = 10^3\,\text{kg/m}^3$, $h = 2$ sm, $\eta = 10^{-2}$ Pa s, $C_s = 1500$ m/s, $g = 9.8$ m/s^2, $\varsigma = 2.81\eta$

liquide, vitesse moyenne et densité) avec la précision jusqu'aux membres du deuxième degré de petitesse selon amplitude des pulsations des parois.

Sur la figure 5b on peut voir, que les pulsations des parois mènent toujours à la diminution du débit du liquide. La méthode utilisée ne permet pas étudier le courant à proximité des points spéciales : 0 Hz, 37500 Hz, 75000 Hz etc. En ce cas, la solution trouvée est la suivante selon le petit paramètre tendant à l'infini (les constantes $C_{s,c}^{\pm}$, $U_{s,c}^{\pm}$, $U_{ys,yc}^{\pm}$, $V_{s,c}^{\pm}$, $R_{s,c}^{\pm}$ accèdent au infini).

L'addition moyenne selon le temps par rapport à la vitesse longitudinale $\bar{u}_2$ a la forme de la cloche avec la plus grande déclinaison de la vitesse de zéro au centre du canal (figure 5a).

L'influence de la compressibilité manifeste dans l'apparition de l'hétérogénéité de la densité, idépendante du temps dans le canal (fig. 6).

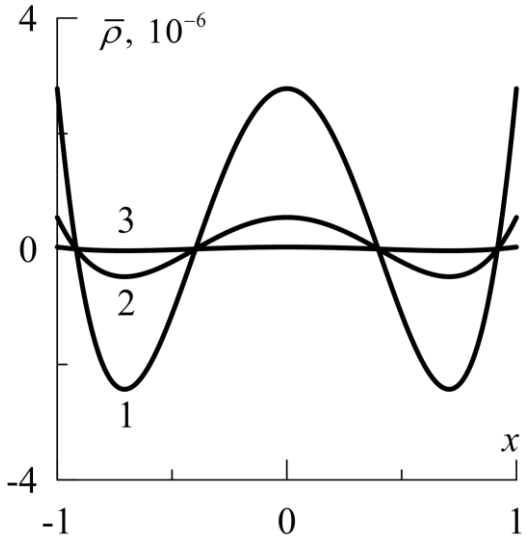

Fig. 6. Dépendance de la densité $\bar{\rho}$, moyenne selon le temps, de la coordonnée pour les fréquences des pulsations des parois 500 Hz (1), 1000 Hz (2), 1500 Hz (3)

Dans le **troisième chapitre** on a examiné l'interaction des bulles ascendentes et de la particule tombante dans l'eau dans champ acoustique. L'influence de la particule sur le mouvement du liquide on peut considerer négligeable . Auparavant ce problème était étudié par Lubimov D.V. , Lubomova T.P. et Klimenko L. S.[7] Ils ont examiné le cas des fortes pressions sonores dans le cadre d'approximation, où l'influence des oscillations propres des bulles peut compter comme peu importante. Pour telles pressions sonores la méthode de Lubimov D.V., Lubomova T.P. et Klimenko L.S. découvre que l'influence du son sur le mouvement d'une bulle et une particule est très petite. Dans la recherche, présente dans cette thèse on a fait la méthode en cadre de laquelle on compte les pulsations propres à la bulle. Cela permet de découvrir l'augumentation du rayon de collision des particules et des bulles pour les frequences du son définies, même dans les cas des faibles presssions acoustiques.

La vitesse des bulles peut décrite par une équitation

$$\frac{\rho_L}{2}\frac{d\vec{U}}{dt} - F_H(t) + \frac{3}{2R}\rho_L\vec{U}\frac{dR}{dt} - \frac{C_D}{2}\rho\pi R^2\left|\vec{U}\right|\vec{U} - \rho_L\vec{g} = 0, \qquad (55)$$

où[8]

[7] Klimenko L.S. Generation of flow and particle behavior near the bubble in an oscillating liquid / / Thesis for the degree Degree of Candidate of Physical and Mathematical Sciences. Perm, 2011.

[8] Takemura F., Magnaudet J. The history force on a rapidly shrinking bubble rising at finite Reynolds number// Phys. Fluids - 2004 - V.16 - 3247

$$F_H(t) = -6\pi\eta \int_{-\infty}^{t} \left\{ \left[\pi\nu \int_{\tau}^{t} \frac{dt'}{R(t')^2} \right]^{1/(2\alpha)} + \frac{1}{G(\tau)} \left[\frac{\pi}{16} \left(\frac{\mathrm{Re}(\tau)}{f_H(\mathrm{Re}(\tau))} \right)^3 \times \right. \right.$$

$$\left. \left. \times \left[\frac{\pi}{16} \left(\frac{\mathrm{Re}(\tau)}{f_H(\mathrm{Re}(\tau))} \right)^3 \left(\nu \int_{\tau}^{t} \frac{dt'}{R(t')^2} \right)^2 \right]^{1/\alpha} \right\} \frac{d}{d\tau} (\mathrm{R}(\tau)(\vec{\mathrm{U}}(\tau) - \vec{\mathrm{u}}_0)) d\tau,$$

$$f_H(\mathrm{Re}) = 0.75 + 0.105\,\mathrm{Re},\ \ \mathrm{Re}(t) = 2R(U - u_0)/\nu,\ \ \alpha = 2,\ G(\tau) = 1.$$

$\vec{U}$ - vitesse de bulles, R - rayon de bulles, ρ_L - densité du liquide, ν - coefficient de viscosité cinématique, C_D - coefficient de viscosité. On compte les bulles sphériques au rayon qui se change conformément à l'équitation de Rayleigh–Plesset

$$R\frac{d^2R}{dt^2} + \frac{3}{2}\left(\frac{dR}{dt}\right)^2 - \frac{p_{g0}}{\rho_L}\left(\frac{R_0}{R}\right)^{3\gamma} = \frac{p_p}{\rho_L} - \frac{p(t)}{\rho_L},$$

où p_{g0} - pression du gaz à l'instant initial, R_0 - rayon de la bulle à l'instant initial.

Le sommant $p(t) = A\sin\omega t$ dans la partie droite de l'équation décrit l'effet que le son produit sur la bulle de gaz. Comme dans le recherche de Lubimov D. V., Lubimova T.P. et Klimenko L.S. on considère que la longueur de l'onde sonore est plus importante que les dimentions du problème. Les vitesses des mouvements des particules de l'environnement dans les champs sonores faibles sont de l'ordre $10^{-4} - 10^{-6}$ m/sec., ce qui est beaucoup moins importante que la vitesse de la bulle de gaz et de particule, c'est pourquoi on peut nier l'influence du son sur le courant de liquide. Le son ne provoque que le changement de forme de bulle de gaz.

Le courant de liquide provoqué par l'existence de la bulle de gaz est considéré comme potentiel, ce qui permet d'utiliser la formule suivante pour calculer la vitesse du liquide

$$\vec{\mathrm{u}}_L = \frac{R^3}{2r^3}\left[-\vec{U} + \frac{3}{r^2}\left(\vec{U}\cdot\vec{r}\right)\vec{r}\right] + \frac{R^2\vec{r}}{r^3}\dot{R}$$

où $\vec{r}$ - le rayon du centre de la bulle jusqu'au point où on effectue le calcul de vitesse du liquide.

Dans les applications liées à la flottation la particule est approximativement 100 fois plus petite que la bulle de gaz et l'influence de la particule sur le courant de liquide produite par la présence de la bulle peut être considérée comme négligeablement petite. Cela permet appliquer à ce problème l'équation de Boussinesq pour la déscription du mouvement de particule:

$$m_p\left(\frac{d\vec{U}_p}{dt} + \frac{d\vec{U}}{dt}\right) = 3\pi d_p\eta(\vec{\mathrm{u}}_L - \vec{U}_p) + \frac{1}{6}\pi d_p^3(\rho_p - \rho)\vec{g} - \frac{\pi}{6}d_p^3\nabla p +$$

$$+ \frac{\pi}{12}d_p^3\rho\frac{d}{dt}(\vec{\mathrm{u}}_L - \vec{U}_p) - \frac{3}{2}d_p^2\sqrt{\pi\eta\rho}\int_0^t \frac{d(\vec{U}_p - \vec{\mathrm{u}}_L)}{d\tau}\frac{d\tau}{\sqrt{(t-\tau)}},$$

où d_p - le diamètre de particule, $\vec{\mathrm{u}}_L$ - la vitesse du liquide dans le centre de particule, si la particule n'existait pas, $\vec{U}_p$ - la vitesse de la particule, m_p - la masse de la particule.

On a découvert que sous l'influence du son la section de collision de la particule avec la bulle de gaz augmente. Quand la fréquence du son est égale à celle de pulsations de la bulle, la section de collision peut atteindre son maximum (figure 7). L'influence de toute autre fréquence

sur le rayon de collision est négligeable. La fréquence propre de la bulle dépende des dimentions

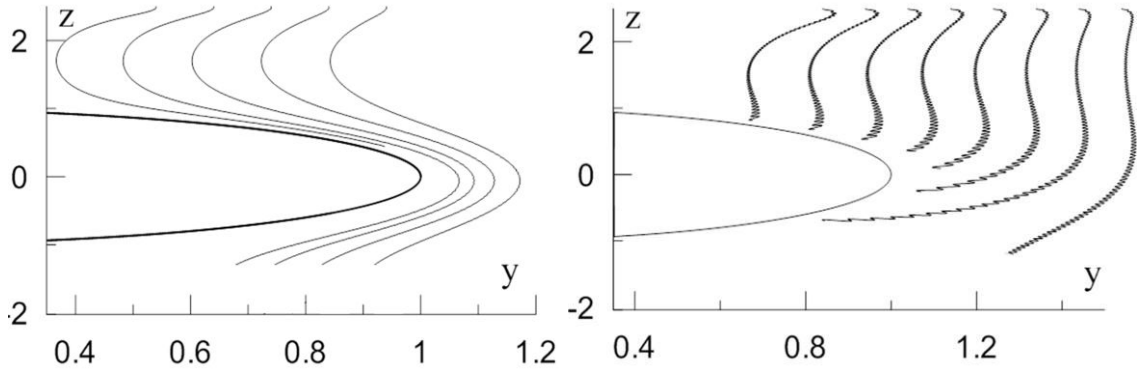

Fig. 7. Trajectoire du mouvement d'une particule en condition d'absence d'influence sonore (figure de droite), au champ acoustique (figure de gauche), fréquence 28160 rad/ s (égal à la fréquence des pulsations propres du bouillon). Les distances sont mesurées aux dimensions initiales du bouillon $R_0 = 700$ mkm.

de la bulle, ce qui signifie que sous influence du son la probabilité de collision des particules et une bulle de certain rayon augmente. Le rayon de collision sous influence du son dont la fréquence est égale à la fréquence des pulsations de la bulle augmente plus pour les particules plus lourdes que pour les particules plus légères.

L'augmentation de la pression acoustique augmente le pic de résonance. Sous pressions acoustiques près de 1000 Pa le rayon de collision est 5 fois plus élèvé grace à l'influence du son à fréquence égale à celle de la bulle. L'approche de Lubimov D. V., Lubimova T.P. et Klimenko L.S. a donné la même augmentation du rayon de collision grace à l'influence du son, mais pour les pressions acoustiques beaucoup plus importantes.

CONCLUSION

On a étudié l'écoulement péristaltique du liquide dans le canal avec une onde donnée de pression sur les limites en cas des rapidités de la progression de l'onde et de nombre d'onde. On a obtenu les dépendances du débit du liquide des paramètres du problème. On a découvert, l'existence de la valeur maximale du débit du liquide, et cela on peut obtenir ne changeant pas les paramètres du problème.

On a étudié l'influence des vibrations longitudinales sur l'écoulement péristaltique avec une onde donnée à limite. On a constaté, que la plus haute influence de vibration est en cas de la coïncidence de la fréquence de l'onde de la pression et de la fréquence des vibrations. On a obtenu les conditions, quand les vibrations augmentent le débit du liquide et quand ils le diminuent.

On a étudié l'influence des pulsations transversales sur le transfert de matière sous influence de la chute de pression et de la force de gravité pour les liquides incompressibles en cas des fréquences finales des pulsations. On a trouvé qu'en cas des fréquences finales des pulsations, à la différence des recherches précédantes , qui ont étudié les cas finales des faibles fréquences, les pulsations mènent à diminution de consommation.

On a étudié l'influence de la compressibilité sur le mouvement du liquide dans le canal vertical sous l'influence de la force de gravité étant donné les parois des pulsations transversales. On a trouvé, que la compressibilité mène à l'apparition de la densité hétérogène, indépendante du temps dans le canal.

On a étudié l'influence du son sur interaction de la particule et du bouillon, émergent dans le liquide. On a trouvé, que le rayon de collision d'une bulle et d'une particule atteint son maximum sous la fréquence du son, égale à la fréquence propre des pulsations de la bulle. Influençant par le son, on peut augmenter la probabilité de capture des particules par les bulles, qui ont le rayon précis, dépendant de la fréquence de l'influence sonore.

2. PERISTALTIC FLOW

2.1. Review

The transport of fluid in vessels with traveling waves spreading over the surface of these vessels is called peristaltic. This kind of transport is fundamental for many biological systems, such as digestive and urinary tracts, that makes its analysis important to understand the reasons of the related deceases. The first studies conducted in 60s, 70s of the XX^{th} century were devoted to peristaltic transport of viscous Newtonian fluid in a channel and in a round pipe. A.H.Shapiro, M.Y. Jaffrine and S.L. Weinberg [1] looked at the solution of a linearized problem about peristaltic transport in the extreme case of infinitely long wave length. Later, linear solution was modified by M.Y. Jaffrine [2] to take small non-linear effects into account. He found the solution in the form of a series of small Reynolds number in a long wave approximation. The results of his research match the experiments conducted by S.L. Weinberg, E.C. Eckstein and A.H.Shapiro [3].

W.H. Lyne [4] studied a time-averaged pulsating flow and found a cellular flow structure. He assumed the vibration amplitude of walls to be small in comparison with the thickness of the boundary layer near the walls. A.Kaneko and H.Honji [5] continued his research and added the members of higher order, that helped them to study the cellular flow structure in details; the results of this research matched the experimental data. G.K. Russel [6] studied the flow structure and its ability to transport solid particles.

The works described above are devoted to the mechanical systems; at the same time the studies aimed at the development of organ models with fundamental peristaltic transport were conducted. P.S. Lykoudis and R. Roos [7] and Y.C. Fung [8] analyzed the work of ureter, pipe connecting kidney with urinary bladder. They had a particular interest in the pressure occurred at the closed end of this pipe. Together they solved the Navier-Stokes equation and the equation for the pipe membrane and concluded that a pressure gradient occurred due to the peristaltic waves is very small, and thus peristaltic waves are incapable to free ureter in case of its blockage. Their work also pointed out that peristaltic transport of a substance in a ureter occurred due to solitons, solitary waves, rather than sinusoidal waves, which are examined in many studies. A detailed analysis of a flow for solitary waves was carried out by J. Jimenez-Lozano [9]. His solution was presented in form of expansion of an amplitude of wall vibrations. Kh. S. Mekheimer [10] looked at the influence of the external magnetic field on peristaltic transport, where he used magnetic hydrodynamic approximation. This research was aimed at the development of physical basis for a method to cure urinary stone decease by magnetic fields. Later, Kh. S. Mekheimer in [11] accounted for the influence on the peristaltic transport of magnetic field occurred due to the fluid motion. Ureter blockage in dogs was studied by H.L. Kim et al. [12]. They observed vermicular motion of ureter, urine flow, hydronephrosis development (kidney decease caused by malfunctioning of urine flow), ureter expansion and movement of artificial stone, which was introduced into ureter between the second and forth lumbar vertebrae.

Besides peristaltic transport, the waves spreading over the vessel surface result in reflux (reverse motion) and the particle trapped by the flow. The first effect is that on average some Lagrange particles move backward the average flow rate, which is the reason of bacteria and toxic substances penetration into the kidney from the urinary bladder. This effect occurs after the

critical value of pressure drop is reached at the channel's ends [13, 14]. The trapping effect is when some Lagrange particles move at the wave velocity. The increase of flow rate results in the expansion of trapping area [15]. The changes in fluid flow direction on the whole with the preservation of the unchanged direction of the traveling wave is predicted for Ostwald–de Waele, Maxwell fluid and some other non-Newtonian fluids [16]. In case of a living organism this may result in retching.

The parameters affecting the peristaltic transport are the amplitude of the walls vibrations, wave number, pipe length and Reynolds number. The increase of the walls vibration amplitude results in the increase of flow rate [17, 18] and pump efficiency coefficient[17]. Friction force acting on the wall decreases [17, 18] and a longitudinal component of pressure gradient increases[19] with the increase of vibration amplitude. If the wave number increases, the flow rate increases first [20, 21, 22, 23], reaches the maximum peak, then starts to decrease [20, 21, 22] and then again to increase [20]. With the Reynolds number increase the flow rate decreases in case of large wave numbers [24], and in the case of small wave numbers it increases [24, 25]. Shun-Fa Khshchang and Yu-Shiuan Shiu [26] showed experimentally that the change of channel length does not result in the change of flow rate.

The influence of the geometry is revealed in the fact that under similar conditions flow rate appears to be less in a flat channel, than in a cylindrical tube [27]. The problem of peristaltic flows in divergence and convergence channels was looked at in [28]. Besides geometry the friction force and flow rate are influenced by the fluid properties: for example, in micropolar fluid the friction force acting on the channel wall is always lower than in the Newtonian fluid, and the flow rate is higher [29].

In biological systems and technical appliances with peristaltic mechanism of substance transfer there is often a pressure drop at the ends of the channel. This drop results in the fact that if a pressure gradient is directed opposite the direction of traveling waves, then in the porous media the flow rate is decreasing with the increase of the Darcy number [19]. The dependence of flow rate in case of varying pressure drop is of resonant nature, the flow rate is maximum when the pressure drop frequency at the channel's ends is equal to the frequency of the traveling waves [30].

The recent studies of peristaltic transport may be divided into six areas: peristaltic transport of the non-Newtonian fluids, peristaltic transport of multilayer fluid systems, influence of magnetic and gravitational fields, different inclusions in peristaltic flow, influence of wall properties on peristaltic transport.

2.1.1. Endoscope in peristaltic flow

Medicine often uses endoscope, which is an optical tool on a flexible tube to examine esophagus, urinary tract and gaster. It is clear that its presence results in significant changes of peristaltic flows in these organs. Typically endoscope is simulated by an endless tube. The increase of endoscope radius leads to the pressure drop decrease [70]. The article [71] states for fluid Jeffrey model that a growth rather than fall of pressure drop may be observed, in case endoscope has higher temperature that the temperature of the tube's walls. Also [71] argues that heat transfer coefficient from the surface of endoscope to the surface of tube decreases with the endoscope radius increase. The increase of temperature difference of endoscope and tube leads

to the growth of pressure drop [72]. Dependence of pressure drop on the difference of inclusions concentration in an endoscope and wall and the dependence of pressure drop on the temperature difference are qualitatively the same [72]. The paper [73] studied the influence of Sore parameter changes on the flow, and the findings were that its increase resulted in particles concentration growth in the space between endoscope and the walls. Friction force acting on the endoscope becomes stronger with the walls vibration amplitude increase and endoscope radius decrease [70, 72], while this force always remains less than the force acting on the tub walls [72, 74].

2.1.2. Peristaltic flow of non-Newtonian fluids

In biological systems lymph, urine, chyme and some other fluids are peristaltically transported. The publications [75, 76] prove that urine of a healthy person is a Newtonian fluid with 1.2-1.4 cP viscosity coefficient. With pathological states its properties may vary significantly resulting in significant viscosity increase. Chymus is typically considered to be a viscoelastic body, and it is approximated by the Oldroyd fluid [77, 78]. In an Oldroyd-B viscoelastic fluid, which is defined by an equation

$$\tau + \lambda_4\left(\frac{\partial \tau}{\partial t} + (\nabla\vec{u})\cdot\tau - \tau\cdot(\nabla\vec{u})^T\right) = \mu_1\left(A_1 + \lambda_5\left(\frac{\partial A_1}{\partial t} - (\nabla\vec{u})\cdot A_1 - A_1\cdot(\nabla\vec{u})^T\right)\right),$$

$$A_1 = (\nabla\vec{u}) + (\nabla\vec{u})^T$$

(where τ is the viscous stress tensor, $\lambda_{4,5}$ are material parameters), increase λ_4 and decrease λ_5 in Oldroyd-B fluid result in the increase in flow rate [80, 77].

The work [16] applied power Ostwald–de Waele model to describe chyme motion in intestine (depending on the value of parameters this model can behave as pseudoplastic, Newtonian or dilatant fluid). Ostwald–de Waele model in pseudoplastic limit is shown to be the most effective in peristaltic transport of fluid. Besides, it has been found that in pseudoplastic fluid the pressure wave length occurring due to peristaltic waves is twice shorter than the one in Newtonian and dilatant fluids.

The behavior of blood can be simulated by Hershel-Burkley [81, 82] and Kasson [83, 84] models. The publication [85] illustrates that the first model rather than the second one corresponds to the experiment's results.

Still, in most cases Kasson model is used to describe blood. Kasson model is defined by an equation:

$$\sqrt{\tau} = \sqrt{\tau_Y} + \sqrt{\eta\dot{\gamma}}\,.$$

If Kasson fluid is transported with peristaltic mechanism, the flow rate is lower than that for Newtonian fluid [84]. Connection between the pressure drop and flow rate for Kasson fluid is non-linear in contrast to Newtonian fluid [86].

Power model as well as a two-layer model with boundary fluid being Newtonian fluid and central part fluid being Kasson fluid are often used to describe blood behavior in small capillaries (with 0.02 cm and less in diameter) [87, 88, 89]. This approach is based on the fact that red blood cells in small vessels concentrate in the middle, while boundary layer has blood plasma only, which may be considered Newtonian fluid.

The work [90] states that flow velocity in reflux area increases with power parameter in Herschel-Bulkley law. Studies with Williamson fluid as a blood model show that Williamson number increase results in flow rate decrease [91].

Besides, Walter's B model of viscoelastic fluid is used to simulate blood flow. The increase of Walter's B liquid parameter characterizing its difference from Newtonian fluid (if it equals zero, then one obtains Newtonian fluid) leads to the decrease of pressure drop [70, 55]. For Jeffrey fluid with the equation –

$$\left[1+\lambda_1\frac{\partial}{\partial t}\right]\tau=\mu(\dot{\gamma}+\lambda_3\ddot{\gamma}),$$

the increase of λ_2 [63,73] and λ_1 [36] parameters results in the decrease of flow rate and efficiency of peristaltic pump [92]. For combined flow arisen from both pressure drop and traveling waves, if the pressure gradient is directed opposite the traveling wave propagation, there exists critical value of pressure drop, when the flow rate starts growing with λ_2 and λ_1 [92]. In Maxwell fluid an average velocity value decreases with the increase of relaxation time [93, 94], and with very large values of this parameter an average flow may become directed opposite the traveling wave propagation [93, 95]. The same change in fluid flow direction may be observed in Jeffrey fluid [95]. For power-law fluids the increase of power law index results in flow rate increase in most cases [59, 43, 37]. The work [46] looks at peristaltic transport of Burgers' fluid with an equation –

$$\left(1+\lambda_1\frac{\partial}{\partial t}+\lambda_2\frac{\partial^2}{\partial t^2}\right)\tau_{ji}=\mu(\dot{\gamma}+\lambda_3\ddot{\gamma}),$$

where τ is the tensor of viscous stress, $\lambda_{1,2,3}$ are material parameters. With either decrease λ_2 or increase of λ_1 and λ_3 parameters pressure drop decreases, while friction force acting on the tube wall increases. The work [54] looks at Eyring-Powell model, to which the following equation is applied –

$$\tau=\mu\dot{\gamma}+\frac{1}{\beta_1}\sinh^{-1}\left(\frac{1}{c_1}\dot{\gamma}\right),$$

where τ is the viscous stress tensor, β_1 and c_1 are material parameters. Pressure drop increases with c_1 and β_1. Friction force acting on the walls decreases with β_1.

The authors of the work [96] found that the increase of Weissenberg number for viscoelastic Sisko fluid leads to the increase of pressure drop [96]. For Johnson–Segalman fluid the work [98] states that flow rate increases with Weissenberg number. H. D. Ceniceros and J. E. Fisher found that large Weissenberg numbers have the threshold value for vibration amplitude; when this threshold value is reached, the increase of Weissenberg number results in flow rate decrease rather than its increase [99].

2.1.3. Peristaltic transport in porous and multilayered media

Porous media being simulated with Darcy law are also considered within the analysis of peristaltic transport, besides the motion of different non-Newtonian fluids. Darcy number decrease leads to the flow rate increase [90, 17, 57, 100, 70, 58, 71, 18], while the efficiency of peristaltic pump decreases [17], friction force acting on fluid from wall increases [100, 18], longitudinal component of pressure gradient increases [19]. Darcy number increase reduces reflux and removes the particle trapping effect [90, 44].

One more group of studies concentrates on peristaltic transport in multilayered media. R. Hemadri Reddy, et al. [101] studied the flow of fluid encased in a porous tube and came to the conclusion that the increase in thickness of porous layer resulted in the decrease of flow rate. With small values of flow rate the friction force acting on the walls grows with the thickness of porous layer, while with large values it drops [101]. The paper [41] looks at the case, when Newtonian fluid was near the walls, while the center of the channel was filled with micropolar fluid. When the layer of Newtonian fluid becomes thinner, this results in the increase of flow rate and friction force acting on the tube surface. The paper [102] considering a three-layer Newtonian fluid states that the increase of viscosity in the center and the decrease of viscosity of boundary fluid increase the flow rate. The decrease of viscosity of the fluid running between them also increases flow rate, but the effect is weak. The same effect is observed for the two-fluid model [27]. In a two-layer fluid with Kasson fluid in the center and Newtonian fluid near the walls the flow rate is always lower than in the case, when the boundary Newtonian fluid is removed [86]. In this two-layer fluid pressure drop and friction force acting on the walls decrease with viscosity of boundary layer [86].

2.1.4. Magnetic and gravitational field influence on peristaltic transport

Many biological fluids are conductive, and some papers analyze the peristaltic flow of fluid in ideal MHD approximation. Conductive fluids showed the increase of longitudinal component of pressure gradient [19], [59], pressure drop [92] and flow rate with the increase of Hartmann number [80, 100, 103, 58, 60, 104, 23]. Friction force acting on the fluid from the walls decreases, while Hartmann number increases until the threshold value [100, 10]. When the Hartmann number reaches the threshold value, the friction force starts to increase with Hartmann number [100]. The increase of external longitudinal magnetic field results in the increase of flow rate [105, 63], and the increase of a transverse magnetic field leads to the decrease [67]. With external magnetic field we may reduce the trapping area to zero [63].

If a tube with traveling waves on the surface is revolving around its axis, then this results in the increase of flow rate with the growth of rotation frequency [106]. Magnetic field directed along the tube axis intensifies this effect [106, 105].

In a gravitational field the increase of slope tube angle [68, 100, 63, 103, 11] and intensity of gravitational field [100, 98] results in the increase of flow rate, generated due to peristaltic waves. It reaches its maximum, if the direction of peristaltic wave propagation and the direction of gravity force match. The increase of slope angle leads to the expansion of trapping area [57].

2.1.5. Influence of temperature on peristaltic transport

If the channel's walls have different temperatures, increase of temperature difference expands the trapping area [47], reduces pressure drop [45] and flow rate [58]. When the temperature difference tends to zero, the temperature dependence on longitudinal coordinate tends to be linear, while in opposite case the profile of temperature turns towards the propagation of peristaltic wave, and for large temperature difference temperature at the channel's center appears to be higher than that of the walls [45, 73]. Gravitational field directed from the cold to hot wall creates the situation, when with Grashof number increase the trapping area of particles by peristaltic flow and position of the maximum of longitudinal velocity move to the warmer wall [45]. The increase of particles concentration shifts the maximum position of longitudinal velocity to cold wall [45]. With gravitational field directed towards traveling wave propagation and with pressure gradient directed backwards Grashof number increase grows the flow rate [58, 59, 71]. The increase in walls vibration amplitude and phase shift (if the original phase shift is the one, when the walls vibrate in counter-phase) results in the increase of the heat transfer from one wall to another [58].

2.1.6. Influence of compressibility on peristaltic transport

In case of compressible fluid, the equation of state should be included in system of Navier-Stokes equation. If we use the equation of state, such as

$$\frac{1}{\rho}\frac{\partial \rho}{\partial p} = k ,$$

where k is isothermal compressibility of liquid, then in case of Newtonian fluid [20, 107, 25] or Maxwell fluid [20] filled with a homogenous porous medium and typical Newtonian fluid, Maxwell fluid [95], [107] or Jeffrey fluid [95] flow rate increases with k, until the parameter k reaches threshold value, when flow rate starts to decrease. For very large relaxation times of Maxwell fluid the flow rate always increases with k [20], [22]. Fluid slip at the boundary results in the situation, when even with large relaxation times the dependence of flow rate on k is bell-shaped [22]. In Newtonian fluid in case of large values of parameter k the flow rate decreases with the increase of Reynolds number, but in case of small or zero value of isothermal compressibility k, the flow rate increases with Reynolds number [95]. In Maxwell fluid at large values of parameter k fluid moves backward the direction of traveling wave propagation [22, 107, 108].

2.1.7. Influence of wall properties on peristaltic transport

In biological systems the wall motion is determined by the work of smooth muscle, meaning that true-to-life description need complicated models, which accounts for properties of muscles. In [31] the model for the coupled problem of wall deformation and fluid flow, based on thin-shell and lubrication theories, and driven by a propagating wave of smooth muscle activation, is proposed for peristaltic pumping in the ureter. D. Takagi [32] used a significantly simpler approach based on the equation for pressure

$$p\big|_{r=R+\xi} = K\frac{\partial^n}{\partial z^n}\xi + \alpha\cos(t-y),$$

where r is the vessel radius at a particular point , and R is the parameter characterizing an average wall position, ξ - wall displacement.

The case $n=0$ corresponds to a linear elasticity of tube, and the case $n=4$ corresponds to a thin shell of bending stiffness $K = h^3E/12(1-\varpi^2)$, where h is the shell thickness, E - the Young modulus and ϖ the Poisson ratio. Additive $\alpha\cos(t-y)$ corresponds to eternal force acting on the vessel surface. The tube is divided into two parts: an occluded region and a peak region. Transverse size of peak increases, while longitudinal size decreases with amplitude α growth.

Later D. Tagaki, et al. [33] studied the behavior of inclusions in peristaltic transport. They have proved that infinite rigid rod located at the center of tube cannot be dislocated by some value of the pointlike external force. Finite-sized particles have been found to have threshold value of pointlike force, at the value above this one the particles velocity equals the wave velocity (this is a well-known trapping effect). The threshold value of force increases with the displacement of particle from the channel centerline. S.K. Pandey and M.K. Chaube [34] studied the flow in a channel with the dynamic boundary conditions proposed in [35] and specified in the form of

$$p\big|_{x=h+\xi} = \left[m\frac{\partial^2}{\partial t^2} + d\frac{\partial}{\partial t} + B\frac{\partial^4}{\partial x^4} - T\frac{\partial^2}{\partial x^2} + K_1\right]\xi + \alpha\cos\frac{2\pi}{\lambda}(y-ct),$$

where m is the wall mass per unit area, d is the wall damping coefficient, K_1 is the spring stiffness, T is the longitudinal tension per unit width, B is the flexural rigidity of the wall. They also set the law of wall motion as

$$\xi = \Xi\cos\frac{2\pi}{\lambda}(x-ct).$$

For the Newtonian fluid this number of boundary conditions is excessive, but S.K. Pandey and M.K. Chaube [34] analyzed the non-Newtonian fluid, with differential equation of forth order:

$$\frac{\partial \mathrm{u}}{\partial t} + (\vec{\mathrm{u}}\cdot\nabla)\vec{\mathrm{u}} = -\frac{\nabla \mathrm{p}}{\rho} + \nu\nabla^2\vec{u} + \nu_1\nabla^4\vec{u}.$$

The diagrams in [34] make us conclude that the increase of wave number results in the increase of average velocity of fluid, then in its decrease. The growth of K and T, viscosity ν decrease lead to increase of average velocity of fluid. The growth of d and ν_1 results in the velocity decrease, and at large values of these parameters the fluid on average moves to the direction opposite the spread of traveling wave. In [36] in their research of peristaltic transport of the Jeffrey fluid T. Hayat, et al. used the same boundary conditions as S.K. Pandey and M.K. Chaube in [34]. In this case one boundary condition is excessive (for the Jeffrey fluid the second Newton law is a differential equation of second order), however, by using analytical methods they found the solution satisfying all boundary conditions. The results of T.Hayat, et al. [36]

stating that the increase of K, T and m leads to the increase of average velocity of fluid, support the results of S.K. Pandey and M.K. Chaube [34]. Later in their research of power-law fluid flow T.Hayat and M. Javed [37] didn't use the slip boundary condition. As a result, they have found out that the increase of all wall characterizing parameters m, d, K and T leads to the growth of flow rate (according to [34] the increase of a parameter d, characterizing the loss of the energy due to wall deformation, results in the decrease of flow rate). Wirth zero coefficients B and K in a boundary condition from the article S.K. Pandey and M.K. Chaube [34], A.V. Ramana-Kumari and G. Radhakrishnamacharya in [38] used it to study peristaltic transport of the Newtonian fluid. They could not set three conditions at the boundary, that is why they didn't use the zero equality condition for normal component of the fluid velocity. This choice of the boundary conditions was not somehow explained. They have found that just like in [34] the increase of the d, T and m parameters led to the increase of flow rate. Later G. Radhakrishnamacharya and G. C. Sankad in [39], D. Srinivasacharya and C. Srinivasulu in [40] and K.M. Prasad in [41] carried out a research within the framework of the approach (used by T. Hayat and M. Javed in [37]) without no-slip boundary condition. Their results supported the conclusions made by T. Hayat and M. Javed in [37]. G. Radhakrishnamacharya, et al. also found that the increase of the T [39, 41], d and m [40] parameters resulted in the increase of trapping area size. Besides, they found that at the increase of parameter T the value of wall vibration amplitude with reflux disappearing decreased [40]. P. Muthu, et al. [42] analyzed the micropolar fluid and set the same boundary conditions as in case of T. Hayat in [37]. They found out that m decrease resulted in the flow rate decrease. They also found that at large values of parameter d the trapping region appeared near the wall.

No-slip boundary condition is an assumption that could, in theory, be violated. The slip length is the main parameter which describes the breakdown of the no-slip condition. With the slip length increase the flow rate and efficiency of peristaltic transport decrease [17, 44], delivery pressure falls [45, 46], and the area of the reverse fluid flow (reflux) expands [47]. Besides, the increase of slip length results in the decrease of trapping area [47]. The influence of the slip on the flow in magnetohydrodynamic approximation was looked at for the symmetrical channel in [48, 49] and for asymmetrical one in [50, 51]. E.F. Elshehawey, et al. in [52] used boundary condition of Saffman in their study of slip effect on peristaltic flows:

$$R\frac{\partial u}{\partial y} = -\frac{\alpha_1}{\sqrt{\mathrm{Da}}}u \text{, if } y = \pm\left[R + \Xi\sin\frac{2\pi}{\lambda}(x - ct)\right],$$

(where R is the average channel radius, α_1 is the slip parameter, Da is the Darcy number, u is the longitudinal fluid velocity, Ξ is the amplitude of wall vibration). They found that the increase of slip parameter α_1 led to the decrease of flow rate, while Darcy number increased.

The shape of the wave running over the walls surface influences significantly the peristaltic flows. In [53, 54] the effects of sinusoidal waves and waves with square, triangle and trapezoid ridges were compared. It was shown that the trapping area was the smallest one for the waves with triangle ridges. The same result was reached at in [55, 56]. For the waves with square ridges the flow rate appeared to be the least, and the friction force acting on the walls was the strongest [54]. In [55] it was found that the situation changed for the opposite one in Sisko fluid: waves with triangle ridges caused the largest friction force and the least pressure rise, and the waves with square ridges caused the least friction force and the highest pressure rise. If the walls

change their coordinate by harmonic law, the largest value of flow rate could be observed at antiphase vibrations, and the smallest value could be seen at in-phase vibrations [57, 58, 59, 60, 37, 61, 62, 63]. Also in [61] it was revealed that the changes of phase shift could suppress reflux and reduce the trapping area.

In this chapter of the thesis, the law of wall's coordinate variation isn't determined a priori. It is found from the initially definite law of pressure-variation on the wall. This way is based on the fact that some hollow organs change diameter under the signals of baroreceptors (sensors that detects the pressure). We studied the effects of various parameters on flow rate and structure of flow. Besides we studied the influence of vibration on the peristaltic flow under long wave approximation.

2.2. Pressure-driven peristaltic flow

2.2.1. Problem Statement

Boundary conditions. Force acting on the element of channel's wall surface from the fluid is defined by a formula

$$P_i = pn_i - \eta\left(\frac{\partial \mathrm{v}_i}{\partial x_k} + \frac{\partial \mathrm{v}_k}{\partial x_i}\right)n_k = pn_i - \eta\left(\frac{\partial \mathrm{v}_i}{\partial x} + \frac{\partial \mathrm{v}_x}{\partial x_i}\right)n_x - \eta\left(\frac{\partial \mathrm{v}_i}{\partial y} + \frac{\partial \mathrm{v}_y}{\partial x_i}\right)n_y, \qquad (2.1)$$

where x and y are transverse and longitudinal coordinates, p is the pressure, η is the dynamic viscosity, v_i is the fluid velocity, n_k is normal to surface. If the channel's wall position is set by an equation

$$x = h + \xi(y,t), \qquad (2.2)$$

then normal to it is defined by an expression

$$\vec{n} = \left(\frac{1}{\sqrt{1+\xi'^2}}, -\frac{\xi'}{\sqrt{1+\xi'^2}}\right). \qquad (2.3)$$

By substituting (2.3) in (2.1), we get

$$P_x = \frac{p}{\sqrt{1+\xi'^2}} - \eta\frac{2}{\sqrt{1+\xi'^2}}\frac{\partial \mathrm{v}_x}{\partial x} + \frac{\xi'\eta}{\sqrt{1+\xi'^2}}\left(\frac{\partial \mathrm{v}_x}{\partial y} + \frac{\partial \mathrm{v}_y}{\partial x}\right), \qquad (2.4)$$

$$P_y = -\frac{\xi' p}{\sqrt{1+\xi'^2}} - \eta\left(\frac{\partial \mathrm{v}_y}{\partial x} + \frac{\partial \mathrm{v}_x}{\partial y}\right)\frac{1}{\sqrt{1+\xi'^2}} + \frac{2\xi'\eta}{\sqrt{1+\xi'^2}}\frac{\partial \mathrm{v}_y}{\partial y}. \qquad (2.5)$$

The force acts on the surface along OX axis

$$P_x = -\kappa(p - \alpha\cos\frac{ct-y}{\lambda}). \qquad (2.6)$$

The force (2.6) tends to change the walls position, so that the pressure at the boundary becomes equal to $\alpha\cos\frac{ct-y}{\lambda}$. By substituting (2.6) in (2.4), we get

$$-\kappa(p - \alpha\cos\frac{ct-y}{\lambda}) = \frac{1}{\sqrt{1+\xi'^2}}\left[p - 2\eta\frac{\partial \mathrm{v}_x}{\partial x} + \xi'\eta\left(\frac{\partial \mathrm{v}_x}{\partial y} + \frac{\partial \mathrm{v}_y}{\partial x}\right)\right]. \qquad (2.7)$$

The walls can't move along the axis OY, that is why the second equation (2.5) does not give any new boundary condition. Present study looks at the case $\kappa \to \infty$, here with pressure deviation from the specified pressure a very strong force is generated, so all the other forces may be neglected. In extreme case $\kappa \to \infty$ the equation (2.7) becomes as follows:

$$p = \alpha\cos\frac{ct-y}{\lambda}. \qquad (2.8)$$

D. Tahaki [32] instead (2.8) specified condition at the tube walls (he analyzed a three-dimensional tube rather than a two-dimensional channel)

$$p\big|_{r=h+\xi} = K\frac{\partial^n}{\partial z^n}\xi + \alpha\sin\frac{2\pi}{\lambda}(y-ct), \tag{2.9}$$

where r is the vessel radius dependent on coordinate y, h is average position of walls and ξ is deviation from its average position. Condition set by D. Tagaki differs from (2.8) with a summand $K\frac{\partial^n}{\partial z^n}\xi$, which was introduced to simulate the influence of wall properties. D. Tagaki examined the extreme case of small wave numbers and wave propagation velocities. Present chapter aims to find more general solution for random wave numbers and wave propagation velocities .

Besides dynamic boundary condition (2.8) used in this research, the walls are defined by kinematic condition as well:

$$x = \pm h \pm \xi: \quad \mathrm{v} = \pm\frac{\partial\xi}{\partial t}, \quad \mathrm{u} = 0, \quad p = a\cos\frac{1}{\lambda}(ct-y). \tag{2.10}$$

where u and v are transverse and longitudinal velocities, x is the transverse coordinate, h is the average position of walls, and ξ is deviation from this average position.

System of equations. Navier-Stokes equation underlies the fluid behavior simulation for incompressible fluid:

$$\frac{\partial \mathrm{v}}{\partial t} + \mathrm{v}\frac{\partial \mathrm{v}}{\partial x} + \mathrm{u}\frac{\partial \mathrm{v}}{\partial y} + \frac{1}{\rho}\frac{\partial \mathrm{p}}{\partial x} - \nu\left(\frac{\partial^2 \mathrm{v}}{\partial x^2} + \frac{\partial^2 \mathrm{v}}{\partial y^2}\right) = 0, \tag{2.11}$$

$$\frac{\partial \mathrm{u}}{\partial t} + \mathrm{v}\frac{\partial \mathrm{u}}{\partial x} + \mathrm{u}\frac{\partial \mathrm{u}}{\partial y} + \frac{1}{\rho}\frac{\partial \mathrm{p}}{\partial y} - \nu\left(\frac{\partial^2 \mathrm{u}}{\partial x^2} + \frac{\partial^2 \mathrm{u}}{\partial y^2}\right) = 0, \tag{2.12}$$

$$\frac{\partial \mathrm{v}}{\partial x} + \frac{\partial \mathrm{u}}{\partial y} = 0. \tag{2.13}$$

Dimensional parameter of a problem is half of the distance between the walls h, half of channel length L', length λ and propagation velocity c of pressure wave at the walls, fluid density ρ, pressure vibration amplitude on the wall a, kinematic viscosity ν.

To get dimensionless parameters let us introduce the measurement units. Axis transverse coordinate x is measured in h, longitudinal coordinate y – in λ, time t – in λ/c, pressure p – in ρc^2, longitudinal velocity u – in c, transverse velocity v – in ch/λ, deviation from average position of wall ξ – in h. As a result, equations (2.11)-(2.13) and boundary conditions (2.10) become as follows:

$$\delta^2\left(\frac{\partial \mathrm{v}}{\partial t} + \mathrm{v}\frac{\partial \mathrm{v}}{\partial x} + \mathrm{u}\frac{\partial \mathrm{v}}{\partial y}\right) + \frac{\partial \mathrm{p}}{\partial x} - \frac{\delta}{C}\left(\frac{\partial^2 \mathrm{v}}{\partial x^2} + \delta^2\frac{\partial^2 \mathrm{v}}{\partial y^2}\right) = 0, \tag{2.14}$$

$$\delta\left(\frac{\partial \mathrm{u}}{\partial t}+\mathrm{v}\frac{\partial \mathrm{u}}{\partial x}+\mathrm{u}\frac{\partial \mathrm{u}}{\partial y}+\frac{\partial \mathrm{p}}{\partial y}\right)-\frac{1}{C}\left(\frac{\partial^2 \mathrm{u}}{\partial x^2}+\delta^2\frac{\partial^2 \mathrm{u}}{\partial y^2}\right)=0, \tag{2.15}$$

$$\frac{\partial \mathrm{v}}{\partial x}+\frac{\partial \mathrm{u}}{\partial y}=0, \tag{2.16}$$

$$x=\pm 1\pm\xi:\quad \mathrm{v}=\pm\frac{\partial \xi}{\partial t},\quad \mathrm{u}=0,\quad \mathrm{p}=A\cos\left(t-y\right). \tag{2.17}$$

Problem is characterized by four dimensionless parameters: dimensionless velocity of wave propagation $C=hc/\nu$, wave number $\delta=h/\lambda$, channel length $L=L'/\lambda$ and dimensionless amplitude of pressure vibration on the wall $A=a/(\rho c^2)$.

2.2.2. Solution in small-amplitude approximation

Let us consider the case of small amplitude of pressure variation on the walls. We are going to find the solution in the power series of small parameter A:

$$\mathrm{v}=A\mathrm{v}_1+A^2\mathrm{v}_2+...,\ \mathrm{u}=A\mathrm{u}_1+A^2\mathrm{u}_2+..., \tag{2.18}$$

$$\mathrm{p}=A\mathrm{p}_1+A^2\mathrm{p}_2+...,\ \xi=A\xi_1+A^2\xi_2+.... \tag{2.19}$$

System of equations. Assigning to new variables

$$\begin{cases} x'=x/(1+\xi) \\ y'=y \\ t'=t \end{cases}, \tag{2.20}$$

we get boundary conditions (2.17) in the form

$$x'=\pm 1:\mathrm{v}=\pm\frac{\partial \xi}{\partial t'},\quad \mathrm{u}=0,\quad \mathrm{p}=A\cos\left(t'-y'\right), \tag{2.21}$$

and equations (2.14)–(2.16) in the form

$$\begin{aligned}\frac{\partial \mathrm{u}}{\partial t'}=&\frac{a^2+\delta^2q^2}{C\delta}\frac{\partial^2 \mathrm{u}}{\partial x'^2}+\left(\kappa-\mathrm{v}a-\mathrm{u}q\right)\frac{\partial \mathrm{u}}{\partial x'}\\&+2\frac{\delta q}{C}\frac{\partial^2 \mathrm{u}}{\partial x'\partial y'}-u\frac{\partial \mathrm{u}}{\partial y'}+\frac{\delta}{\mathrm{Re}}\frac{\partial^2 \mathrm{u}}{\partial y'^2}-q\frac{\partial \mathrm{p}}{\partial x'}-\frac{\partial \mathrm{p}}{\partial y'},\end{aligned} \tag{2.22}$$

$$\begin{aligned}\frac{\partial \mathrm{v}}{\partial t'}=&\frac{a^2+\delta^2q^2}{C\delta}\frac{\partial^2 \mathrm{v}}{\partial x'^2}+\left(\kappa-\mathrm{v}a-\mathrm{u}q\right)\frac{\partial \mathrm{v}}{\partial x'}\\&+2\frac{\delta q}{C}\frac{\partial^2 \mathrm{v}}{\partial x'\partial y'}-\mathrm{u}\frac{\partial \mathrm{v}}{\partial y'}+\frac{\delta}{\mathrm{Re}}\frac{\partial^2 \mathrm{v}}{\partial y'^2}-\frac{a}{\delta^2}\frac{\partial \mathrm{p}}{\partial x'},\end{aligned} \tag{2.23}$$

$$a\frac{\partial \mathrm{v}}{\partial x'}+q\frac{\partial \mathrm{u}}{\partial x'}+\frac{\partial \mathrm{u}}{\partial y'}=0. \tag{2.24}$$

where

$$q_* = a\left[2a\left(\frac{\partial\xi}{\partial y}\right)^2 - \xi''\right]x', \qquad a = \frac{1}{1+\xi},$$

$$\kappa = -ax'\left(\delta\frac{\dfrac{\partial^2\xi}{\partial y^2} - 2a\left(\dfrac{\partial\xi}{\partial y}\right)^2}{\mathrm{Re}} + \mathrm{v}\big|_{x=-1}\right), \quad q = -a\frac{\partial\xi}{\partial y}x'. \tag{2.25}$$

First-order solution. First-order problem (2.21) - (2.24) takes the form

$$\delta^2\frac{\partial \mathrm{v}_1}{\partial t} + \frac{\partial \mathrm{p}_1}{\partial x} = \frac{\delta}{C}\left(\frac{\partial^2 \mathrm{v}_1}{\partial x^2} + \delta^2\frac{\partial^2 \mathrm{v}_1}{\partial y^2}\right), \tag{2.26}$$

$$\delta C\left(\frac{\partial \mathrm{u}_1}{\partial t} + \frac{\partial \mathrm{p}_1}{\partial y}\right) = \frac{\partial^2 \mathrm{u}_1}{\partial x^2} + \delta^2\frac{\partial^2 \mathrm{u}_1}{\partial y^2}, \tag{2.27}$$

$$\frac{\partial \mathrm{v}_1}{\partial x} + \frac{\partial \mathrm{u}_1}{\partial y} = 0, \tag{2.28}$$

$$x = \pm 1: \quad \mathrm{v}_1 = \pm\frac{\partial\xi_1}{\partial t}, \quad \mathrm{u}_1 = 0, \quad \mathrm{p}_1 = \cos(t-y). \tag{2.29}$$

With the variables

$$\chi_1 = \sqrt{\frac{\delta}{2}}\sqrt{\sqrt{\delta^2+C^2}+\delta}, \ \omega_1 = \sqrt{\frac{\delta}{2}}\sqrt{\sqrt{\delta^2+C^2}-\delta},$$

$$C_1 = -\frac{\sinh\chi_1\sin\omega_1}{\cos^2\omega_1 + \sinh^2\chi_1}, \ C_2 = -\frac{\cosh\chi_1\cos\omega_1}{\cos^2\omega_1 + \sinh^2\chi_1},$$

we write the solution of equation system(2.26)-(2.29) in the form

$$\begin{aligned}\mathrm{v}_1 = {} & \frac{\cosh\chi_1 x\sin\omega_1 x}{\chi_1^2+\omega_1^2}\left[(\omega_1 C_1 - \chi_1 C_2)\cos(t\text{ - }y) - (\omega_1 C_2 + \chi_1 C_1)\sin(t\text{ - }y)\right] \\ & - \frac{\sinh\delta x}{\delta\cosh\delta}\sin(t\text{ - }y) + \frac{\sinh\chi_1 x\cos\omega_1 x}{\chi_1^2+\omega_1^2}\left[(\chi_1 C_1 + \omega_1 C_2)\cos(t\text{ - }y) + \right. \\ & \left. - (\chi_1 C_2 - \omega_1 C_1)\sin(t\text{ - }y)\right]\end{aligned} \tag{2.30}$$

for the transverse velocity,

$$\begin{aligned}\mathrm{u}_1 = {} & \frac{\cosh\delta x}{\cosh\delta}\cos(t\text{ - }y) + \sinh\chi_1 x\sin\omega_1 x\left[C_1\cos(t\text{ - }y) - C_2\sin(t\text{ - }y)\right] + \\ & + \cosh\chi_1 x\cos\omega_1 x\left[C_2\cos(t\text{ - }y) + C_1\sin(t\text{ - }y)\right]\end{aligned} \tag{2.31}$$

for longitudinal velocity,

$$p_1 = \cosh(\delta x)\cos(t-y)/\operatorname{ch}\delta \tag{2.32}$$

for pressure,

$$\xi_1 = \frac{\cosh\chi_1 \sin\omega_1}{\chi_1^{\,2}+\omega_1^{\,2}}\left[(\omega_1 C_1 - \chi_1 C_2)\sin(t\text{ - }y)+(\omega_1 C_2 + \chi_1 C_1)\cos(t\text{ - }y)\right]$$
$$+\frac{\sinh\delta}{\delta\cosh\delta}\cos(t\text{ - }y)+\frac{\sinh\chi_1\cos\omega_1}{\chi_1^{\,2}+\omega_1^{\,2}}\left[(\chi_1 C_1+\omega_1 C_2)\sin(t\text{ - }y)+\right. \tag{2.33}$$
$$\left.+(\chi_1 C_2-\omega_1 C_1)\cos(t\text{ - }y)\right].$$

for deviation from average position.

Expanding (2.33) into power series of wave number, we get

$$\xi_1 = -\frac{C\delta}{3}\sin(t-y)+O(\delta^2). \tag{2.34}$$

D. Tagaki [32] received in first order by A for ξ expression which has the following form:

$$\xi_1 = -2\pi C\delta\frac{16\cos(y-t)-K\sin(y-t)}{16^2+K^2}. \tag{2.35}$$

At $K=0$ expressions (2.35) and (2.34) differ in numerical coefficient, this being connected with difference in problem geometry: D. Tagaki studied a tube rather than a channel. They also differ in a phase, that is connected with different phase in boundary conditions on pressure (2.9) and (2.17). For phases to match one should make transformation $t\to t-\frac{\pi}{2}$ in (2.35). The dependences on the parameters in (2.35) and in (2.34) are qualitatively the same.

Averaged profile of flow. The equations in the second order are cumbersome and as result we haven't found the solution for the order higher than the first order in an explicit form. However, with the first-order solution we may calculate an average value of longitudinal velocity u_2 in the second order. In this case we should time-average Navier-Stokes equation for longitudinal velocity component u_2 in the second order of A:

$$\frac{\partial \mathrm{u}_2}{\partial t}-x\frac{\partial\xi_1}{\partial y}\frac{\partial p_1}{\partial x}+\frac{\partial p_2}{\partial y}+\mathrm{u}_1\frac{\partial \mathrm{u}_1}{\partial y}+\frac{x\delta}{C}\frac{\partial^2\xi_1}{\partial y^2}\frac{\partial \mathrm{u}_1}{\partial x}-\frac{1}{C\delta}\frac{\partial^2\mathrm{u}_2}{\partial x^2}+$$
$$+\frac{2\xi_1}{C\delta}\frac{\partial^2\mathrm{u}_1}{\partial x^2}+\frac{2x\delta}{C}\frac{\partial\xi_1}{\partial y}\frac{\partial^2\mathrm{u}_1}{\partial x\partial y}+\mathrm{v}_1\frac{\partial \mathrm{u}_1}{\partial x}-\frac{\delta}{C}\frac{\partial^2\mathrm{u}_2}{\partial y^2}+x\frac{\partial \mathrm{u}_1}{\partial x}\left(\mathrm{v}_1\big|_{x=-1}\right)=0. \tag{2.36}$$

First-order solution depends on $(t-y)$, rather than on t time and y coordinate separately. Let us consider that the second-order solution will also depend on $(t-y)$ only. With this we may transform the equation (2.36) into

$$\frac{\partial \mathrm{u}_2}{\partial t}-x\frac{\partial\xi_1}{\partial y}\frac{\partial p_1}{\partial x}-\frac{\partial p_2}{\partial t}-\mathrm{u}_1\frac{\partial \mathrm{u}_1}{\partial t}+\frac{x\delta}{C}\frac{\partial^2\xi_1}{\partial y^2}\frac{\partial \mathrm{u}_1}{\partial x}-\frac{1}{C\delta}\frac{\partial^2\mathrm{u}_2}{\partial x^2}+$$
$$+\frac{2\xi_1}{C\delta}\frac{\partial^2\mathrm{u}_1}{\partial x^2}+\frac{2x\delta}{C}\frac{\partial\xi_1}{\partial y}\frac{\partial^2\mathrm{u}_1}{\partial x\partial y}+\mathrm{v}_1\frac{\partial \mathrm{u}_1}{\partial x}-\frac{\delta}{C}\frac{\partial^2\mathrm{u}_2}{\partial t^2}+x\frac{\partial \mathrm{u}_1}{\partial x}\left(\mathrm{v}_1\big|_{x=-1}\right)=0. \tag{2.37}$$

Time averaged summands $\frac{\partial \mathrm{u}_2}{\partial t}$, $\frac{\partial \mathrm{p}_2}{\partial t}$, $\frac{\partial^2\mathrm{u}_2}{\partial t^2}$, $\mathrm{u}_1\frac{\partial \mathrm{u}_1}{\partial t}$ are zero. If that was not the case, then velocity, its square or pressure would grow up infinitely. As a result, equation for time-averaged velocity component $\bar{\mathrm{u}}_2$ takes the form

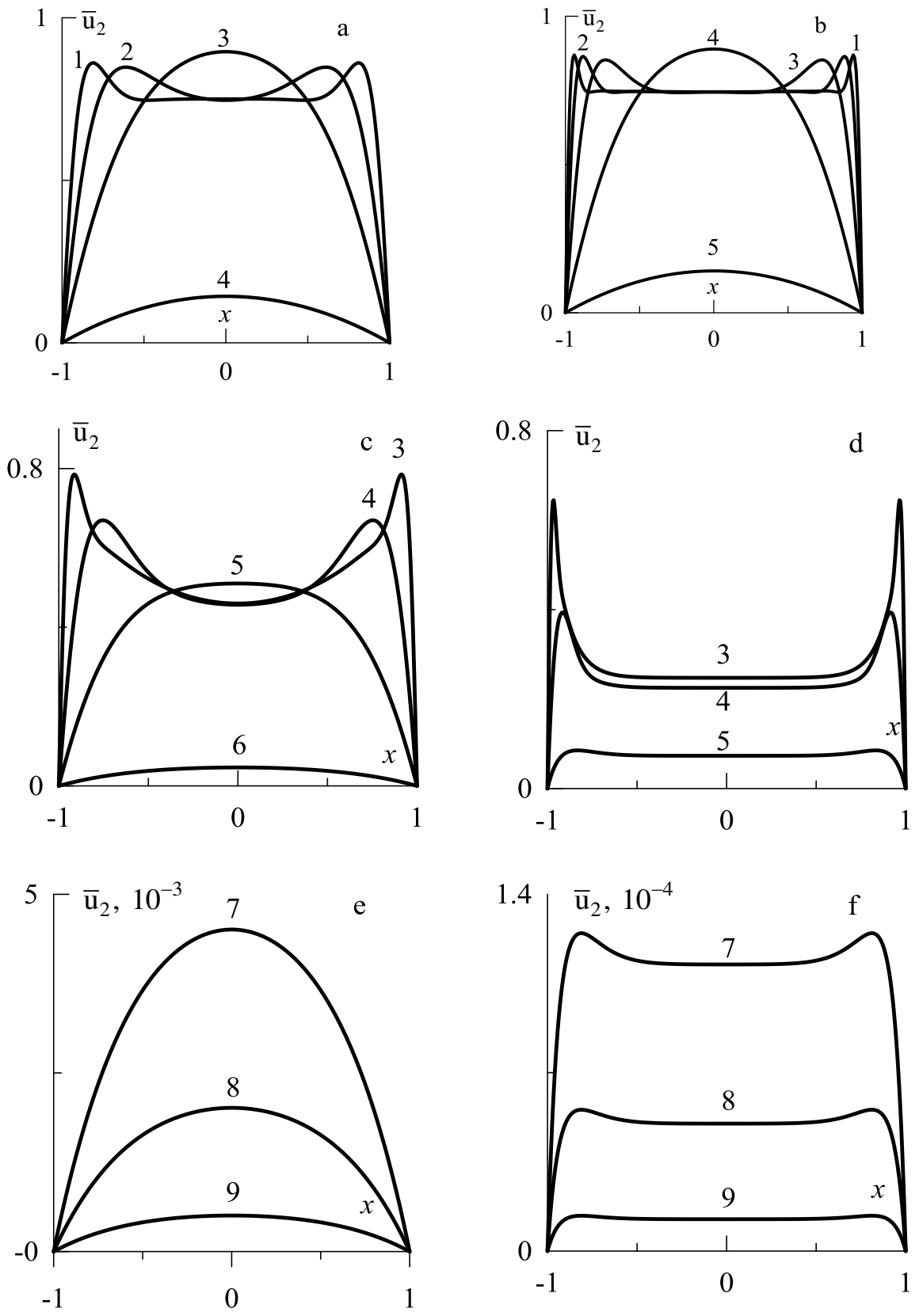

Fig. 2.1. Dependency of time-averaged longitudinal velocity on transverse coordinate for $\delta = 0.01$ (a), $\delta = 0.1$ (b), $\delta = 1$ (c, e), $\delta = 10$ (d, f) and for $C = 20000$ (1), $C = 5000$ (2), $C = 1000$ (3), $C = 100$ (4), $C = 10$ (5), $C = 1$ (6), $C = 0.3$ (7), $C = 0.2$ (8), $C = 0.1$ (9)

$$\frac{1}{C\delta}\frac{\partial^2 \mathrm{u}_2}{\partial x^2} = -x\frac{\partial \xi_1}{\partial y}\frac{\partial p_1}{\partial x} + \frac{x\delta}{C}\frac{\partial^2 \xi_1}{\partial y^2}\frac{\partial \mathrm{u}_1}{\partial x} + \frac{2\xi_1}{C\delta}\frac{\partial^2 \mathrm{u}_1}{\partial x^2} + \\ + \frac{2x\delta}{C}\frac{\partial \xi_1}{\partial y}\frac{\partial^2 \mathrm{u}_1}{\partial x \partial y} + \mathrm{v}_1\frac{\partial \mathrm{u}_1}{\partial x} + x\frac{\partial \mathrm{u}_1}{\partial x}\left(\mathrm{v}_1\big|_{x=-1}\right), \tag{2.38}$$

where dash denotes time-averaging. By time averaging (2.38), then integrating the expression twice by x, we get

$$\overline{\mathrm{u}}_2 = c_1 + c_2 x + \frac{C\delta}{2\pi}\iiint_0^{2\pi}\left(-x\frac{\partial \xi_1}{\partial y}\frac{\partial p_1}{\partial x} + \frac{x\delta}{C}\frac{\partial^2 \xi_1}{\partial y^2}\frac{\partial \mathrm{u}_1}{\partial x} + \frac{2\xi_1}{C\delta}\frac{\partial^2 \mathrm{u}_1}{\partial x^2}\right. \\ \left. + \frac{2x\delta}{C}\frac{\partial \xi_1}{\partial y}\frac{\partial^2 \mathrm{u}_1}{\partial x \partial y} + \mathrm{v}_1\frac{\partial \mathrm{u}_1}{\partial x} + x\frac{\partial \mathrm{u}_1}{\partial x}\mathrm{v}_1\big|_{x=-1}\right) dt dx dx \tag{2.39}$$

Constants c_1 and c_2 are identified from the conditions at the boundary:

$$x = \pm 1:\ \overline{\mathrm{u}}_2 = 0. \tag{2.40}$$

Fig. 2.1 shows the profile of time-averaged longitudinal velocity $\overline{\mathrm{u}}_2$ in the second order (in the first order time-averaged longitudinal velocity equals zero). Velocity $\overline{\mathrm{u}}_2$ increases with δ decrease and increase of wave velocity C. At small velocities of wave propagation C the profile of longitudinal velocity is bell shaped with maximum at the channel center (Fig.2.1a: curves 3 and 4). With the increase of wave propagation velocity plateau occurs in the central part and boundary layers near the walls (Fig.2.1a: curves 1 and 2, and Fig.2.1e-f). Boundary layer thickens with C and δ increase, while the area with nearly constant average velocity expands in the central part.

Flow rate. Fluid transport is characterized by its flow rate: volume of fluid flowing through transverse section of a channel in a unit time. Expression for time-averaged flow rate in original

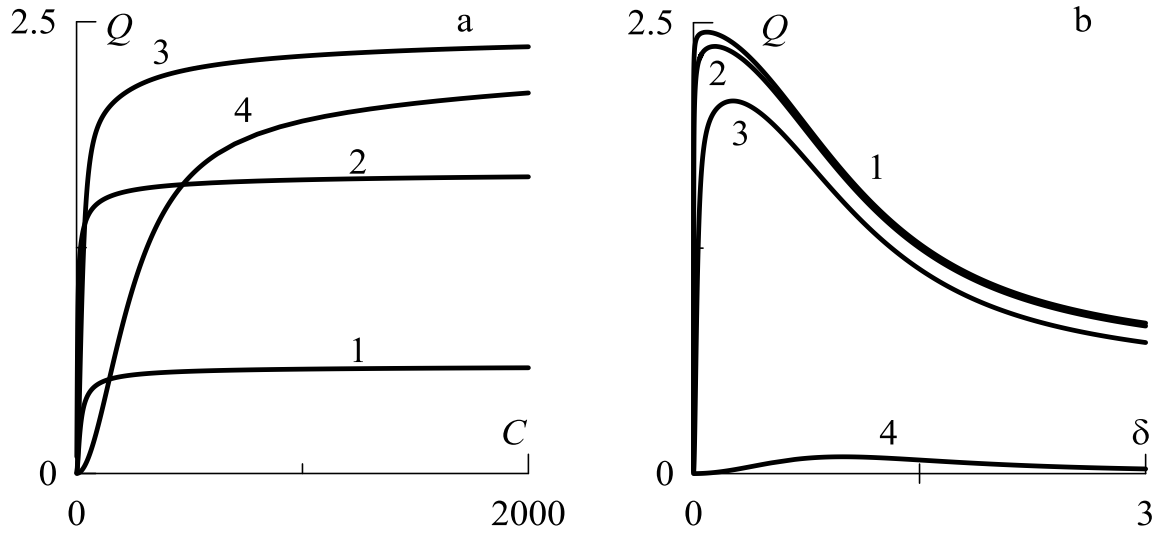

Fig. 2.2. Flow rate dependency on a: wave velocity C for $\delta = 0.01$ (1), $\delta = 0.1$ (2), $\delta = 1$ (3), $\delta = 10$ (4), and b: wave number δ for $C = 20000$ (1), $C = 2000$ (2), $C = 100$ (3), $C = 1$ (4)

untransformed (unshaded (2.20)) coordinate system takes the form

$$Q = \frac{1}{2\pi} \int_0^{2\pi} \int_{-1-\xi}^{1+\xi} \mathrm{u} dx dt. \tag{2.41}$$

After transformation to shaded coordinates the expression for flow rate takes the form

$$Q = \frac{1}{2\pi} \int_0^{2\pi} \int_{-1}^{1} \mathrm{u}(1+\xi) dx' dt'. \tag{2.42}$$

By substituting power series (2.18) in (2.42), we obtain a formula for flow rate in the second order by A:

$$Q_2 = \frac{1}{2\pi} \int_0^{2\pi} \int_{-1}^{1} (\mathrm{u}_2 + \mathrm{u}_1 \xi_1) dx' dt'. \tag{2.43}$$

Fig. 2.2 represents the dependency of flow rate on problem parameters. Rate dependency on wave number is non-monotonous; there is maximum value of flow rate, which may be reached by changing the problem parameters. It approximately equals 2.5, which corresponds to velocity of order 10^{-3} m/s for water in a centimeter channel. Flow rate grows with wave propagation velocity and at large values of C it reaches horizontal asymptote, which is explained by the formation of boundary layers.

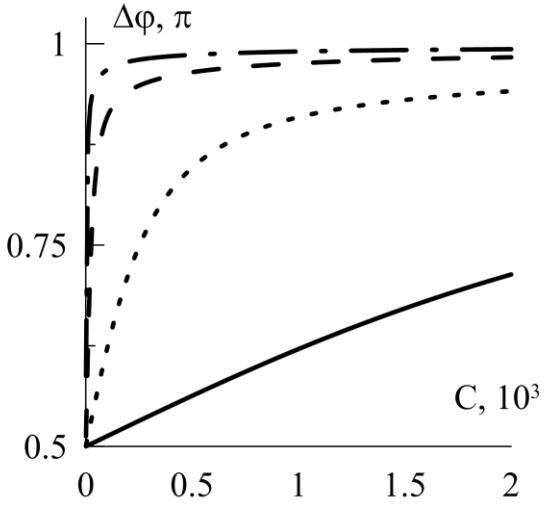

Fig. 2.3. Dependency of phases shift on pressure wave at the boundary and wall surface traveling wave on wave velocity (solid line: $\delta = 0.001$, dotted: $\delta = 0.01$, dashed: $\delta = 0.1$, dot-and-dash: $\delta = 1$)

Shift of phases. One of the important peculiarities of the system under analysis is the shift of the wave traveling on the wall surface (which is characterized by value of ξ, deviation from average wall position) relatively to pressure wave at the boundary. Fig.2.3 shows that with wave velocity decrease C shift of phases tends to $\frac{\pi}{2}$, while with the increase it tends to π. The increase of wave number makes shift of phases reach asymptote $\Delta\varphi = \pi$ quicker.

2.2.3. Solution in long wave approximation

The usage of boundary condition (2.17) on pressure is connected with the baroreceptors in esophagus walls, intestine, ureter. These sensors perceive pressure in boundary layer of fluid. A.D. Nozdrachev [131] states that reflex arc of nervous system of this type including sensor part with basis being a baroreceptor is enclosed within the walls and that is one observes no direct subordination to central nervous system.

Let us estimate the value of parameter δ. Large intestine is up to 1.5 meters in length and 3 centimeters in radius, the frequency of peristaltic waves in large intestine is 0.2-0.6 c^{-1}. Circumferential muscles constrict and form occlusion of 1-3 centimeters, while the content of the intestine moves to the neighboring area of 15-20 cm in width. Thus, we may state that for the large intestine

$$\delta = h / \lambda \sim 0.1 \div 0.2 . \tag{2.44}$$

The length of ureter is about 30 centimeters with 3 to 10 mm in diameter. The wave velocity is 2-3 cm/min, frequency is from 0.02 to 0.1 c^{-1}, wave length is from 2 to 15 cm. Urine viscosity is $\nu = 0.007$ cm^2/c [46]. Thus, we may state that for the ureter

$$\delta = 0.001 \div 0.1. \tag{2.45}$$

The obtained values make us conclude that wave number δ in most cases may be considered to be small, that is why it is quite natural to seek solution in form of power series of δ. Note that the solution in small amplitude approximation is more general then solution in long-wave approximation (for small δ).

In long-wave approximation the expressions for velocities, pressure and changes of wall coordinates are looked for in a power series of small parameter δ:

$$\mathrm{u} = \mathrm{u}_1\delta + \mathrm{u}_2\delta^2 + \mathrm{u}_3\delta^3 + \ldots, \ \mathrm{v} = \mathrm{v}_1\delta + \mathrm{v}_2\delta^2 + \mathrm{v}_3\delta^3 + \ldots \tag{2.46}$$

$$\xi = \xi_1\delta + \xi_2\delta^2 + \xi_3\delta^3 + \ldots, \ \mathrm{p} = \mathrm{p}_1\delta + \mathrm{p}_2\delta^2 + \mathrm{p}_3\delta^3 + \ldots \tag{2.47}$$

The solution is in the fact that the series (2.46) and (2.47) are substituted in equations system (2.14)-(2.17). Then multipliers at similar powers δ are grouped and the coefficients at successive powers δ are set to zero. Before the series (2.46) and (2.47) are substituted into the boundary conditions (2.17), these boundary conditions are decomposed into a series being centered at $x = \pm 1$:

$$x = \pm 1: \ \mathrm{p} \pm \xi \frac{\partial \mathrm{p}}{\partial x} + \frac{\xi^2}{2}\frac{\partial^2 \mathrm{p}}{\partial x^2} + \ldots = A\cos(t - y),$$
$$\mathrm{v} \pm \xi \frac{\partial \mathrm{v}}{\partial x} + \frac{\xi^2}{2}\frac{\partial^2 \mathrm{v}}{\partial x^2} + \ldots = \pm\frac{\partial \xi}{\partial t}, \ \mathrm{u} \pm \xi \frac{\partial \mathrm{u}}{\partial x} + \frac{\xi^2}{2}\frac{\partial^2 \mathrm{u}}{\partial x^2} + \ldots = 0.$$

The program to find the solution to the equation system in a long-wave approximation is given in Appendix 1. Longitudinal velocity found with this program is defined by an expression

$$\mathrm{u} = \frac{AC\delta}{2}\sin(t-y)(x^2-1) + \\ + \frac{AC^2\delta^2}{24}\left[\cos(t-y)(x^2-1)(x^2-5) + 8A\sin^2(t-y)\right] + O(\delta^3), \tag{2.48}$$

transverse velocity - by

$$\mathrm{v} = \frac{AC\delta}{6}x(x^2-3)\cos(t-y) - \\ - \frac{AC^2\delta^2}{120}\left[(x^2-5)^2 - 80A\cos(t-y)\right]x\sin(t-y) + \mathrm{O}(\delta^3), \tag{2.49}$$

law of wall coordinates change - by

$$\xi_{1,2} = \xi = -\frac{AC\delta}{3}\sin(t-y) + \\ + \frac{AC^2\delta^2}{30}\left[5A - 2\cos(t-y)(5A\cos(t-y)-2)\right] + O(\delta^3), \tag{2.50}$$

pressure - by

$$\mathrm{p} = A\cos(t-y) + \frac{A\delta^2}{2}(x^2-1)\cos(t-y) + O(\delta^3). \tag{2.51}$$

Flow rate in a long-wave approximation is expressed as follows

$$Q = \frac{1}{2\pi}\int_0^{2\pi}\int_{-1-\xi}^{1+\xi}\mathrm{u}\,dx\,dt = \frac{A^2C^2\delta^2}{3} + \\ + \frac{A^2C^2\delta^4}{9}\left[\left(\frac{25}{12}A^2 - \frac{31}{63}\right)C^2 - \frac{22}{5}\right] + O(\delta^6). \tag{2.52}$$

Fig. 2.4 shows that at small δ and C the approximation of small amplitudes, which was looked at in the previous paragraph, and the approximation of long waves used in this paragraph give close results.

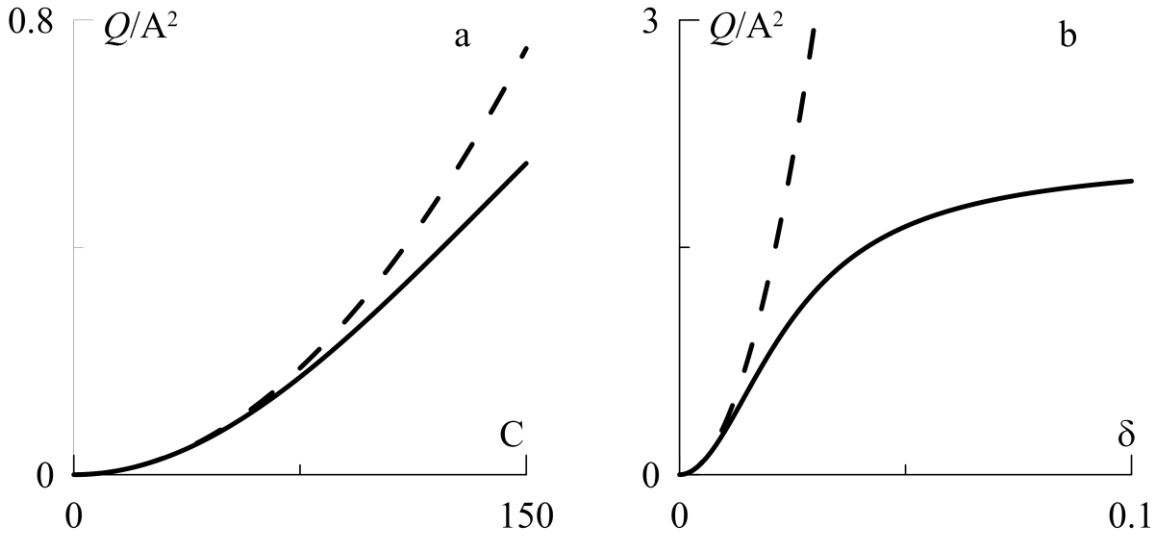

Fig. 2.4. Flow rate dependency on a: wave velocity C for $\delta = 0.01$, b: wave number δ for $C = 100$ (solid line: approximation of small amplitudes, dashed line: approximation of long waves)

D. Tagaki[32], who solved problem close to the one considered in this work, found an expression for flow rate

$$Q = \frac{4}{16^2 + K^2} A^2 C^2 \delta^2 + O(A^3, \delta^3, C^3), \tag{2.53}$$

At $D = 0$ expressions (2.53) and (2.52) differ in numerical coefficient, that is connected with different problem geometry: D. Tagaki studied a tube rather than a channel. The dependences on the parameters in (2.53) and in (2.52) are qualitatively the same.

Using series (2.50) we can find the maximum deviation of wall points from their time-averaged position in the form

$$\Xi = \frac{AC\delta}{3} + \frac{A^2 C^2 \delta^2}{6} + O(\delta^3) \tag{2.54}$$

Formula (2.54) show, that for small A, C and δ maximum deviation from average wall position Ξ increases linearly with these parameters. D. Tagaki received the same result in [32].

2.3. Influence of longitudinal vibrations on peristalsis

2.3.1. Problem statement

This section of the paper considers the influence of longitudinal channel vibrations on fluid transport. We study the flow of Newtonian fluid with viscosity ν and density ρ in a channel of $2L'$ in length and *2h* as an average distance between the walls. To simulate vibrations we introduce inertia force as harmonic function with amplitude g and frequency $\tilde{\omega}$.

After transformation to dimensionless variables, which are introduced in paragraph 2.1.1., the system of equation becomes as follows

$$\delta^2\left(\frac{\partial \mathrm{v}}{\partial t}+\mathrm{v}\frac{\partial \mathrm{v}}{\partial x}+\mathrm{u}\frac{\partial \mathrm{v}}{\partial y}\right)+\frac{\partial \mathrm{p}}{\partial x}-\frac{\delta}{C}\left(\frac{\partial^2 \mathrm{v}}{\partial x^2}+\delta^2\frac{\partial^2 \mathrm{v}}{\partial y^2}\right)=0,$$

$$\delta\left(\frac{\partial \mathrm{u}}{\partial t}+\mathrm{v}\frac{\partial \mathrm{u}}{\partial x}+\mathrm{u}\frac{\partial \mathrm{u}}{\partial y}+\frac{\partial \mathrm{p}}{\partial y}\right)-\frac{1}{C}\left(\frac{\partial^2 \mathrm{u}}{\partial x^2}+\delta^2\frac{\partial^2 \mathrm{u}}{\partial y^2}\right)=M\delta\cos wt, \tag{2.55}$$

$$\frac{\partial \mathrm{v}}{\partial x}+\frac{\partial \mathrm{u}}{\partial y}=0,$$

$$x=\pm 1\pm\xi:\quad \mathrm{v}=\pm\frac{\partial \xi}{\partial t},\quad \mathrm{u}=0,\quad \mathrm{p}=A\sin(t-y). \tag{2.56}$$

Besides the wave velocity $C=hc/\nu$, wave number $\delta=h/\lambda$ and dimensionless amplitude of pressure oscillations at the wall $A=a/(\rho c^2)$, which characterize peristaltic flow, this equation system has dimensionless vibration amplitude $\mathrm{M}=\lambda g/c^2$ and vibration frequency $w=\tilde{\omega}\lambda/c$.

2.3.2. General solution

We assume that dimensionless wave number δ is small, and find the solution in a series with this parameter:

$$\mathrm{u}=\mathrm{u}_1\delta+\mathrm{u}_2\delta^2+\mathrm{u}_3\delta^3+\ldots,\ \mathrm{v}=\mathrm{v}_1\delta+\mathrm{v}_2\delta^2+\mathrm{v}_3\delta^3+\ldots \tag{2.57}$$

$$\xi=\xi_1\delta+\xi_2\delta^2+\xi_3\delta^3+\ldots,\ \mathrm{p}=\mathrm{p}_1\delta+\mathrm{p}_2\delta^2+\mathrm{p}_3\delta^3+\ldots \tag{2.58}$$

Series (2.57) and (2.58) are substituted in equation system (2.55). Then multipliers at similar powers δ are grouped and the coefficients at successive powers δ are set to zero. Before the series (2.57) and (2.58) are substituted into the boundary conditions (2.56), these boundary conditions are decomposed into a series being centered at $x=\pm 1$:

$$x=\pm 1:\ \mathrm{p}\pm\xi\frac{\partial \mathrm{p}}{\partial x}+\frac{\xi^2}{2}\frac{\partial^2 \mathrm{p}}{\partial x^2}+\ldots=A\cos\left(t-y\right),$$

$$\mathrm{v}\pm\xi\frac{\partial \mathrm{v}}{\partial x}+\frac{\xi^2}{2}\frac{\partial^2 \mathrm{v}}{\partial x^2}+\ldots=\pm\frac{\partial \xi}{\partial t},\ \mathrm{u}\pm\xi\frac{\partial \mathrm{u}}{\partial x}+\frac{\xi^2}{2}\frac{\partial^2 \mathrm{u}}{\partial x^2}+\ldots=0.$$

The longitudinal velocity found in such a way equals

$$\mathrm{u} = \frac{1-x^2}{2}\delta C\left(A\cos(t-y)+M\cos wt\right)+\frac{C^2\delta^2}{24}\Big(8A^2\cos^2(t-y)+$$
$$+8AM\cos(t-y)\cos wt+(x^4-6x^2+5)(A\sin(t-y)+Mw\sin wt)\Big)+O(\delta^3),$$

pressure equals

$$p = A\sin(t-y)+\frac{1}{2}A\delta^2(x^2-1)\sin(t-y)+O(\delta^3), \tag{2.59}$$

transverse velocity equals

$$\mathrm{v} = \frac{x(x^2-3)}{6}\delta CA\sin(t-y)-\frac{xC^2\delta^2A}{120}(\cos(t-y)(80A\sin(t-y)-(x^2-5)^2)$$
$$+40M\sin(t-y)\cos wt)+O(\delta^3).$$

Vibration-caused additive to flow rate becomes

$$\Delta Q = -\frac{5}{18}\frac{C^4\delta^4A^2M^2}{w^2-1}+\mathrm{O}(\delta^5). \tag{2.60}$$

As we can see from (2.60), if the vibration frequencies are higher than the pressure wave at the wall ($w>1$), vibrations affect the peristaltic transport negatively – flow rate in a channel reduces. Otherwise ($w<1$), vibrations lead to the flow rate increase.

2.3.3. Solution at w close to 1

The case $w=1$ requires special consideration. Let us consider the system behavior in the neighborhood of this value, let us assume that $w=1+\gamma\delta^2$, where $\gamma\delta^2$ is small value. In this case a typical method of small parameter does not help to find solution, and one should use a method of multiple scales, when together with quick time t, slow times $t_1=\delta t$ and $t_2=\delta^2 t$ are also introduced. Equation system (2.55) is rewritten in the form

$$\delta^2\left(\frac{\partial \mathrm{v}}{\partial t}+\delta\frac{\partial \mathrm{v}}{\partial t_1}+\delta^2\frac{\partial \mathrm{v}}{\partial t_2}+\mathrm{v}\frac{\partial \mathrm{v}}{\partial x}+\mathrm{u}\frac{\partial \mathrm{v}}{\partial y}\right)+\frac{\partial \mathrm{p}}{\partial x}-\frac{\delta}{C}\left(\frac{\partial^2\mathrm{v}}{\partial x^2}+\delta^2\frac{\partial^2\mathrm{v}}{\partial y^2}\right)=0,$$

$$\frac{\partial \mathrm{u}}{\partial t}+\delta\frac{\partial \mathrm{u}}{\partial t_1}+\delta^2\frac{\partial \mathrm{u}}{\partial t_2}+\mathrm{v}\frac{\partial \mathrm{u}}{\partial x}+\mathrm{u}\frac{\partial \mathrm{u}}{\partial y}+\frac{\partial \mathrm{p}}{\partial y}-\frac{1}{\delta C}\left(\frac{\partial^2\mathrm{u}}{\partial x^2}+\delta^2\frac{\partial^2\mathrm{u}}{\partial y^2}\right)=M\cos(t+\gamma t_2), \tag{2.61}$$

$$\frac{\partial \mathrm{v}}{\partial x}+\frac{\partial \mathrm{u}}{\partial y}=0,$$

and boundary conditions take the following form

$$x=\pm1\pm\xi:\quad \mathrm{v}=\pm\frac{\partial\xi}{\partial t}+\delta\frac{\partial\xi}{\partial t_1}+\delta^2\frac{\partial\xi}{\partial t_2},\quad \mathrm{u}=0,\quad \mathrm{p}=A\sin(t-y). \tag{2.62}$$

We are going to find the solution of equation system (2.61) in the series of small parameter δ:

$$\mathrm{v} = \mathrm{v}_1\delta + \mathrm{v}_2\delta^2 + ...;\ \ \mathrm{u} = \mathrm{u}_1\delta + \mathrm{u}_2\delta^2 + ...; \mathrm{p} = A\sin(t-y) + \mathrm{p}_2\delta^2 + ...; \tag{2.63}$$

$$\xi = \bar{\xi}_0(y, t_{1,2}) + (\xi_1(t, t_{1,2}, y) + \bar{\xi}_1(y, t_{1,2}))\delta + (\xi_2(t, t_{1,2}, y) + \bar{\xi}_2(y, t_{1,2}))\delta^2 + ... \tag{2.64}$$

First-order solution. In the first order the problem takes the following form

$$\frac{\partial^2 \mathrm{u}_1}{\partial x^2} = -C(A\cos(t-y) + M\cos(t+\gamma t_2)),\ \ \frac{\partial \mathrm{v}_1}{\partial x} + \frac{\partial \mathrm{u}_1}{\partial y} = 0, \tag{2.65}$$

$$x = \pm 1 \pm \bar{\xi}_0 :\quad \mathrm{v}_1 = \pm\frac{\partial \xi_1}{\partial t},\quad \mathrm{u}_1 = 0,\quad \mathrm{p}_1 = 0\,. \tag{2.66}$$

The longitudinal velocity found equals

$$\mathrm{u}_1 = \frac{C}{2}(A\cos(t-y) + M\cos(t+\gamma t_2))((1+\xi_0)^2 - x^2)\,, \tag{2.67}$$

transverse velocity is

$$\begin{aligned}\mathrm{v}_1 = Cx\Bigg(&\frac{1}{6}Ax^2\sin(t-y) - \frac{1}{2}A\sin(t-y)(1+\xi_0)^2 \\ &-(A\cos(t-y) + M\cos(t+\gamma t_2))(1+\xi_0)\frac{\partial \xi_0}{\partial y}\Bigg),\end{aligned} \tag{2.68}$$

deviation from average wall position is

$$\begin{aligned}\xi_1 = \xi_0(y, t_2) + C(1+\xi_0)\Bigg(&\frac{1}{3}(1+\xi_0)^2 A\cos(t-y) \\ &-(1+\xi_0)\frac{\partial \xi_0}{\partial y}(A\sin(t-y) + M\sin(t+\gamma t_2))\Bigg).\end{aligned}$$

Second-order solution. The problem in the second order has the following form

$$\frac{\partial p_2}{\partial x} = \frac{1}{C}\frac{\partial^2 \mathrm{v}_1}{\partial x^2},\quad \frac{\partial^2 \mathrm{u}_2}{\partial x^2} = C\frac{\partial \mathrm{u}_1}{\partial t},\quad \frac{\partial \mathrm{u}_2}{\partial y} + \frac{\partial \mathrm{v}_2}{\partial x} = 0; \tag{2.69}$$

$$x = \pm 1 \pm \xi_0 : \mathrm{v}_2 \pm \xi_1\frac{\partial \mathrm{v}_1}{\partial x} = \pm\frac{\partial \xi_2}{\partial t} \pm \frac{\partial \xi_1}{\partial t_1} \pm \frac{\partial \xi_0}{\partial t_2},\ \mathrm{u}_2 \pm \xi_1\frac{\partial \mathrm{u}_1}{\partial x} = 0,\ \mathrm{p}_2 = 0.$$

(2.70)

While solving the equation system (2.69) secular terms, which cause the solution divergence on large times, appear. The requirements to make these terms zero are aimed to obtain the equation for time-independent deviation from average wall position ξ_0:

$$\left[\frac{AM}{6}(\xi_0+1)\sin(y+\gamma t_2) - \frac{5}{6}A\frac{\partial \xi_0}{\partial y}(A + M\cos(y+\gamma t_2))\right](\xi_0+1)^4 C^2 = \frac{\partial \xi_0}{\partial t_2} \tag{2.71}$$

With a variable $z = y + \gamma t_2$ we transform an equation (2.71) to be as follows

$$\frac{AM}{6}(\xi_0+1)^5 C^2 \sin z - \left[\frac{5}{6}A(\xi_0+1)^4 C^2(A + M\cos z) + \gamma\right]\frac{\partial \xi_0}{\partial z} = 0 \tag{2.72}$$

This differential equation may be transformed to algebraic

$$(M\cos z + A)AC^2(\xi_0+1)^5 + 6\xi_0\gamma + \tilde{C} = 0 \tag{2.73}$$

or

$$\xi_0 + 1 = -\left(\frac{6\gamma\xi_0 + \tilde{C}}{AC^2(M\cos z + A)} \right)^{\frac{1}{5}}, \tag{2.74}$$

where $\tilde{C}$ is an constant. To consider the case with large γ decompose ξ_0 and $\tilde{C}$ into a series of γ^{-1}:

$$\xi_0 = \xi_0^I \frac{1}{\gamma} + \xi_0^{II} \frac{1}{\gamma^2} + \xi_0^{III} \frac{1}{\gamma^3}, \quad \tilde{C} = \tilde{C}_0 + \tilde{C}_1 \frac{1}{\gamma} + \tilde{C}_2 \frac{1}{\gamma^2}. \tag{2.75}$$

By substituting (2.75) in (2.73), and decomposing the obtained expression in series at powers $\frac{1}{\gamma}$, we get

$$\xi_0^{\mathrm{I}} = -\frac{AC^2 M\cos z}{6}, \quad \xi_0^{\mathrm{II}} = \frac{5}{72} MC^4 A^2 (M\cos 2z + 2A\cos z). \tag{2.76}$$

В результате для расхода жидкости с точностью до второго порядка по обратной к γ переменной получается выражение

The flow rate in the power series of $\frac{1}{\gamma}$ is

$$\begin{aligned} Q &= \lim_{T_i\to\infty} \frac{1}{T_2}\int_0^{T_2} \frac{1}{T_1}\int_0^{T_1} \frac{1}{T_0}\int_0^{T_0}\int_{-1-\xi}^{1+\xi} u\,dx\,dt\,dt_1\,dt_2 = \\ &= \delta^2 C^2 A^2 \left[\frac{1}{3} - \frac{5C^2M^2}{36\gamma} + \frac{5C^2A^2M^2}{18\gamma^2} \right] + \mathrm{O}\left(\frac{1}{\gamma^3}, \delta^3 \right). \end{aligned} \tag{2.77}$$

If we put $w = 1 + \gamma\delta^2$ into equation (2.60) (formula for flow rate, which works away from $w = 1$) and decompose in series of δ, then in the second order the additive flow rate appearing from vibrations will take the following form

$$\Delta Q = -\frac{5C^4\delta^2A^2M^2}{36\gamma} + \mathrm{O}(\delta^3), \tag{2.78}$$

that coincide with (2.77).

Let us consider the solution of equations (2.73) for small relations M/A<<1. To do this let us decompose ξ_0 and constant $\tilde{C}$ into a series

$$\xi_0 = \frac{M}{A}\xi_0^I + \left(\frac{M}{A}\right)^2 \xi_0^{II} + \left(\frac{M}{A}\right)^3 \xi_0^{III}, \quad \tilde{C} = \left(\frac{M}{A}\right)\tilde{C}_1 + \left(\frac{M}{A}\right)^2 \tilde{C}_2 + \ldots \tag{2.79}$$

By substituting (2.79) in (2.73), we get after simplifications

$$\xi_0 = -\frac{\cos z}{5 + 6\frac{\gamma}{A^2C^2}} \frac{M}{A} + 15 \frac{\frac{\gamma}{A^2C^2} + \frac{1}{2}}{\left(5 + 6\frac{\gamma}{A^2C^2}\right)^3} \left(\frac{M}{A}\right)^2 \cos 2z + O\left(\frac{M}{A}\right)^3 \tag{2.80}$$

Expression (2.80) shows that when the vibration frequency and the pressure wave frequency are getting closer, then a slowly traveling wave with frequency equals the difference of frequencies of

two effects appears. In a particular case of frequencies equality the traveling wave become stationary relief.

Found in this approximation expression for flow rate takes the following form

$$Q=\lim_{T_i\to\infty}\frac{1}{T_2}\int_0^{T_2}\frac{1}{T_1}\int_0^{T_1}\frac{1}{T_0}\int_0^{T_0}\int_{-1-\xi}^{1+\xi}udxdtdt_1dt_2=\frac{C^2A^2\delta^2}{3}-\frac{5A^2C^2\delta^2}{2}\frac{1+2\Gamma}{(5+6\Gamma)^2}\frac{M^2}{A^2}$$
$$-\frac{5\left[2916\Gamma^3+2025\Gamma+325+4152\Gamma^2\right]}{4(6\Gamma+5)^6}A^2C^2\delta^2\frac{M^4}{A^4}+\mathrm{O}\left(\delta^3,\left(\frac{M}{A}\right)^6\right), \tag{2.81}$$

where $\Gamma=\dfrac{\gamma}{A^2C^2}$. Expression (2.81) shows that at $\Gamma>-0.5$ vibration influence reduces flow rate, while in contrast cases it increases the flow rate.

When $\Gamma=-\dfrac{5}{6}$, we can't get the algebraic equation (2.73) from differential equation (2.71). Let us find the solution of differential equation (2.71) for $\Gamma=-\dfrac{5}{6}$. By substituting in (2.71) series (2.79), in the first order of $\left(\dfrac{M}{A}\right)$ we get

$$\left[\sin(y+\gamma t_2)-5\frac{\partial\xi_0^I}{\partial y}\right]\frac{A^2C^2}{6}=\frac{\partial\xi_0^I}{\partial t_2} \tag{2.82}$$

Considering that $\gamma=-\dfrac{5}{6}A^2C^2$, we get

$$\left[\sin(y-\frac{5}{6}A^2C^2t_2)-5\frac{\partial}{\partial y}\xi_0^I\right]\frac{A^2C^2}{6}=\frac{\partial}{\partial t_2}\xi_0^I \tag{2.83}$$

The solution for the equation (2.83) is

$$\xi_0^I=\frac{y}{5}\sin(y-\frac{5}{6}A^2C^2t_2). \tag{2.84}$$

For a long channel (this is the case we are looking at) the law of wall motion (2.84) results in their collision and channel obstruction. The results illustrate that for some values of parameters the original assumption about the possibility to provide the specified pressure at the boundary by moving the walls is invalid.

Finally, the longitudinal vibrations influence the flow in a channel in such a way, that for vibration frequencies higher that pressure wave frequency at the wall the vibrations negatively affect the peristaltic transport - the flow rate decreases. Otherwise, vibrations lead to the flow rate increase. When the vibration frequency and the pressure wave frequency at the wall are close, then a slowly traveling wave with frequency being equal to the difference of frequencies of effects appears. In a particular case of frequencies equality the traveling wave become stationary relief.

3. FLOW IN PULSATING CHANNELS

A two-dimensional liquid flow in the field of the gravitational force in a channel with pulsating walls at the presence of pressure drop is studied in this chapter. This problem was previously analyzed as a particular case of peristaltic flow by S.L.Weinberg [109] and M.S.Longuet-Higgins [110], who illustrated that the pulsations resulted in increase of the flow rate, which occurred due to the pressure drop. Later, N.I.Arinchin [113] used this effect to explain the significant increase of blood flow in the working muscles. Building the research by G.V. Anrep, et al [150], he proposed that the muscles with high frequency vibrations squeeze and relax dependent vessels and as the result, the increase of flow rate is observed. G.A.Lyukhov and I.V.Shugan [111, 112] suggested that the effect found by S.L.Weinberg [109] and M.S.Longuet-Higgins [110] could be used to improve the pumps performance and they have calculated the energy consumption required to increase the flow rate by means of pulsations. Kwi-joo Lee, etc. [151] arrived at a differential equation for the flow rate on the bases of the assumptions, some of which (for example, an assumption about local Poiseuille profile of longitudinal velocity) being not evident. Kwi-joo Lee, et al. [151] came to the conclusion that the flow rate increases with the increase in the amplitude of the walls pulsation and decreases with the decrease of the Womersley number (product of the distance between the walls by square root from frequency ratio to kinematic liquid viscosity). Their theory states that for the small walls pulsation amplitudes the pulsations result in the flow rate increase and the high walls pulsation amplitudes could lead to both the flow rate increase and its decrease depending on the Womersley number value.

We study the solution to the problem about the flow in a channel with pulsating walls applying the solution class of Navier-Stokes equations with a linear dependence from coordinate being longitudinal with respect to the channel axis. Earlier, T.W.Secomb [139] considered this type of solution for this problem focusing on the analysis of the case with the absent of pressure differences at the channel ends. The research of T.W.Secomb illustrates the existence of nonzero time-averaged velocity field of flow; this flow, however, does not contribute into the time-averaged flow rate. Later P.Hall and D.T.Papageorgiou [140] considered the stability of this solution. Their numerical calculations showed that the increase of the Womersley number for high amplitudes of walls pulsations led to the chaos according to the Feigenbaum scenario via the cascade of period doubling.

The problem about the channel walls pulsation influence on the solute concentration distribution and the problem about the squeezing flow are close to the ones considered in this article. S. Tsangaris [152] was among the first studies on the first problem. Later S.L.Waters [153] looked at this problem and found out that the solute flow increased as the diffusion coefficient was decreasing, the Womersley number was increasing and the walls permeability coefficient was increasing. Going deeper into the problem S.L.Waters [153] presented a mathematical model of oxygen supply to the heart after laser myocardial revascularization.

The problem of the squeezing flow is characterized by the approaching walls squeezing liquid from the channel. For some laws of walls movements there are analytical solutions to this problem [154-155]. K.J.Zwick, et al [114] experimentally studied this issue. They analyzed the flow of Newtonian and viscoplastic liquids between two round plates, which were under the acting force comprising oscillating and constant components. In case of viscoplastic liquid they found that the plates vibration resulted in significant increase of flow rate, while no such effect was found in case of Newtonian liquid.

The purpose of the present chapter is to examine the influence of channel walls pulsations on the fluid transport for the large Womersley numbers. This problem is solved under the approximation of

small-amplitude wall pulsation. The first section deals with the review on the literature. The second one describes general problem statement. The third section of the paper states and solves the problem in zero and first order by wall pulsation amplitude. The fourth section states the problem and its time-averaged solution in the second order by the amplitude. In the fifth and sixth sections we use the found solutions to analyze the influence of channel walls pulsations on the flow rate and time-averaged velocity field of flow. At the end of this chapter we study the influence of compressibility on the flow in pulsating channel.

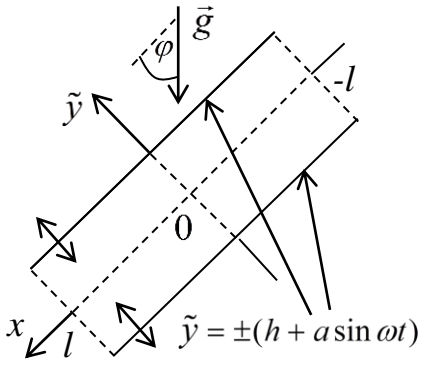

Fig.3.1. Geometry of the problem

3.1. Problem Statement

Let us consider a two-dimensional flow of viscous incompressible fluid flow in a channel, which walls harmonically pulsate with the frequency ω and the amplitude a at the presence of the gravity and pressure difference 2Δ at the ends of the channel with the length $2l$ (Fig.3.1).

The fluid flow is described by a system of Navier-Stokes equations for the viscous incompressible Newtonian fluid and by a continuity equation:

$$\rho\left(\frac{\partial \mathrm{U}}{\partial t}+\mathrm{U}\frac{\partial \mathrm{U}}{\partial x}+\mathrm{v}\frac{\partial \mathrm{U}}{\partial \tilde{y}}\right)=-\frac{\partial \tilde{p}}{\partial x}+\eta\left(\frac{\partial^2 \mathrm{U}}{\partial x^2}+\frac{\partial^2 \mathrm{U}}{\partial \tilde{y}^2}\right)+\rho \mathrm{g}\cos\varphi, \tag{3.1}$$

$$\rho\left(\frac{\partial \mathrm{v}}{\partial t}+\mathrm{U}\frac{\partial \mathrm{v}}{\partial x}+\mathrm{v}\frac{\partial \mathrm{v}}{\partial \tilde{y}}\right)=-\frac{\partial \tilde{p}}{\partial \tilde{y}}+\eta\left(\frac{\partial^2 \mathrm{v}}{\partial x^2}+\frac{\partial^2 \mathrm{v}}{\partial \tilde{y}^2}\right)-\rho g\sin\varphi\ , \tag{3.2}$$

$$\frac{\partial \mathrm{u}}{\partial x}+\frac{\partial \mathrm{v}}{\partial \tilde{y}}=0\,, \tag{3.3}$$

where x and $\tilde{y}$ are longitudinal and transverse with the relation to the axis of channel coordinates, t is time; U and v are longitudinal and transverse components of velocity, p is pressure; g is the acceleration of gravity, ρ - is fluid density, η is dynamic viscosity, φ - angle between the channel axis and the direction of gravity force.

The position of the upper and lower channel wall in a given time moment is determined by the equation

$$\tilde{y}=\pm(h+a\sin\omega t). \tag{3.4}$$

The position of the channel ends are specified by the equations

$$x=-l \ \text{и} \ x=l. \tag{3.5}$$

The walls points move only along the OY axis. No-slip boundary conditions are identified on the lower and the upper walls:

$$\tilde{y}=\pm(h+a\sin\omega t)\ :\ \mathrm{u}=0\,,\ \mathrm{v}=\pm a\cos\omega t\,, \tag{3.6}$$

Pressure-drop boundary condition is specified at the channel ends:

$$\tilde{p}\big|_{x=l}-\tilde{p}\big|_{x=-l}=2\Delta\,, \tag{3.7}$$

Choose the following units of measurement: length - h, time - $1/\omega$, pressure - $\eta\omega$, velocity - $h\omega$. The problem in a dimensionless form is characterized by four parameters: the Womersley number

W, the Richardson number Ri, dimensionless amplitude of pulsations A and dimensionless channel length L:

$$\mathrm{W} = h\sqrt{\frac{\rho\omega}{2\eta}},\ \mathrm{Ri} = \frac{g\cos\varphi - \delta_p/(L\rho)}{\omega^2 h},\ A = \frac{a}{h}, L = \frac{l}{h}.$$

After the pressure transformation

$$\tilde{p} \to p - \rho y g \sin\varphi + x\Delta/l \tag{3.8}$$

the nondimensionalization and the transformation of transverse coordinate

$$\tilde{y} \to y(1 + A\sin t), \tag{3.9}$$

the system of Navier-Stokes equations (20)-(21) and continuity equations (22) has the following form

$$\begin{aligned}(1+A\sin t)^2\left[\frac{\partial \mathrm{U}}{\partial t} + \mathrm{U}\frac{\partial \mathrm{U}}{\partial x} + \frac{\mathrm{v} - yA\cos t}{1+A\sin t}\frac{\partial \mathrm{U}}{\partial y}\right] = \\ = \frac{1}{2\mathrm{W}^2}\left[\left(-\frac{\partial p}{\partial x} + \frac{\partial^2 \mathrm{U}}{\partial x^2}\right)(1+A\sin t)^2 + \frac{\partial^2 \mathrm{U}}{\partial y^2}\right] + (1+A\sin t)^2\,\mathrm{Ri},\end{aligned} \tag{3.10}$$

$$\frac{\partial \mathrm{v}}{\partial t} + \mathrm{U}\frac{\partial \mathrm{v}}{\partial x} + \frac{\mathrm{v} - yA\cos t}{1+A\sin t}\frac{\partial \mathrm{v}}{\partial y} = \frac{1}{2\mathrm{W}^2}\left(\frac{\partial^2 \mathrm{v}}{\partial x^2} + \frac{1}{(1+A\sin t)^2}\frac{\partial^2 \mathrm{v}}{\partial y^2} - \frac{\partial p}{\partial y}\right), \tag{3.11}$$

$$\frac{\partial \mathrm{U}}{\partial x} + \frac{1}{1+A\sin t}\frac{\partial \mathrm{v}}{\partial y} = 0, \tag{3.12}$$

and the boundary conditions are the following ones:

$$y = \pm 1:\ \mathrm{U} = 0,\ \mathrm{v} = \pm A\cos t. \tag{3.13}$$

$$p\big|_{x=L} = p\big|_{x=-L}. \tag{3.14}$$

The purpose of the coordinate transformation (26) is to set the boundary conditions at the fixed boundary.

Pressure transformation (25) leads to the exclusion of summand with Δ from the boundary condition (24). At the same time the Richardson number Ri contains a member $\Delta/(L\rho)$ besides the gravity acceleration g. This transformation results in the exclusion of summand $\rho g \sin\alpha$ from the equation for transverse velocity (28).

3.2. Solution in first and zero orders

The solution of the problem was obtained in a form suggested by T.W.Secomb [139]:

$$\mathrm{U} = \mathrm{u}(y,t) - \frac{x}{1+A\sin t}\frac{\partial \mathrm{v}(y,t)}{\partial y}, \tag{3.15}$$

$$\mathrm{v} = \mathrm{v}(y,t),\ p = \phi(y,t) + x^2\gamma(t). \tag{3.16}$$

Equation of continuity is always valid for the solution (32)-(33). After the introduction $\mathrm{u}(y,t)$ according to the formula (32) the boundary condition for the longitudinal velocity U in (30) is the following one:

$$y = \pm 1:\ \frac{\partial \mathrm{v}}{\partial y} = 0,\ \mathrm{u} = 0. \tag{3.17}$$

Dimensional amplitude of walls pulsation is considered to be small in comparison with the distance between the walls, which enables one to find the solution by the method of small parameter in the form of a series in powers of dimensionless amplitude A:

$$\mathrm{u}(y,t)=\mathrm{u}_0(y)+A\mathrm{u}_1(y,t)+A^2\mathrm{u}_2(y,t)+\ldots,\ \mathrm{v}(y,t)=A\mathrm{v}_1(y,t)+A^2\mathrm{v}_2(y,t)+\ldots, \tag{3.18}$$

$$p=Ap_1(x,y,t)+A^2p_2(x,y,t)+\ldots \tag{3.19}$$

After substitution (3.18), (3.19) and (32) in the equation (27) and boundary condition (3.17) we get the problem in zero order of A as

$$\frac{\partial^2\mathrm{u}_0}{\partial y^2}=-2W^2\mathrm{Ri}, \tag{3.20}$$

$$y=\pm1:\ \mathrm{u}_0=0. \tag{3.21}$$

The problem solution is the following one:

$$\mathrm{u}_0=-\mathrm{W}^2\mathrm{Ri}(y^2-1). \tag{3.22}$$

Expression (3.22) describes the profile of flat Poiseuille flow in the channel with fixed walls.

The problem in the first order has the following form

$$\begin{aligned}\frac{\partial\mathrm{u}_1}{\partial t}-x\frac{\partial^2\mathrm{v}_1}{\partial y\partial t}+\mathrm{RiW}^2\left[(y^2-1)\frac{\partial\mathrm{v}_1}{\partial y}+2y\left(y\cos t-\mathrm{v}_1\right)\right]=\\ =\frac{1}{2\mathrm{W}^2}\left(\frac{\partial^2\mathrm{u}_1}{\partial y^2}-x\frac{\partial^3\mathrm{v}_1}{\partial y^3}-\frac{\partial p_1}{\partial x}\right)+2\mathrm{Ri}\sin t,\end{aligned} \tag{3.23}$$

$$\frac{\partial\mathrm{v}_1}{\partial t}=\frac{1}{2\mathrm{W}^2}\left(\frac{\partial^2\mathrm{v}_1}{\partial y^2}-\frac{\partial p_1}{\partial y}\right) \tag{3.24}$$

$$y=\pm1:\ \mathrm{u}_1=0,\ \mathrm{v}_1=\pm\cos t. \tag{3.25}$$

The solution for the problem of the first order is the pressure in the form

$$p_1=p_{1s}(x,y)\sin t+p_{1c}(x,y)\cos t, \tag{3.26}$$

transverse velocity in the form

$$\mathrm{v}_1=\mathrm{v}_{1s}(\mathrm{y})\sin t+\mathrm{v}_{1c}(\mathrm{y})\cos t, \tag{3.27}$$

and longitudinal velocity in the form

$$\mathrm{u}_1=\mathrm{u}_{1s}(\mathrm{y})\sin t+\mathrm{u}_{1c}(\mathrm{y})\cos t. \tag{3.28}$$

To simplify the expression for the coefficients at sinuses and cosines in (34)-(36) we will introduce a variable

$$S=\left((2\mathrm{W}^2+1)\cosh 2\mathrm{W}+(2\mathrm{W}^2-1)\cos 2\mathrm{W}-2\mathrm{W}(\sinh 2\mathrm{W}+\sin 2\mathrm{W})\right)^{-1}. \tag{3.29}$$

Then the coefficients in the expression (34) for the pressure are written in the following way

$$p_{1s}=(y^2-x^2)\mathrm{W}^2f_1,$$

$$p_{1c}=-(y^2-x^2)\mathrm{W}^2f_2,$$

where

$$f_1=\mathrm{W}S\left[2\mathrm{W}(\cosh 2\mathrm{W}+\cos 2\mathrm{W})-\sin 2\mathrm{W}-\sinh 2\mathrm{W}\right]. \tag{3.30}$$

$$f_2=\mathrm{W}S\left[\sinh 2\mathrm{W}-\sin 2\mathrm{W}\right], \tag{3.31}$$

coefficients in the expression (35) for the transverse velocity:

$$\mathrm{v}_{1s}=f_3\sin\mathrm{W}y\cosh\mathrm{W}y+f_4\cos\mathrm{W}y\sinh\mathrm{W}y+f_2y, \tag{3.32}$$

$$\mathrm{v}_{1c}=f_4\sin\mathrm{W}y\cosh\mathrm{W}y-f_3\cos\mathrm{W}y\sinh\mathrm{W}y+f_1y, \tag{3.33}$$

where

$$f_3=2S\left[\mathrm{W}\cos\mathrm{W}\cosh\mathrm{W}-(\cos\mathrm{W}+\mathrm{W}\sin\mathrm{W})\sinh\mathrm{W}\right], \tag{3.34}$$

$$f_4=-2S\left[(\mathrm{W}\cos\mathrm{W}-\sin\mathrm{W})\cosh\mathrm{W}+\mathrm{W}\sinh\mathrm{W}\sin\mathrm{W}\right], \tag{3.35}$$

and the coefficients in the expression (36) for the longitudinal velocity:

$$\mathrm{u}_{1s} = \mathrm{Ri}\Big(\Big[(f_6 + f_7(y^2-1))y\cos \mathrm{W}y + (f_8 + f_9(y^2-1))\sin \mathrm{W}y\Big]\sinh \mathrm{W}y + f_{14} +$$
$$+\Big[(f_{10}(y^2-1) + f_{11})\cos \mathrm{W}y + (f_{12} + f_{13}(y^2-1))y\sin \mathrm{W}y\Big]\cosh \mathrm{W}y + f_5(y^2-1)\Big),$$

$$\mathrm{u}_{1c} = \mathrm{Ri}\Big(\Big[(f_{11} + f_{10}(y^2-1))\sin \mathrm{W}y - (f_{12} + f_{13}(y^2-1))y\cos \mathrm{W}y\Big]\sinh \mathrm{W}y - f_1 +$$
$$+\Big[(f_6 + f_7(y^2-1))y\sin \mathrm{W}y - (f_9(y^2-1) + f_8)\cos \mathrm{W}y\Big]\cosh \mathrm{W}y - f_2\mathrm{W}^2(y^2+1)\Big),$$

where

$$f_5 = \mathrm{W}^2(f_1-2),\ f_6 = -\frac{2}{3}\left(\frac{9}{8}f_3 + \mathrm{W}^2 f_4\right)\mathrm{W}^2,\ f_7 = \mathrm{W}^4 f_4/3,\ f_9 = -3\mathrm{W}^3(f_4+f_3)/4,$$

$$f_{10} = 3(f_3-f_4)\mathrm{W}^3/4,\ f_{12} = -2\mathrm{W}^2(f_3\mathrm{W}^2 - 9f_4/8)/3,\ f_{13} = f_3\mathrm{W}^4/3,\ f_{14} = 2(f_1-1)\mathrm{W}^2 - f_2,$$

$$f_8 = \frac{-f_{12}\sinh 2\mathrm{W} + f_6\sin 2\mathrm{W} - 2(2f_2\mathrm{W}^2 + f_1)\cosh \mathrm{W}\cos W - 2f_{14}\sin \mathrm{W}\sinh \mathrm{W}}{\cos 2\mathrm{W} + \cosh 2\mathrm{W}},$$

$$f_{11} = \frac{-f_6\sinh 2\mathrm{W} - f_{12}\sin 2\mathrm{W} + 2(2f_2\mathrm{W}^2 + f_1)\sin \mathrm{W}\sinh \mathrm{W} - 2f_{14}\cos \mathrm{W}\cosh \mathrm{W}}{\cos 2\mathrm{W} + \cosh 2\mathrm{W}}.$$

This solution shows that the assumption about the quadratic dependency of a longitudinal velocity from transverse coordinate, made by Kwi-joo Li, et al. [151], is not valid.

In order to investigate the influence of the walls pulsations on the liquid transport one should know the time-averaged second-order solution, besides the first-order solution.

3.3. Time-averaged second-order solution

Let us look at the A second-order problem. After the substitution (3.18), (3.19), (32) and (3.22) in (27) we get the following equation:

$$E_1(y,t)x + E_2(y,t) = 0. \tag{3.36}$$

Here

$$E_1 = \frac{1}{2\mathrm{W}^2}\frac{\partial^3 \mathrm{v}_2}{\partial y^3} + \frac{1}{2x\mathrm{W}^2}\frac{\partial p_2}{\partial x} + e_1\sin^2 t + e_2\cos^2 t + e_3\sin t\cos t - \frac{\partial^2 \mathrm{v}_2}{\partial t\partial y}, \tag{3.37}$$

$$E_2 = \frac{\partial \mathrm{u}_2}{\partial t} + \left(\frac{\partial \mathrm{v}_2}{\partial y}(y^2-1) - 2\mathrm{v}_2 y\right)\mathrm{W}^2\mathrm{Ri} - \frac{1}{2\mathrm{W}^2}\frac{\partial^2 \mathrm{u}_2}{\partial y^2} + \tag{3.38}$$
$$+(e_4\sin t + e_6\cos t)\sin t + e_5\cos^2 t,$$

where

$$e_1 = \frac{1}{2\mathrm{W}^2}\left(\frac{2}{x}\frac{\partial p_{1s}}{\partial x} - \frac{\partial^3 \mathrm{v}_{1s}}{\partial y^3}\right) + \frac{\partial \mathrm{v}_{1c}}{\partial y} + \left(\frac{\partial \mathrm{v}_{1s}}{\partial y}\right)^2 - \mathrm{v}_{1s}\frac{\partial^2 \mathrm{v}_{1s}}{\partial y^2},$$

$$e_2 = (y - \mathrm{v}_{1c})\frac{\partial^2 \mathrm{v}_{1c}}{\partial y^2} + \left(\frac{\partial \mathrm{v}_{1c}}{\partial y}\right)^2 + \frac{\partial \mathrm{v}_{1c}}{\partial y},$$

$$e_3 = \frac{1}{2\mathrm{W}^2}\left(\frac{2}{x}\frac{\partial p_{1c}}{\partial x} - \frac{\partial^3 \mathrm{v}_{1c}}{\partial y^3}\right) + 2\frac{\partial \mathrm{v}_{1s}}{\partial y}\frac{\partial \mathrm{v}_{1c}}{\partial y} + (y - \mathrm{v}_{1c})\frac{\partial^2 \mathrm{v}_{1s}}{\partial y^2} - \mathrm{v}_{1s}\frac{\partial^2 \mathrm{v}_{1c}}{\partial y^2},$$

$$e_4 = \mathrm{v}_{1s}\frac{\partial \mathrm{u}_{1s}}{\partial y} - (\mathrm{u}_{1s} + \mathrm{u}_0)\frac{\partial \mathrm{v}_{1s}}{\partial y} - 2\mathrm{u}_{1c} - (1 + 2\mathrm{W}^2 y\mathrm{v}_{1s})\mathrm{Ri},$$

$$e_5 = (v_{1c} - y)\frac{\partial \mathrm{u}_{1c}}{\partial y} - \mathrm{u}_{1c}\frac{\partial \mathrm{v}_{1c}}{\partial y},$$

$$e_6 = (\mathrm{v}_{1c} - y)\frac{\partial \mathrm{u}_{1s}}{\partial y} - (\mathrm{u}_{1s} + \mathrm{u}_0)\frac{\partial \mathrm{v}_{1c}}{\partial y} + 2\mathrm{u}_{1s} + 2\mathrm{W}^2\mathrm{Ri}(y - \mathrm{v}_{1c})y - \mathrm{u}_{1c}\frac{\partial \mathrm{v}_{1s}}{\partial y} + \mathrm{v}_{1s}\frac{\partial \mathrm{u}_{1c}}{\partial y}.$$

The boundary conditions for the second-order problem are presented in the following way

$$y = \pm 1:\ \mathrm{u}_2 = 0,\ \frac{\partial \mathrm{v}_2}{\partial y} = 0,\ \mathrm{v}_2 = 0. \tag{3.39}$$

In equation (3.36), $E_1(y,t)$ and $E_2(y,t)$ must independently equal to zero.

Transverse velocity. The equation

$$E_1(y,t) = 0 \tag{3.40}$$

with the boundary conditions (3.39) defines a second-order problem for the transverse velocity.

We average the equation (3.40) over time to calculate the time-averaged transverse velocity $\overline{\mathrm{v}}_2$ and as a result get

$$\frac{\partial^3 \overline{\mathrm{v}}_2}{\partial y^3} = -\frac{1}{x}\frac{\partial \overline{p}_2}{\partial x} - \mathrm{W}^2(e_1 + e_2), \tag{3.41}$$

where $\overline{p}_2$ is time-averaged pressure. The boundary conditions for the second-order transverse velocity are the following ones:

$$y = \pm 1:\ \frac{\partial \overline{\mathrm{v}}_2}{\partial y} = 0,\ \overline{\mathrm{v}}_2 = 0. \tag{3.42}$$

The solution for the problem (3.41)-(3.42) is presented in the following way:

$$\begin{aligned} \overline{\mathrm{v}}_2 = {} & f_{20}(\sin 2\mathrm{W}y - \sinh 2\mathrm{W}y) + \left(f_{15}y\cos \mathrm{W}y + f_{16}\sin \mathrm{W}y\right)\cosh \mathrm{W}y + \\ & + \left(f_{17}y\sin \mathrm{W}y + f_{18}\cos \mathrm{W}y\right)\sinh \mathrm{W}y + f_{21}y + f_{22}y^3, \\ \frac{\partial \overline{p}_2}{\partial x} = {} & -x\left(\mathrm{W}^2(f_1^2 + f_2^2) + 6f_{22}\right), \end{aligned} \tag{3.43}$$

where

$$f_{20} = \frac{\mathrm{W}}{8}\left(f_4^2 + f_3^2\right),\ f_{18} = \frac{5}{2}(f_1 f_4 + f_2 f_3),\ f_{17} = \frac{\mathrm{W}}{2}\left(f_4(f_1 + f_2 - 1) + (1 + f_2 - f_1)f_3\right),$$

$$f_{16} = \frac{5}{2}(f_1 f_3 - f_2 f_4),\ f_{15} = \frac{\mathrm{W}}{2}\left(f_4(1 + f_2 - f_1) - (f_1 + f_2 - 1)f_3\right),$$

$$f_{22} = f_{20}\left(\mathrm{W}(\cosh 2\mathrm{W} - \cos 2\mathrm{W}) + \frac{\sin 2\mathrm{W} - \sinh 2\mathrm{W}}{2}\right) + \left(-\mathrm{W}(f_{16} + f_{18})\cos \mathrm{W} + \right.$$

$$\left. + ((f_{15} - f_{17})\mathrm{W} + f_{16})\sin \mathrm{W}\right)\frac{\cosh \mathrm{W}}{2} - \left(((f_{17} + f_{15})\mathrm{W} - f_{18})\cos \mathrm{W} + \mathrm{W}(f_{16} - f_{18})\sin \mathrm{W}\right)\frac{\sinh \mathrm{W}}{2},$$

$$f_{21} = f_{20}\left(3\frac{\sinh 2\mathrm{W} - \sin 2\mathrm{W}}{2} + \mathrm{W}(\cos 2\mathrm{W} - \cosh 2\mathrm{W})\right) + \left((\mathrm{W}(f_{16} + f_{18}) - 2f_{15})\cos \mathrm{W} - (3f_{16} + \right.$$

$$\left. (f_{15} - f_{17})\mathrm{W})\sin \mathrm{W}\right)\frac{\cosh \mathrm{W}}{2} + \left(((f_{17} + f_{15})\mathrm{W} - 3f_{18})\cos \mathrm{W} + ((f_{16} - f_{18})\mathrm{W} - 2f_{17})\sin \mathrm{W}\right)\frac{\sinh \mathrm{W}}{2}.$$

Longitudinal velocity. Second-order longitudinal velocity is defined by the equation

$$E_2(y,t) = 0 \tag{3.44}$$

with the boundary condition (3.39). By introducing a function

$$F(y)=2\mathrm{W}^2\left(\mathrm{W}^2\mathrm{Ri}\left(\frac{\partial\overline{\mathrm{v}}_2}{\partial y}(y^2-1)-2\overline{\mathrm{v}}_2 y\right)+\frac{e_4+e_5}{2}\right),$$

and averaging (3.44) in time we get the equation for the time-averaged longitudinal velocity $\overline{\mathrm{u}}_2$:

$$\frac{\partial^2\overline{\mathrm{u}}_2}{\partial y^2}=F(y). \tag{3.45}$$

The boundary condition for the longitudinal second-order velocity is the following one

$$y=\pm 1:\overline{\mathrm{u}}_2=0. \tag{3.46}$$

The problem (3.45)-(3.46) is solved in the following way:

$$\overline{\mathrm{u}}_2=\int_1^y\int_0^{z_2}F(z_1)dz_1dz_2. \tag{3.47}$$

Due to its cumbersomeness the expression for $\overline{\mathrm{u}}_2$ is not given here in its explicit form.

3.4. Flow rate

Provided we know the zero-order and the first-order solution and time-averaged second-order solution, we can calculate the flow rate. Instantaneous flow rate is defined by the equation

$$Q=\int_{-1-A\sin t}^{1+A\sin t}\mathrm{U}d\tilde{y}. \tag{3.48}$$

After transformation of transverse coordinate (26), expression (3.48) takes the following form

$$Q=\int_{-1}^{1}\mathrm{U}(1+A\sin t)dy, \tag{3.49}$$

By substituting (32) instead of U, we get

$$Q=\int_{-1}^{1}\left(\mathrm{u}-\frac{x}{1+A\sin t}\frac{\partial\mathrm{v}}{\partial y}\right)(1+A\sin t)dy. \tag{3.50}$$

By opening the brackets in (3.50) and integrating, we find that

$$Q=\int_{-1}^{1}\mathrm{u}\cdot(1+A\sin t)dy-x(\mathrm{v}\big|_{y=1}-\mathrm{v}\big|_{y=-1}), \tag{3.51}$$

By substituting the transverse velocity at the channel walls from the boundary conditions (30) in (3.51), we get

$$Q=\int_{-1}^{1}\mathrm{u}\cdot(1+A\sin t)dy-2Ax\cos t, \tag{3.52}$$

By substituting the series (3.18) in (3.52), we present (3.52) in the following form

$$Q=Q_0+Q_1A+Q_2A^2+O(A^3), \tag{3.53}$$

where

$$Q_0=\int_{-1}^{1}\mathrm{u}_0dy, \tag{3.54}$$

$$Q_1=\int_{-1}^{1}\left(\mathrm{u}_0\sin(t)+\mathrm{u}_1\right)dy-2x\cos t, \tag{3.55}$$

$$Q_2 = \int_{-1}^{1} \left(\mathrm{u}_1 \sin(t) + \mathrm{u}_2 \right) dy \,. \tag{3.56}$$

With time averaging (3.53), we get the flow rate as

$$\bar{Q} = \bar{Q}_0 + \bar{Q}_1 A + \bar{Q}_2 A^2 + O(A^3)\,, \tag{3.57}$$

$$\bar{Q}_0 = \int_{-1}^{1} \bar{\mathrm{u}}_0 dy\,, \tag{3.58}$$

$$\bar{Q}_1 = \frac{1}{2\pi} \int_0^{2\pi} Q_1 dt, \tag{3.59}$$

$$\bar{Q}_2 = \int_{-1}^{1} \left(\frac{1}{2\pi} \int_0^{2\pi} \mathrm{u}_1 \sin(t) dt + \bar{\mathrm{u}}_2 \right) dy \,. \tag{3.60}$$

The expressions for the instantaneous and time-averaged zero-order flow rate are the same:

$$Q_0 = \int_{-1}^{1} \mathrm{u}_0 dy = \frac{4}{3} \mathrm{W}^2 \mathrm{Ri}\,. \tag{3.61}$$

Expansion term Q_0 corresponds to the contribution of Poiseuille flow in a channel with fixed walls.

By substituting u_0 from (3.22) and u_1 from (36) in (3.55), we get the following expression for the first-order instantaneous flow rate

$$Q_1 = \left(\frac{4}{3} \mathrm{W}^2 \mathrm{Ri} + \int_{-1}^{1} \mathrm{u}_{1\mathrm{s}} dy \right) \sin(t) + \int_{-1}^{1} \mathrm{u}_{1\mathrm{c}} dy \cos t - 2x \cos t. \tag{3.62}$$

Time-averaged Q_1 equals zero:

$$\bar{Q}_1 = 0. \tag{3.63}$$

In the first order the channel walls pulsations do not contribute into time-averaged flow rate.

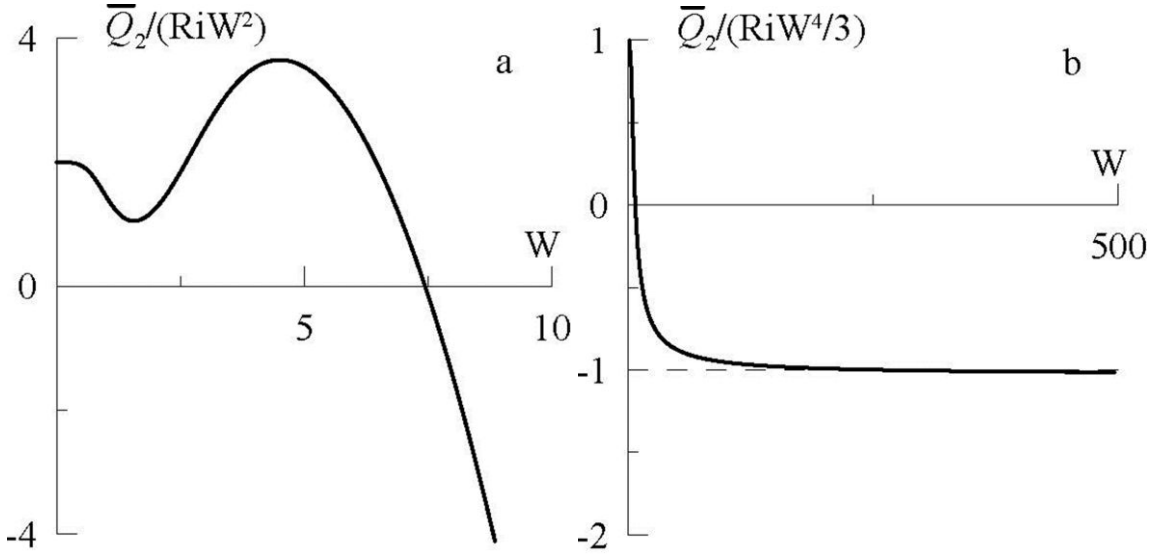

Fig.3.2. Dependence of time-averaged second-order flow rate $\bar{Q}_2$ (divided by RiW^2 (a) and $\mathrm{RiW}^4/3$ (b)) on the Womersley number

By substituting the expression (36) for u_1 in (3.60), we get a formula for time-averaged second-order flow rate:

$$\bar{Q}_2 = \int_{-1}^{1} \left(\frac{\mathrm{u}_{1s}}{2} + \bar{\mathrm{u}}_2 \right) dy . \qquad (3.64)$$

Fig.3.2 shows dependence $\bar{Q}_2$ on the Womersley number calculated by the equation (47). As we can see from Fig. 3.2a, at $\mathrm{W} \to 0$ time-averaged second-order flow rate is positive and equals to

$$\bar{Q}_2 \approx 2\mathrm{W}^2\mathrm{Ri} , \qquad (3.65)$$

which corresponds with the formula, obtained earlier by G.A.Lyakhov and I.V.Shugan [112] for this limiting case. G.A.Lyakhov and I.V.Shugan [112] predicted the increase flow rate ($\bar{Q}_2 > 0$) due to the walls pulsations, and this increase can be observed up to the Womersley number $\mathrm{W}_0 \approx 7.5$. At $\mathrm{W} > \mathrm{W}_0$ the sign Q_2 changes into the opposite one. Let us note here that for the small-amplitude pulsation the theory of Kwi-joo Lee, et al. [151] states $\bar{Q}_2$ to be always positive.

For the blood flow (viscosity $\eta = (1.2-5)$ mPa c, density $\rho = 10^3$ kg/m^3) in muscles dependent capillary ($h = 5$ mkm), the Womersley number $\mathrm{W}_0 \approx 7.5$ corresponds to the frequency of about 10^6 Hz. Thus, the effect of periodic capillary squeezing and relaxing by the working muscles on the blood flow rate is positive even at high frequency, as it was earlier suggested by N.I.Arichin [113] on the basis of his experiments.

In technical applications (for example, when one uses the channel walls pulsations to increase the pump performance efficiency) the characteristic dimension of a channel is about a centimeter. In this case the Womersley number $\mathrm{W}_0 \approx 7.5$ will correspond to the frequency of about 1 Hz, i.e. in order to have positive effect from the walls pulsations, the frequency of these pulsations should be low.

Fig. 3.2a illustrates the dependency of the flow rate on the Womersley number with its maximum $\bar{Q}_{2\max} \approx 3.7\mathrm{RiW}^2$ at $W = 4.4$. This maximum is connected with the presence of a nonzero time-averaged longitudinal velocity in the second order $\bar{\mathrm{v}}_2$ (equation (3.43)). If $\bar{\mathrm{v}}_2$ equaled zero, then the dependency of flow rate on the Womersley number would be monotonous with the intersection point with $\bar{Q}_2 = 0$ at $W \approx 1$.

The increase of flow rate for small value of Womersley number due to the pulsations is

$$\chi = \frac{Q_0 + A^2 Q_{2\max}}{Q_0} \approx \frac{\frac{4}{3} + 3.7A^2}{\frac{4}{3}} \approx 1 + 2.8A^2 . \qquad (3.66)$$

For the pulsations with the amplitude $A = 0.1$ in case of small value of Womersley number the increase of flow rate is about 1%. In order to make the pulsations effect on the flow rate more significant (of about 10-20%), one should increase the amplitude up to $A = 0.2$. Experiments [113, 150] show that in the working muscles the blood flow increases many times, but the present theory cannot explain such a situation. In this case the summand in the second order of small parameter in (3.66) will exceed the summand in zero order.

Fig. 2b shows that for large values of the Womersley number W an increase of flow rate occurred due to pulsations is negative and approximately equals

$$Q_2 \approx -k \frac{\mathrm{RiW}^4}{3} , \qquad (3.67)$$

where k is the coefficient equal to approximately one. Equation (3.67) enables one to evaluate the decrease in flow rate due to pulsations:

$$\chi = \frac{Q_0 + A^2 Q_{2\max}}{Q_0} \approx \frac{\frac{4}{3} - k\frac{\mathrm{W}^2}{3}A^2}{\frac{4}{3}} \approx 1 - \frac{k}{4}W^2A^2. \qquad (3.68)$$

For $W = 10$ and $A = 0.1$ the equation (3.68) presupposes the flow rate to be decreased by 25% due to the walls pulsations.

3.5. Time-averaged velocity

Let us consider time-averaged velocity of flow. To do this in the found solution we must perform backward transformation from the time dependent coordinate $y = \tilde{y}/(1 + A\sin t)$ to a physical coordinate $\tilde{y}$. As a result, series of longitudinal velocity (3.18) is the following one

$$\mathrm{u}(\tilde{y},t) = \mathrm{u}_0\left(\frac{\tilde{y}}{1+A\sin t},t\right) + A\mathrm{u}_1\left(\frac{\tilde{y}}{1+A\sin t},t\right) + A^2\mathrm{u}_2\left(\frac{\tilde{y}}{1+A\sin t},t\right) + \ldots \qquad (3.69)$$

By decomposing (3.69) into power series around $A = 0$ up to the second order we get

$$\begin{aligned}\mathrm{u}(\tilde{y},t) = \mathrm{u}_0(\tilde{y}) + \left(\mathrm{u}_1(\tilde{y}) - \tilde{y}\frac{\partial \mathrm{u}_0(\tilde{y})}{\partial \tilde{y}}\sin t\right)A + \\ + \left(\mathrm{u}_2(\tilde{y}) - \tilde{y}\frac{\partial \mathrm{u}_1(\tilde{y})}{\partial \tilde{y}}\sin t + \tilde{y}\left(\frac{\partial \mathrm{u}_0(\tilde{y})}{\partial \tilde{y}} + \frac{\tilde{y}}{2}\frac{\partial^2 \mathrm{u}_0(\tilde{y})}{\partial \tilde{y}^2}\right)\sin^2 t\right)A^2.\end{aligned} \qquad (3.70)$$

By substituting (3.22), (35) and (36) in (3.70) we get

$$\begin{aligned}\mathrm{u}(\tilde{y},t) = \mathrm{u}_0 + \left((\mathrm{u}_{1s} + 2\tilde{y}^2\mathrm{W}^2 Ri)\sin t + \mathrm{u}_{1c}\cos t\right)A + \\ + \left(\mathrm{u}_2 - \tilde{y}\left(\frac{\partial \mathrm{u}_{1s}}{\partial \tilde{y}} + 3\tilde{y}\mathrm{W}^2\mathrm{Ri}\right)\sin^2 t - \frac{\partial \mathrm{u}_{1c}}{\partial \tilde{y}}\tilde{y}\cos t\sin t\right)A^2\end{aligned} \qquad (3.71)$$

By time averaging (3.71) we get

$$\bar{\mathrm{u}}(\tilde{y}) = \mathrm{u}_0(\tilde{y}) + \mathrm{q}_2(\tilde{y})A^2, \qquad (3.72)$$

where

$$\mathrm{q}_2(\tilde{y}) = \bar{\mathrm{u}}_2(\tilde{y}) - \frac{\tilde{y}}{2}\left(\frac{\partial \mathrm{u}_{1s}}{\partial \tilde{y}} + 3\tilde{y}\mathrm{W}^2\mathrm{Ri}\right). \qquad (3.73)$$

Complete longitudinal velocity is defined by the equation (32), which can be presented in the following way after the transfer from y coordinate to $\tilde{y}$ coordinate:

$$\mathrm{U} = \mathrm{u}(\tilde{y},t) - x\frac{\partial \mathrm{v}(\tilde{y},t)}{\partial \tilde{y}}. \qquad (3.74)$$

Series for the transverse velocity $\mathrm{v}(\tilde{y},t)$ after the transfer from y coordinate to $\tilde{y}$ coordinate is presented in the following way:

$$\mathrm{v}(\tilde{y},t) = A\mathrm{v}_1\left(\frac{\tilde{y}}{1+A\sin t},t\right) + A^2\mathrm{v}_2\left(\frac{\tilde{y}}{1+A\sin t},t\right) + \ldots \qquad (3.75)$$

By decomposing (3.75) into a series in powers of A up to the second order we get

$$\mathrm{v}(\tilde{y},t) = \mathrm{v}_1(\tilde{y},t)A + \left(\mathrm{v}_2(\tilde{y},t) - \tilde{y}\frac{\partial \mathrm{v}_1(\tilde{y},t)}{\partial \tilde{y}}\sin t\right)A^2 + \ldots. \qquad (3.76)$$

By substituting (35) in (3.76) and time averaging, we get

$$\overline{\mathrm{v}}(\tilde{y},t)=\left(\overline{\mathrm{v}}_2(\tilde{y})-\frac{\tilde{y}}{2}\frac{\partial \mathrm{v}_{1s}}{\partial \tilde{y}}\right)A^2+\ldots \qquad (3.77)$$

After the time average and substitution (3.72) and (3.77), the expression (3.74) is changed into the following one:

$$\overline{\mathrm{U}}=\mathrm{u}_0(\tilde{y})+A^2\left[\mathrm{q}_2(\tilde{y})+\sigma_2(\tilde{y})x\right],. \qquad (3.78)$$

where

$$\sigma_2(\tilde{y})=-\frac{\partial}{\partial \tilde{y}}\left(\overline{\mathrm{v}}_2(\tilde{y})-\frac{\tilde{y}}{2}\frac{\partial \mathrm{v}_{1s}}{\partial \tilde{y}}\right). \qquad (3.79)$$

The formula (3.78) helps to calculate complete time-averaged longitudinal velocity. The first summand in square brackets in this expression is second-order time-averaged longitudinal velocity in the channel center (at $x=0$): it is proportional to the Richardson number; it becomes zero without pressure differences and gravity force.

The second summand in square brackets $\sigma_2(\tilde{y})x$ does not depend on the Richardson number Ri, its appearance is determined by the channel walls pulsation. Pressure difference and gravitational force do not affect the summand. It does not contribute into the time-averaged flow rate. In a special case $\mathrm{Ri}=0$, complete time-averaged longitudinal velocity up to second order is defined by this summand.

Calculated by the formula (3.73) the dependence of time-averaged second-order longitudinal velocity at $x=0$ on transverse coordinate, $\mathrm{q}_2(\tilde{y})$, is shown at Fig. 3.3. At small Womersley numbers,

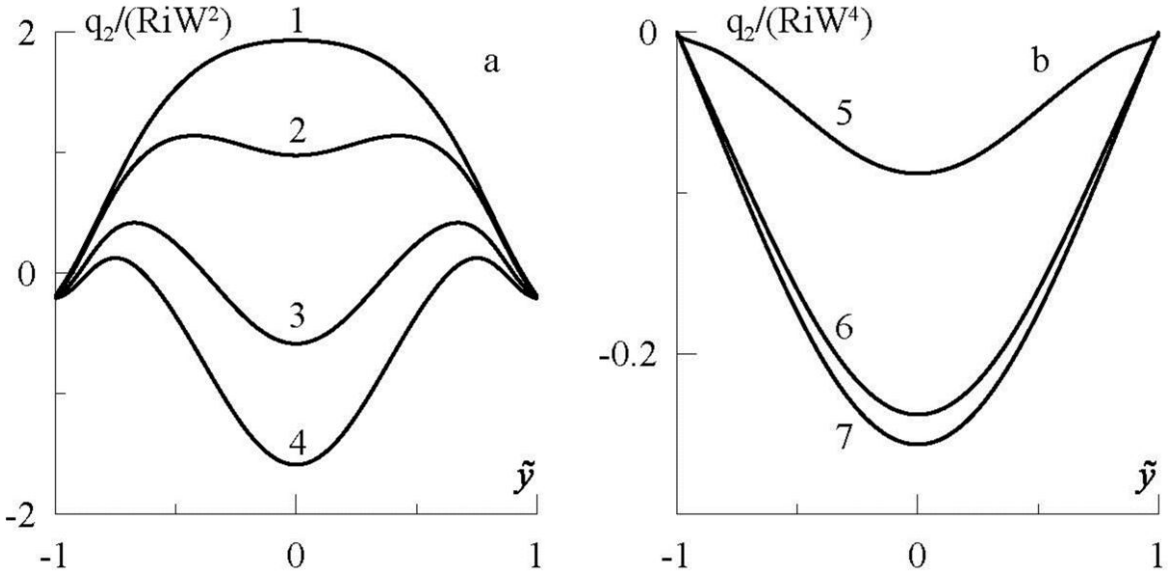

Fig.3.3. Dependence of time-averaged second-order longitudinal velocity (divided by RiW^2 (a) and RiW^4 (b)) on transverse coordinate at $x=0$ for W=5 (1), 6 (2), 7 (3), 7.5 (4), 10 (5), 50 (6), 100 (7)

q_2 is positive for practically all $\tilde{y}$ and has one point of extremum in the central part of the channel, where it reaches maximum value (Fig.3.3a, curve 1). At large values of the Womersley number (Fig.3a, curves 2-4) there are two extremum points near the walls and one minimum point in the center of the channel ($\tilde{y}=0$). Further increase of the Womersley number results in the situation, when q_2 becomes negative for all values of coordinate $\tilde{y}$ with the only point of extremum in the central part of the channel ($\tilde{y}=0$). Fig.3b illustrates, that as the Womersley number is increased, $q_2(\tilde{y})$ tends to the

asymptote $\mathrm{RiW}^4 f(\tilde{y})$, where $f(\tilde{y})$ is $\tilde{y}$ dependent, but not the Womersley and Richardson numbers dependent function.

Fig. 3.4 and 3.5 show the dependence of time-averaged full longitudinal velocity on transverse coordinate, with the velocity being divided by the longitudinal coordinate ($\bar{U}/x = \sigma_2(\tilde{y})$) and time-

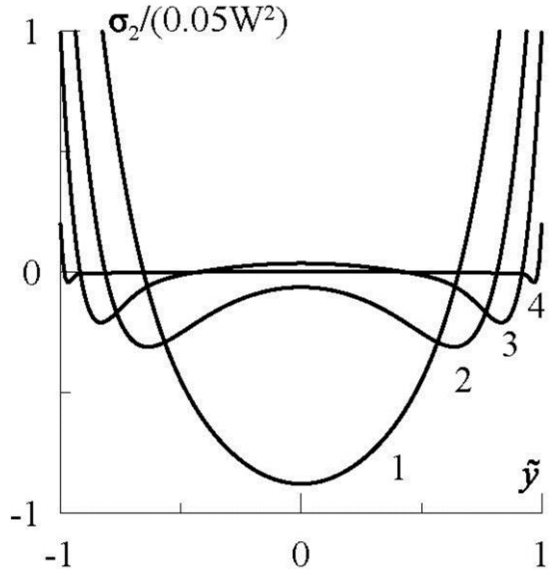

Fig. 3.4. Dependence of time-averaged longitudinal velocity divided by x coordinate on transverse coordinate $\tilde{y}$ for $\mathrm{Ri} = 0$ and W=3 (1), 5 (2), 10 (3), 50 (4)

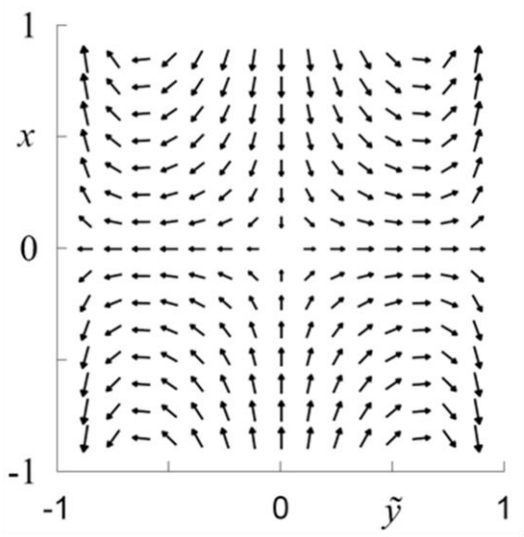

Fig. 3.5. Time-averaged velocity field for Ri=0 and W=5

averaged velocity field for $\mathrm{Ri} = 0$ (with no pressure difference and gravity). This time-averaged velocity field is multidirectional with zero flow rate. Earlier this flow was studied by T.U. Secomb [139], who examined this case only ($\mathrm{Ri} = 0$).

3.6. Conclusion

It has been found that at the Womersley numbers less than $\mathrm{W}_0 \approx 7.5$ the walls pulsations result in the increase of the flow rate, as it was obtained earlier by G.A.Lyakhov and I.V.Shugan. The paper predicted that for the Womersley numbers $\mathrm{W} > \mathrm{W}_0$ the pulsations result in the decrease of flow rate. The higher value of the Womersley number is, the more significant the predicted decrease of flow rate appears to be.

The Womersley number at the point of sign changes $\bar{Q}_2$ is about one, thus leading us to conclude that in the sphere of positive values $\bar{Q}_2$ viscosity determined effects dominate over the inertia effects, occurred due to the liquid flow cause by the walls pulsations. At negative $\bar{Q}_2$ inertial effects are the dominating ones.

Time-averged velocity field, occurred due to the pulsating walls, pressure difference and gravity, may be divided into two components. The first one is solely connected with the pulsation of

walls: pressure difference and gravity force do not affect it. It does not contribute into the time-averaged flow rate.

The second component of the time-averaged velocity field arises from the joint influence of pulsations, pressure difference and gravity. The distribution of this component along the transverse coordinate has the point of extremum in the center of the channel with the small Womersley numbers having the maximum and the large Womersley numbers having the minimum.

Evaluations made on the basis of the obtained equations for the blood flow in the capillaries showes that periodic squeeze and relax of capillaries by the working muscles results in blood flow increase, as Y.I.Arichin assumed on the basis of his experiments. Further research development in this direction may be connected with considering such facttors, as liquid compressibility and complex rheological blood properties, pulse waves, peculiarities of capillary walls and muscle fiber structure.

3.7. Influence of compressibility

3.7.1. Problem statement

The first part of this chapter looks at the influence of channel pulsations on fluid transfer assuming that it is incompressible. Such an assumption is valid for pulsations with small frequencies only. Here we take into account fluid compressibility. In this case in addition to those dimensional parameters which have been introduced earlier the second viscosity $\tilde{\xi}$ and sound velocity C appear.

Problem research is based on the Navier-Stokes equations for compressible fluid:

$$\rho\frac{\partial \mathrm{u}}{\partial t}+\rho\mathrm{u}\frac{\partial \mathrm{u}}{\partial x}+\rho\mathrm{v}\frac{\partial \mathrm{u}}{\partial y}=-\frac{\partial \mathrm{p}}{\partial x}+\eta\left[\frac{\partial^2 \mathrm{u}}{\partial y^2}+\frac{\partial^2 \mathrm{u}}{\partial x^2}\right]+\left[\tilde{\xi}+\frac{\eta}{3}\right]\frac{\partial}{\partial x}\left[\frac{\partial \mathrm{v}}{\partial y}+\frac{\partial \mathrm{u}}{\partial x}\right]+\rho g,$$

$$\rho\frac{\partial \mathrm{v}}{\partial t}+\rho\mathrm{u}\frac{\partial \mathrm{v}}{\partial x}+\rho\mathrm{v}\frac{\partial \mathrm{v}}{\partial y}=-\frac{\partial \mathrm{p}}{\partial y}+\eta\left[\frac{\partial^2 \mathrm{v}}{\partial x^2}+\frac{\partial^2 \mathrm{v}}{\partial y^2}\right]+\left[\tilde{\xi}+\frac{\eta}{3}\right]\frac{\partial}{\partial y}\left[\frac{\partial \mathrm{v}}{\partial y}+\frac{\partial \mathrm{u}}{\partial x}\right], \tag{3.80}$$

$$\frac{\partial \rho}{\partial t}+\frac{\partial \mathrm{u}\rho}{\partial x}+\frac{\partial \mathrm{v}\rho}{\partial y}=0,$$

and equation of fluid condition:

$$\mathrm{p}=C^2(\rho-\rho_i), \tag{3.81}$$

where ρ_i is equilibrium value of density. The boundary conditions are

$$y=\pm(h+\alpha\sin\omega t):\ \mathrm{v}=\pm\alpha\omega\cos\omega t,\ \mathrm{u}=0. \tag{3.82}$$

Let us assume that there is no pressure drop at the channel's ends, and fluid moves by the gravity force directed along the channel.

Let us introduce the measurement units as follows. Channel axis transverse coordinate x is measured in h, longitudinal coordinate y – in h, time t – in $1/\omega$, pressure p – in $\eta\omega$, density – in ρ_i, longitudinal velocity and transverse velocity v – in $h\omega$. Problem is characterized by six dimensionless parameters: dimensionless pulsation frequency Ω, second dimensionless pulsation frequency Ω_2,

Froude number Fr, dimensionless sound velocity c, dimensionless pulsation amplitude A and dimensionless channel length L:

$$\Omega=\frac{\omega h^2\rho_i}{\eta};\Omega_2=\frac{\omega h^2\rho_i}{\tilde{\xi}+\frac{\eta}{3}};\mathrm{Fr}=\frac{-g}{h\omega^2};\alpha=\frac{A}{h};c^2=\frac{C^2\rho_i}{\eta\omega};L=\frac{L'}{h}. \tag{3.83}$$

In dimensionless form the equations are as follows

$$\rho\left(\frac{\partial \mathrm{u}}{\partial t}+\mathrm{u}\frac{\partial \mathrm{u}}{\partial x}+\mathrm{v}\frac{\partial \mathrm{u}}{\partial y}\right)=\frac{1}{\Omega}\left[\frac{\partial^2\mathrm{u}}{\partial y^2}+\frac{\partial^2\mathrm{u}}{\partial x^2}-\frac{\partial \mathrm{p}}{\partial x}\right]+\frac{1}{\Omega_2}\frac{\partial}{\partial x}\left[\frac{\partial \mathrm{v}}{\partial y}+\frac{\partial \mathrm{u}}{\partial x}\right]+\rho\mathrm{Fr}, \tag{3.84}$$

$$\rho\left(\frac{\partial \mathrm{v}}{\partial t}+\mathrm{u}\frac{\partial \mathrm{v}}{\partial x}+\mathrm{v}\frac{\partial \mathrm{v}}{\partial y}\right)=-\frac{1}{\Omega}\frac{\partial \mathrm{p}}{\partial y}+\frac{1}{\Omega}\left[\frac{\partial^2\mathrm{v}}{\partial x^2}+\frac{\partial^2\mathrm{v}}{\partial y^2}\right]+\frac{1}{\Omega_2}\frac{\partial}{\partial y}\left[\frac{\partial \mathrm{v}}{\partial y}+\frac{\partial \mathrm{u}}{\partial x}\right], \tag{3.85}$$

$$\frac{\partial\rho}{\partial t}+\frac{\partial \mathrm{u}\rho}{\partial x}+\frac{\partial \mathrm{v}\rho}{\partial y}=0,$$

$$\mathrm{p}=c^2(\rho-1), \tag{3.86}$$

and boundary conditions take the following form -

$$y=\pm(1+A\sin t):\ \mathrm{v}=\pm A\cos t,\ \mathrm{u}=0. \tag{3.87}$$

$$x=\pm L:\ p=0.$$

After transformation to new coordinates -

$$\tilde{y}=\frac{y}{1+A\sin t},\tilde{t}=t,\tilde{x}=x, \tag{3.88}$$

equations system (3.84)-(3.86) is as follows

$$\rho\left(\frac{\partial \mathrm{u}}{\partial \tilde{t}}-\frac{\tilde{y}A\cos t}{1+A\sin\tilde{t}}\frac{\partial \mathrm{u}}{\partial \tilde{y}}+\mathrm{u}\frac{\partial \mathrm{u}}{\partial \tilde{x}}+\frac{\mathrm{v}}{1+A\sin\tilde{t}}\frac{\partial \mathrm{u}}{\partial \tilde{y}}\right)=$$

$$=\frac{1}{\Omega}\left[\frac{1}{(1+A\sin\tilde{t})^2}\frac{\partial^2\mathrm{u}}{\partial\tilde{y}^2}+\frac{\partial^2\mathrm{u}}{\partial\tilde{x}^2}-\frac{\partial \mathrm{p}}{\partial\tilde{x}}\right]+\frac{1}{\Omega_2}\frac{\partial}{\partial\tilde{x}}\left[\frac{1}{1+A\sin t}\frac{\partial \mathrm{v}}{\partial\tilde{y}}+\frac{\partial \mathrm{u}}{\partial\tilde{x}}\right]+\rho\mathrm{Fr},$$

$$\rho\left(\frac{\partial \mathrm{v}}{\partial \tilde{t}}-\frac{\tilde{y}A\cos\tilde{t}}{1+A\sin\tilde{t}}\frac{\partial \mathrm{v}}{\partial\tilde{y}}+\mathrm{u}\frac{\partial \mathrm{v}}{\partial\tilde{x}}+\frac{\mathrm{v}}{1+A\sin\tilde{t}}\frac{\partial \mathrm{v}}{\partial\tilde{y}}\right)=-\frac{1}{\Omega(1+A\sin\tilde{t})}\frac{\partial \mathrm{p}}{\partial\tilde{y}}+$$

$$+\frac{1}{\Omega}\left[\frac{\partial^2\mathrm{v}}{\partial\tilde{x}^2}+\frac{1}{(1+A\sin\tilde{t})^2}\frac{\partial^2\mathrm{v}}{\partial\tilde{y}^2}\right]+\frac{1}{\Omega_2}\frac{1}{1+A\sin\tilde{t}}\frac{\partial}{\partial\tilde{y}}\left[\frac{1}{1+A\sin\tilde{t}}\frac{\partial \mathrm{v}}{\partial\tilde{y}}+\frac{\partial \mathrm{u}}{\partial\tilde{x}}\right], \tag{3.89}$$

$$\frac{\partial\rho}{\partial\tilde{t}}-\frac{\tilde{y}A\cos\tilde{t}}{1+A\sin\tilde{t}}\frac{\partial\rho}{\partial\tilde{y}}+\frac{\partial \mathrm{u}\rho}{\partial\tilde{x}}+\frac{1}{1+A\sin\tilde{t}}\frac{\partial \mathrm{v}\rho}{\partial\tilde{y}}=0,$$

$$\mathrm{p}=c^2(\rho-1), \tag{3.90}$$

and the boundary conditions -(3.87) are the following ones :

$$\tilde{y}=\pm1:\ \mathrm{v}=\pm A\cos t,\ \mathrm{u}=0, \tag{3.91}$$

Further we will omit tilde above y, x and t.

Let us assume that u, p and v do not depend on longitudinal coordinate. In this case the equations system (3.89) is as follows

$$\rho\left(\frac{\partial \mathrm{u}}{\partial t}+\frac{\mathrm{v}-yA\cos t}{1+A\sin t}\frac{\partial \mathrm{u}}{\partial y}\right)=\frac{1}{\Omega}\frac{1}{(1+A\sin t)^2}\frac{\partial^2 \mathrm{u}}{\partial y^2}+\rho \mathrm{Fr},$$

$$\rho\left(\frac{\partial \mathrm{v}}{\partial t}+\frac{\mathrm{v}-yA\cos t}{1+A\sin t}\frac{\partial \mathrm{v}}{\partial y}\right)=-\frac{1}{\Omega(1+A\sin t)}\frac{\partial \mathrm{p}}{\partial y}+\left(\frac{1}{\Omega}+\frac{1}{\Omega_2}\right)\frac{1}{(1+A\sin t)^2}\frac{\partial^2 \mathrm{v}}{\partial y^2}, \tag{3.92}$$

$$\frac{\partial \rho}{\partial t}-\frac{yA\cos t}{1+A\sin t}\frac{\partial \rho}{\partial y}+\frac{1}{1+A\sin t}\frac{\partial \mathrm{v}\rho}{\partial y}=0,$$

By substituting (3.90) in (3.92), we finally get

$$\rho\left(\frac{\partial \mathrm{u}}{\partial t}+\frac{\mathrm{v}-yA\cos t}{1+A\sin t}\frac{\partial \mathrm{u}}{\partial y}\right)=\frac{1}{\Omega}\frac{1}{(1+A\sin t)^2}\frac{\partial^2 \mathrm{u}}{\partial y^2}+\rho \mathrm{Fr}, \tag{3.93}$$

$$\rho\left(\frac{\partial \mathrm{v}}{\partial t}+\frac{\mathrm{v}-yA\cos t}{1+A\sin t}\frac{\partial \mathrm{v}}{\partial y}\right)=-\frac{c^2}{\Omega(1+A\sin t)}\frac{\partial \rho}{\partial y}+\left(\frac{1}{\Omega}+\frac{1}{\Omega_2}\right)\frac{1}{(1+A\sin t)^2}\frac{\partial^2 \mathrm{v}}{\partial y^2}, \tag{3.94}$$

$$\frac{\partial \rho}{\partial t}-\frac{yA\cos t}{1+A\sin t}\frac{\partial \rho}{\partial y}+\frac{1}{1+A\sin t}\frac{\partial \mathrm{v}\rho}{\partial y}=0. \tag{3.95}$$

The next paragraph finds the solution for the obtained equation system (3.93)-(3.95) with a method of small parameter.

3.7.2. Approximation of small amplitudes

Let us consider a case of small amplitude of wall vibrations ($A<<1$). We are going to find the solution in the series of A:

$$\mathrm{v}=A\mathrm{v}_1+A^2\mathrm{v}_2+\ldots\quad \mathrm{u}=\mathrm{u}_0+A\mathrm{u}_1+A^2\mathrm{u}_2+\ldots;\ \mathrm{p}=\mathrm{p}_0+A\mathrm{p}_1+A^2\mathrm{p}_2+\ldots;$$

$$\rho=\rho_0+A\rho_1+A^2\rho_2+\ldots$$

Zero order. In zero order the equation system under study is as follows

$$\frac{1}{\Omega}\frac{\partial^2 \mathrm{u}_0}{\partial y^2}+\rho_0\mathrm{Fr}=0,$$

$$-c^2\frac{\partial \rho_0}{\partial y}+\frac{\partial^2 \mathrm{v}_0}{\partial y^2}=0, \tag{3.96}$$

$$\frac{\partial \rho_0}{\partial t}+\frac{\partial \mathrm{v}_0\rho_0}{\partial y}=0,$$

The solution of this equation system:

$$\mathrm{u}_0=-\frac{y^2-1}{2}\Omega\mathrm{Fr},\ \mathrm{p}_0=0,\ \rho_0=1,\ \mathrm{v}_0=0.$$

Thus, in zero order, as it should be, we have a solution describing the Poiseuille flow.

First order. In the first order the problem takes the following form

$$\frac{\partial \mathrm{u}_1}{\partial t} + y^2 \Omega \mathrm{Fr} \cos t - y \Omega \mathrm{Fr} \mathrm{v}_1 = \frac{1}{\Omega} \frac{\partial^2 \mathrm{u}_1}{\partial y^2} + \rho_1 \mathrm{Fr} + 2\mathrm{Fr} \sin t,$$

$$\frac{\partial \mathrm{v}_1}{\partial t} = -\frac{c^2}{\Omega} \frac{\partial \rho_1}{\partial y} + \left(\frac{1}{\Omega} + \frac{1}{\Omega_2} \right) \frac{\partial^2 \mathrm{v}_1}{\partial y^2}, \tag{3.97}$$

$$\frac{\partial \rho_1}{\partial t} + \frac{\partial \mathrm{v}_1}{\partial y} = 0,$$

$$y = \pm 1 : \ \mathrm{v}_1 = \pm \cos t \, , \ \mathrm{u}_1 = 0. \tag{3.98}$$

The solution of this problem is longitudinal velocity in form

$$\begin{aligned} \mathrm{u}_1 = {} & C_s^+ e^{\Omega' y} \sin(t + \Omega' y) + C_s^- e^{-\Omega' y} \sin(t - \Omega' y) + C_c^+ e^{\Omega' y} \cos(t + \Omega' y) + \\ & + C_c^- e^{-\Omega' y} \cos(t - \Omega' y) + U_s^- e^{-\delta y} \sin(t - yk) + U_c^- e^{-\delta y} \cos(t - yk) + \\ & + U_s^+ e^{\delta y} \sin(t + yk) + U_c^+ e^{\delta y} \cos(t + yk) + y \left[U_{ys}^- e^{-\delta y} \sin(t - yk) + \right. \\ & \left. + U_{yc}^- e^{-\delta y} \cos(t - yk) + U_{ys}^+ e^{\delta y} \sin(t + yk) + U_{yc}^+ e^{\delta y} \cos(t + yk) \right] \\ & - y^2 \Omega \mathrm{Fr} \sin t, \end{aligned} \tag{3.99}$$

transverse velocity in the form

$$\begin{aligned} \mathrm{v}_1 = {} & V_{1s}^- e^{-\delta y} \sin(t - yk) + V_{1c}^- e^{-\delta y} \cos(t - yk) \\ & + V_{1s}^+ e^{\delta y} \sin(t + yk) + V_{1c}^+ e^{\delta y} \cos(t + yk), \end{aligned} \tag{3.100}$$

and density in the form

$$\begin{aligned} \rho_1 = {} & R_{1s}^- e^{-\delta y} \sin(t - yk) + R_{1c}^- e^{-\delta y} \cos(t - yk) \\ & + R_{1s}^+ e^{\delta y} \sin(t + yk) + R_{1c}^+ e^{\delta y} \cos(t + yk), \end{aligned} \tag{3.101}$$

where the variables are introduced:

$$k = \sqrt{\frac{\Omega \Omega_2}{2} \frac{\sqrt{\Omega_2^2 c^4 + (\Omega_2 + \Omega)^2} + \Omega_2 c^2}{c^4 \Omega_2^2 + (\Omega_2 + \Omega)^2}} ; \tag{3.102}$$

$$\delta = \sqrt{\frac{\Omega \Omega_2}{2} \frac{\sqrt{\Omega_2^2 c^4 + (\Omega_2 + \Omega)^2} - \Omega_2 c^2}{c^4 \Omega_2^2 + (\Omega_2 + \Omega)^2}} ; \tag{3.103}$$

$$\Omega' = \sqrt{\frac{\Omega}{2}} \tag{3.104}$$

Formulas to calculate the constants $C_{s,c}^{\pm}$, $U_{s,c}^{\pm}$, $U_{ys,yc}^{\pm}$, $V_{s,c}^{\pm}$, $R_{s,c}^{\pm}$ are given in Appendix 3.

The equations (3.99), (3.100) and (3.101) show that the vibrations of channel's walls result in the appearance of two types of waves. The waves of the first type (first four terms in (3.99)) are transverse:

$$\begin{aligned} \mathrm{u}_{1tr} = {} & C_s^+ e^{\Omega' y} \sin(t + \Omega' y) + C_s^- e^{-\Omega' y} \sin(t - \Omega' y) \\ & + C_c^+ e^{\Omega' y} \cos(t + \Omega' y) + C_c^- e^{-\Omega' y} \cos(t - \Omega' y), \end{aligned}$$

$$v_{1tr} = 0,\ \rho_{1tr} = 0.$$

They cause the vibrations of fluid particles along the channel and run in transverse direction. Damp coefficient and the wave number of these waves equal parameter Ω', which is the Womersley number by nature. To find the depth of wave penetration into the fluid let us look at the specific example: a 2 cm thick channel with water falling under the gravity force, and the channel's walls vibrate with 24 kHz frequency. In this case

$$\Omega = \frac{\rho\omega h^2}{\eta} \sim \frac{10^3 \cdot 24000 \cdot 2 \cdot \pi \cdot 4 \cdot 10^{-4}}{10^{-2}} \sim 6 \cdot 10^6,$$

$$\Omega' \sim 2500,$$

an dimensional damp coefficient and the wave number are

$$\Omega' / h = 5000 / (2 \cdot 10^{-2}) \sim 10^5 \ \text{m}^{-1}.$$

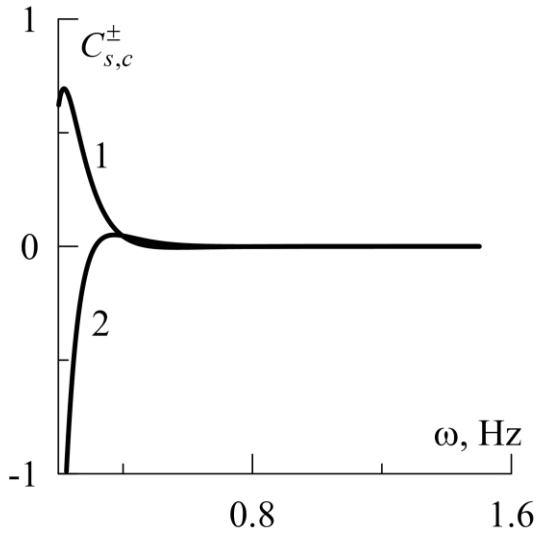

Fig. 3.8. Dependency of amplitudes of transverse wave $C^{\pm}_{s,c}$ on dimensional frequency of channel pulsation for 1 - $C^{\pm}_{c}$, 2 - $C^{\pm}_{s}$ for $\Omega = 375$, $\Omega_2 = 120$, $c = 1.5 \cdot 10^5$, $\text{Fr} = 5.5$ ($\rho = 10^3$ kg/м^3, $h = 2$ cm, $\eta = 10^{-2}$ Pa s, $C = 1500$ m/s, $g = 9.8$ m/s^2, $\tilde{\xi} = 2.81\eta$)

Here the penetration depth is 10^{-5} m or 10^{-3} cm. Thus, the depth of penetration of this wave appears to be about 1,000 times less than the channels size. If we decrease the frequency in 10^4 times, then the penetration depth will be about 1 millimeter and 10 times less the channel's thickness. Thus, the low frequency transverse waves influence the flow in a channel the most.

Fig. 3.8 shows that the amplitude of the transverse waves $C^{\pm}_{s,c}$ decays very quickly with the frequency increase. For the high frequency vibrations of walls with 25000 Hz vibration frequency the amplitude of the wave $C^{\pm}_{s,c} \sim 10^{-753}$ and transverse waves should be small to negligible, however, due to the fact that this small amplitude is multiplied by exponent with input variable included $\Omega' = \sqrt{24000}$, the resulting value appears to be small, but not so small, as one could have thought.

Fig. 3.9 illustrates the dependency on y coordinate of longitudinal velocity appeared due to the transverse waves. Near the walls its value will be $10^{-7} - 10^{-8}$ (Fig. 3.9a). The transverse waves'

influence the flow only in small boundary area, their influence in other areas may be neglected (Fig. 3.9b).

Besides pure transverse waves, the vibrations of the walls cause another type of waves, which is characterized by the fact that the particles of the medium move both perpendicular and longitudinally relative to the channel axis. The relation between wave vector and wave frequency is described by the equation (3.102), which is as follows in dimensional form

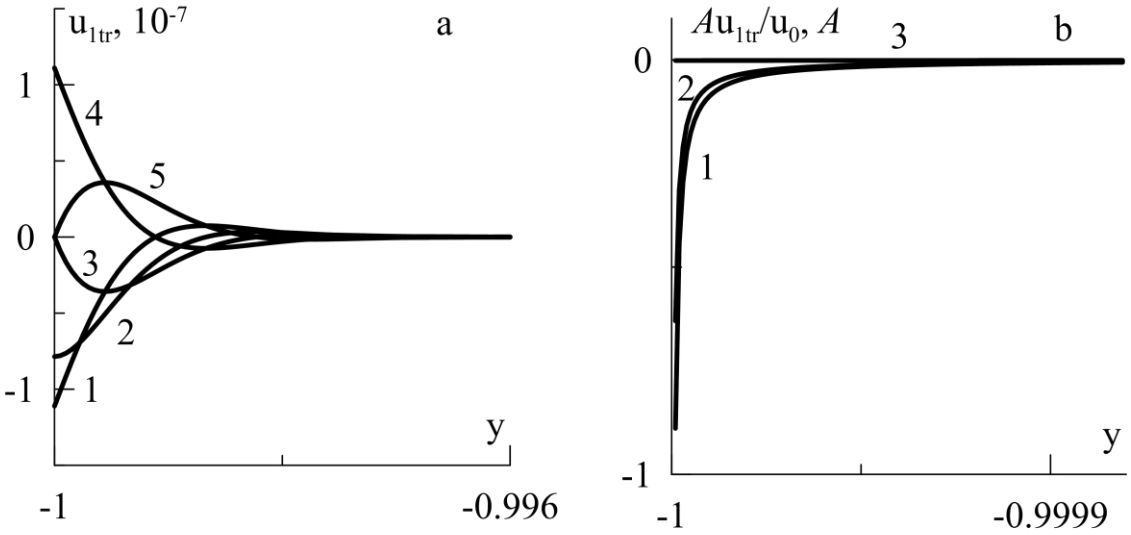

Fig.3.9. a – dependency of additive to longitudinal velocity caused by transverse waves, b – the same dependency divided by the longitudinal velocity in zero order for $\Omega = 375$, $\Omega_2 = 120$, $c = 1200$, $\mathrm{Fr} = 5.5$ in the moment of time $t = 0$ (1), $t = \frac{\pi}{4}$ (2), $t = \frac{\pi}{2}$ (3), $t = \pi$ (4), $t = \frac{3\pi}{2}$ (5)

$$k' = \omega \sqrt{\frac{\rho_i}{2\eta} \frac{\sqrt{\left(\frac{C^2\rho_i}{\eta}\right)^2 + \omega^2\left(\frac{4}{3} + \frac{\xi}{\eta}\right)^2} + \frac{C^2\rho_i}{\eta}}{\left(\frac{C^2\rho_i}{\eta}\right)^2 + \omega^2\left(\frac{4}{3} + \frac{\xi}{\eta}\right)^2}} . \qquad (3.105)$$

At small values of frequency ω linear term contributes the most in dispersion relation:

$$k' = \frac{1}{C}\omega - \frac{1}{24}\frac{(4\eta + 3\tilde{\xi})}{C^5\rho^2}\omega^3 + O(\omega^5) . \qquad (3.106)$$

Otherwise, at large frequencies the expression (3.105) tends to asymptote

$$k' = \sqrt{\frac{3\rho\omega}{2(4\eta + 3\tilde{\xi})}} + \frac{3}{4}\frac{\rho C^2}{(4\eta + 3\tilde{\xi})^{3/2}}\sqrt{\frac{6\rho}{\omega}} + O(\omega^{-3/2}) . \qquad (3.107)$$

Damp coefficient of the wave is described by the relation (3.103), which is as follows in dimensional form

$$\delta' = \omega \sqrt{\frac{\rho_i}{2\eta} \frac{\sqrt{\left(\frac{C^2\rho_i}{\eta}\right)^2 + \omega^2\left(\frac{4}{3}+\frac{\tilde{\xi}}{\eta}\right)^2} - \frac{C^2\rho_i}{\eta}}{\left(\frac{C^2\rho_i}{\eta}\right)^2 + \omega^2\left(\frac{4}{3}+\frac{\tilde{\xi}}{\eta}\right)^2}}\,. \tag{3.108}$$

This coefficient is always positive, except for a trivial case when frequency equals zero. At small values of frequency the damp coefficient grows with it in accordance with the quadratic law

$$\delta' = \frac{(4\eta+3\tilde{\xi})}{6C^3\rho}\omega^2 - \frac{5(4\eta+3\tilde{\xi})^3}{432C^7\rho^3}\omega^4 + \mathrm{O}(\omega^6)\,. \tag{3.109}$$

Evaluation of the convergence area for series (3.109) may be based on the d'Alembert's ratio test with the ratio of $(n+1)$ term to n^{th} term:

$$\frac{|\delta'_{n+1}|}{|\delta'_n|}\frac{100\rho^2C^4}{\omega^2(4\eta+3\xi)^2} = 6.9,\ 8.75,\ 9.4,\ 9.8,...\ \text{for}\ n = 1,2,.. \tag{3.110}$$

Thus, for the series convergence it is necessary to have

$$\omega < \sqrt{10}\,\frac{\rho C^2}{4\eta+3\tilde{\xi}}\,. \tag{3.111}$$

For water the limiting frequency (3.109) is going to be 10^{10} Hz.

Otherwise at large frequencies the expression (3.108) tends to asymptote

$$\delta' = \sqrt{\frac{3\rho\omega}{2(4\eta+3\tilde{\xi})}} - \frac{3\rho C^2}{4(4\eta+3\tilde{\xi})^{3/2}}\sqrt{\frac{6\rho}{\omega}} + \mathrm{O}(\omega^{-3/2})\,. \tag{3.112}$$

Let us see how large the frequencies should be to apply the formula (3.112) for water. The ratio of $(n+1)$ term to n^{th} term in a series (3.112) is as follows

$$10^{-10}\frac{|\delta'_{n+1}|}{|\delta'_n|}\omega = 3,\ 4.6,\ 5.2,\ 5.4,\ 5.6,\ 5.7\ \text{for}\ n = 1,2,.. \tag{3.113}$$

Thus, the pulsation frequency should be more than 10^{10} Hz for the series (3.112) to converge in case of water.

To understand how deep the waves penetrate into the fluid, let us look at the some example, as for the transverse waves: a 2 cm thick channel with water falling under the gravity force, and the channel's walls vibrate with 25 kHz frequency. In this case the dimensionless damp coefficient is

$$\delta \sim 2.65\cdot 10^{-6}, \tag{3.114}$$

and the dimensional one is

$$\delta' \sim 1.32813195026\cdot 10^{-4}\ \mathrm{m}^{-1}. \tag{3.115}$$

Formula (3.109) gives the following value

$$\delta' \sim 1.32813195027\cdot 10^{-4}\ \mathrm{m}^{-1}. \tag{3.116}$$

that is in this case one may use the formula (3.109) with no loss of accuracy. Here obtained penetration depth is 10^4 m, that is the waves do not decay inside a channel filled with water.

With 25 kHz frequency, as it is shown in Fig. 3.10a, the value of longitudinal velocity part corresponding the waves of the second type is about 0.1 A. Taking into account the fact that first-order velocity for $\Omega = 375$ and $\mathrm{Fr} = 5.5$ is about 700, we see that the waves contribute into the main flow quite little. Fig. 3.10 shows that waves overlapping inside the channel causes the standing wave with a nod appear at the center of the channel.

With 25 kHz frequency the specific value of amplitude of density vibrations is $2A$ or talking about the dimensional form - $2\rho_i \frac{\alpha}{h}$. Typically the correlation $\frac{\alpha}{h}$ is a value, which is less than 0.001, so the density change will be less than 1%, that allow the use of equation (3.81), where density and pressure are linearly connected.

Second-order density. To identify the influence of walls' vibrations on the substance transport one should know the second-order solution. The second-order continuity equation is as follows

$$\frac{\partial \rho_2}{\partial t} + \frac{\partial \rho_1}{\partial t}\sin t - y\cos t\frac{\partial \rho_1}{\partial y} + \frac{\partial \mathrm{v}_1\rho_1}{\partial y} + \frac{\partial \mathrm{v}_2\rho_0}{\partial y} = 0, \tag{3.117}$$

equation for longitudinal velocity:

$$\begin{aligned}\frac{1}{\Omega}\frac{\partial^2 \mathrm{u}_2}{\partial y^2} = &-4\mathrm{Fr}\rho_1\sin t - 6\mathrm{Fr}\rho_0\sin^2 t - \frac{2\sin t}{\Omega}\frac{\partial^2 u_1}{\partial y^2} \\ &- 3\rho_0 y\frac{\partial \mathrm{u}_0}{\partial y}\cos t\sin t + \rho_0\frac{\partial \mathrm{u}_2}{\partial t} + \rho_1\frac{\partial \mathrm{u}_1}{\partial t} + 4\rho_0\frac{\partial \mathrm{u}_1}{\partial t}\sin t \\ &+ \rho_0\mathrm{v}_1\frac{\partial \mathrm{u}_1}{\partial y} + \rho_0\mathrm{v}_2\frac{\partial \mathrm{u}_0}{\partial y} + \rho_1\mathrm{v}_1\frac{\partial \mathrm{u}_0}{\partial y} + 3\rho_0\mathrm{v}_1\frac{\partial \mathrm{u}_0}{\partial y}\sin t \\ &- \rho_0 y\frac{\partial \mathrm{u}_1}{\partial y}\cos t - \rho_1 y\frac{\partial \mathrm{u}_0}{\partial y}\cos t - \frac{\sin^2 t}{\Omega}\frac{\partial^2 \mathrm{u}_0}{\partial y^2} - \mathrm{Fr}\rho_2,\end{aligned} \tag{3.118}$$

equation for transverse velocity:

$$\begin{aligned}&2\rho_0\frac{\partial \mathrm{v}_1}{\partial t}\sin t + \rho_0\mathrm{v}_1\frac{\partial \mathrm{v}_1}{\partial y} + \frac{c^2}{\Omega}\frac{\partial \rho_2}{\partial y} + \left(\frac{1}{\Omega_2} + \frac{1}{\Omega}\right)\frac{\partial^2 \mathrm{v}_2}{\partial y^2} \\ &+ \rho_1\frac{\partial \mathrm{v}_1}{\partial t} + \rho_0\frac{\partial \mathrm{v}_2}{\partial t} - \rho_0 y\frac{\partial \mathrm{v}_1}{\partial y}\cos t + \frac{c^2}{\Omega}\frac{\partial \rho_1}{\partial y}\sin t = 0.\end{aligned} \tag{3.119}$$

Transverse velocity v_2 should be periodic time function. Averaging (3.117)in time with taking into account periodic behavior of v_2 and limit in density growth we get

$$\int_0^{2\pi}\left[\frac{\partial \rho_1}{\partial t}\sin t - y\cos t\frac{\partial \rho_1}{\partial y} + \frac{\partial \mathrm{v}_1\rho_1}{\partial y}\right]dt = 0, \tag{3.120}$$

By substitution we may see that this equality is correct. Averaging (3.119) in time with the requirements of periodic behavior we get

$$\frac{\partial \overline{\rho}_2}{\partial y} = \frac{\Omega}{2\pi c^2}\int_0^{2\pi}\left(\rho_0\frac{\partial \mathrm{v}_1}{\partial y}(y\cos t - \mathrm{v}_1) - 2\rho_0\frac{\partial \mathrm{v}_1}{\partial t}\sin t - \rho_1\frac{\partial \mathrm{v}_1}{\partial t} - \frac{c^2}{\Omega}\frac{\partial \rho_1}{\partial y}\sin t\right)dt, \tag{3.121}$$

Here for $\overline{\rho}_2$, time-independent term in the expression for density we get

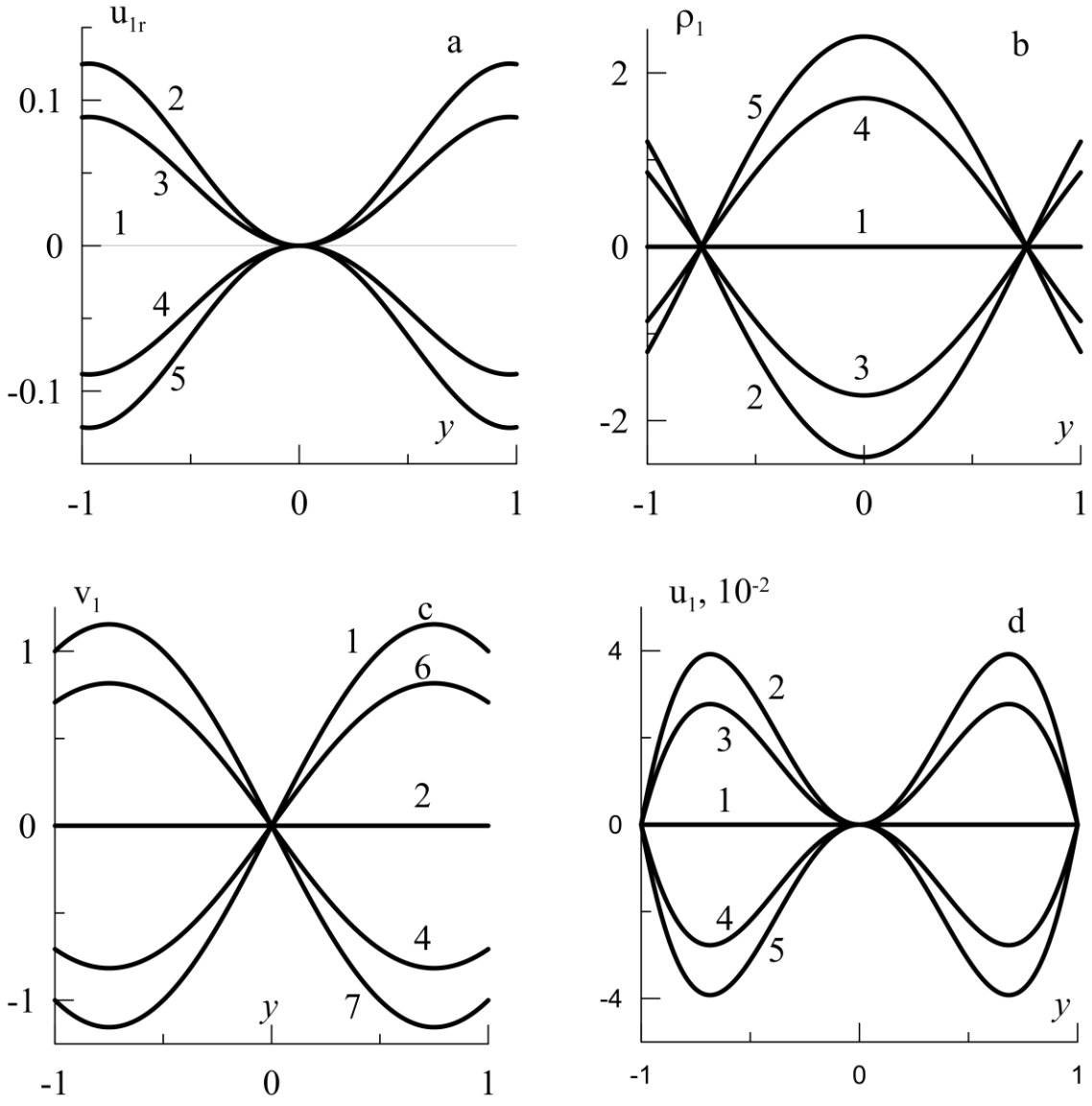

Fig. 3.10. Dependency of coordinate a – part of longitudinal velocity corresponding to the second type waves, b – complete density, c – complete transverse velocity, d – complete longitudinal velocity at the time moments $t=0$ (1), $t=\frac{\pi}{2}$ (2), $t=\frac{3\pi}{4}$ (3), $t=\frac{5\pi}{4}$ (4), $t=\frac{3\pi}{2}$ (5), $t=\frac{\pi}{4}$ (6), $t=\pi$ (7) для $\Omega=375$, $\Omega_2=120$, $c=1200$, $\mathrm{Fr}=5.5$.

$$\begin{aligned}\bar{\rho}_2 = C + \Big(&\Big[y\Omega(\delta^2+k^2)\cos k(y+1) - k(c^2(\delta^2+k^2)-\Omega)\sin k(y+1)\Big]\cosh\delta(y-1)\\ &+\Big[-y\Omega(\delta^2+k^2)\cos k(y-1) + k(c^2(\delta^2+k^2)-\Omega)\sin k(y-1)\Big]\cosh\delta(y+1)\\ &-\delta(c^2(\delta^2+k^2)+\Omega)\sinh\delta(y+1)\cos k(y-1) + \delta(c^2(\delta^2+k^2)\\ &+\Omega)\sinh\delta(y-1)\cos k(y-1) + \delta(c^2(\delta^2+k^2)+\Omega)\sinh\delta(y-1)\cos k(y+1)\\ &+\Omega(\delta^2+k^2)(\cosh 2\delta y - \cos 2yk)\Big) / (2c^2(\delta^2+k^2)(\cos 2k - \cosh 2\delta)),\end{aligned} \tag{3.122}$$

where C is constant, which is identified from an assumption about the zero equality of y coordinate-averaged density $\bar{\rho}_2$.

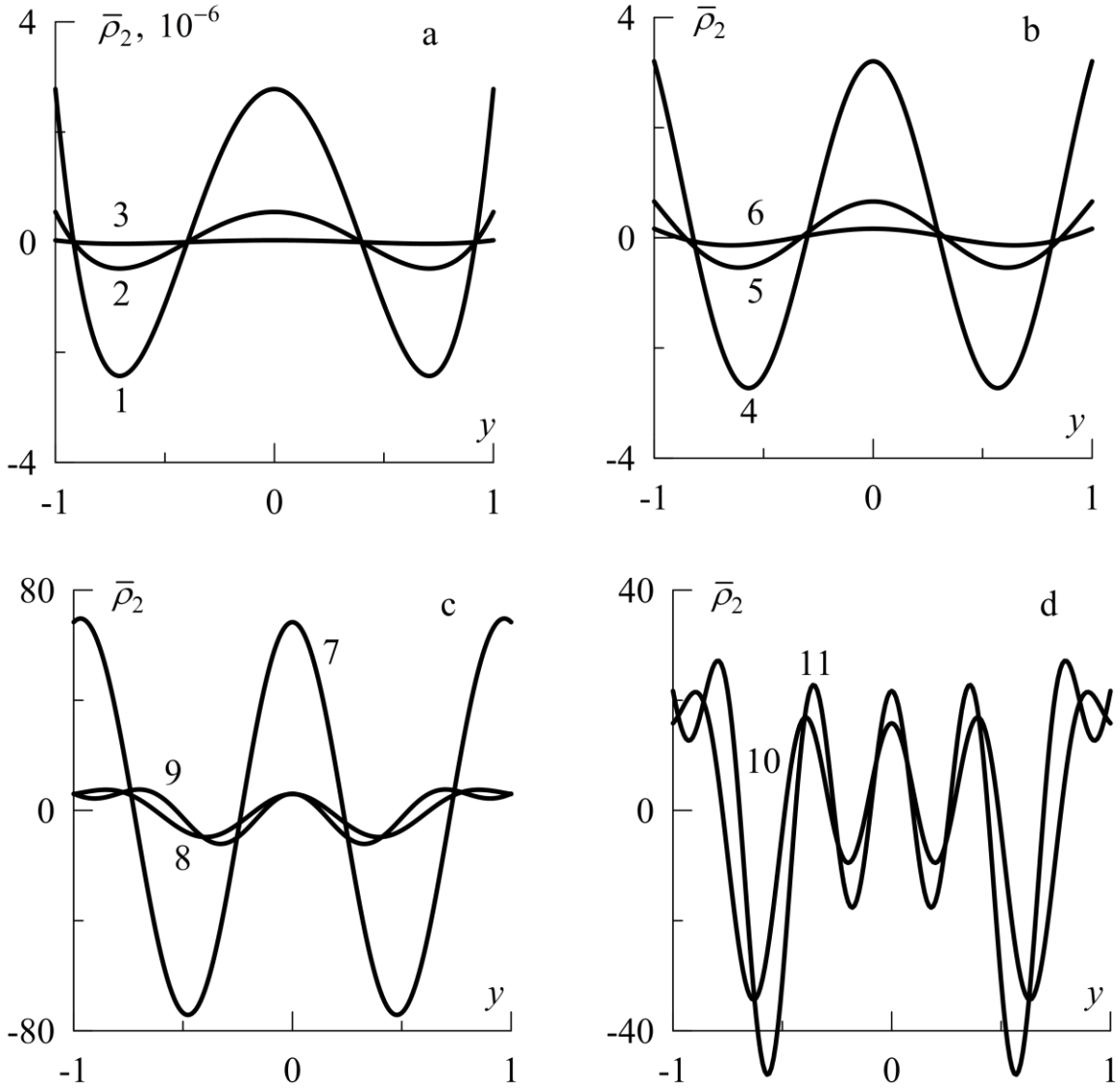

Fig. 3.11. Dependency of time-averaged density $\bar{\rho}_2$ on coordinate for the walls pulsation frequency 500 Hz (1), 1000 Hz (2), 1500 (3) Hz, $2\cdot10^4$ Hz(4), $2.5\cdot10^4$ Hz (5), $3\cdot10^4$ Hz (6), $4\cdot10^4$ Hz (7), $5\cdot10^4$ Hz (8), $6\cdot10^4$ Hz (9), $9\cdot10^4$ Hz (10), 10^5 Hz (11) at $\rho=10^3$ kg/м^3, $h=2$ cm, $\eta=10^{-2}$ Pa s, $C=1500$ m/s, $g=9.8$ m/s^2, $\tilde{\xi}=2.81\eta$

Fig.3.11 shows that with the increase of the frequency $\bar{\rho}_2$ may both increase and decrease, but it reaches the largest values with large frequencies. The number of antinodes grows with frequency. For $4\cdot10^4$ Hz frequencies the vibration amplitude of dimensional frequency is about $70\left(\frac{\alpha}{h}\right)^2\rho_i$; assuming that $\frac{\alpha}{h}=10^{-5}$, $\rho_i=1000$ kg/m^2, then the vibration amplitude of density is $7\cdot10^{-6}$ kg/m^2, with vibration amplitude of pressure being about 16 Pa, that is the pressure is changed just a little.

Velocity profile and flow rate. With v_2 periodicity, having averaged the equation (3.118) we get

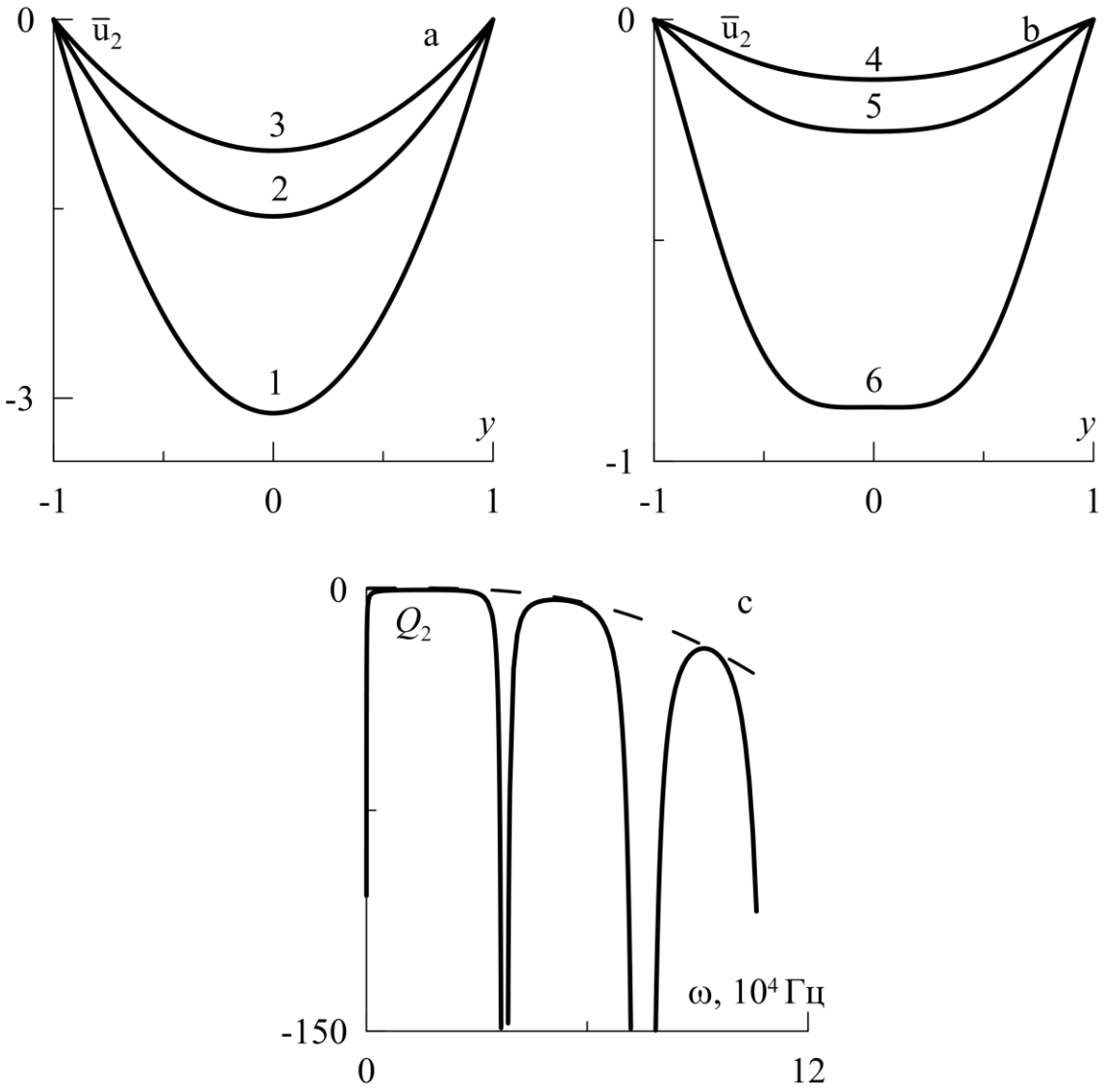

Fig. 3.12. a, b – time-averaged profile of velocity part which appears due to pulsations for walls pulsation frequency 500 Hz (1), 1000 Hz (2), 1500 Hz (3), $2\cdot10^4$ Hz (4), $2.5\cdot10^4$ Hz (5), $3\cdot10^4$ Hz (6); c – dependency of dimensionless flow rate on frequency at $\rho = 10^3$ kg/м^3, $h = 2$ cm, $\eta = 10^{-2}$ Pa s, $C = 1500$ m/s, $g = 9.8$ m/s^2, $\tilde{\xi} = 2.81\eta$

$$\frac{1}{\Omega}\frac{\partial^2 \bar{u}_2}{\partial y^2} = -3\mathrm{Fr}\rho_0 - \frac{1}{2\Omega}\frac{\partial^2 u_0}{\partial y^2} - \mathrm{Fr}\bar{\rho}_2 + \frac{1}{2\pi}\int_0^{2\pi}\left[\rho_0\frac{\partial u_2}{\partial t} - 4\mathrm{Fr}\rho_1\sin t\right.$$
$$-\frac{2\sin t}{\Omega}\frac{\partial^2 u_1}{\partial y^2} + \rho_1\frac{\partial u_1}{\partial t} + 4\rho_0\frac{\partial u_1}{\partial t}\sin t + \rho_0 v_1\frac{\partial u_1}{\partial y} + \rho_1 v_1\frac{\partial u_0}{\partial y}$$
$$\left.+3\rho_0 v_1\frac{\partial u_0}{\partial y}\sin t - \rho_0 y\frac{\partial u_1}{\partial y}\cos t - \rho_1 y\frac{\partial u_0}{\partial y}\cos t\right]dt. \qquad (3.123)$$

The equation (3.123) allows one to find time-averaged profile of velocity part which appears due to pulsations. Integration constants in (3.123) are defined from the boundary conditions

$$y = \pm 1 : \bar{u}_2 = 0 . \qquad (3.124)$$

Fig. 3.12 a, b shows that $\bar{u}_2$ has the maximum at the center of the channel and the minimum at its boundaries. Fig. 3.12c shows that the influence of pulsations on fluid transport is negative. Pulsation-driven part of flow rate is defined by the formula:

$$Q_2 = \frac{1}{2\pi} \int_0^{2\pi} \int_{-1}^{1} (u_1 \sin t + u_2)) dy dt , \qquad (3.125)$$

has a negative sign, while the flow rate in main order has a positive sign. And here the higher the pulsation frequency is, the more significant the decrease of flow rate is. Fig. 3.12c also shows that there are some frequencies with channel pulsations leading to significant decrease of flow rate. For these points the obtained solution does not work, since the coefficients $V_{1s,c}^{\pm}$, $R_{1s,c}^{\pm}$ in first-order solution by amplitude of walls pulsation (3.100) and (3.101), which are given in the Appendix No 3, tend to infinity. It happens when the condition $\cos 2k = \cosh 2\delta$ is met.

4. BEHAVIOR OF BUBBLE AND PARTICLE IN ACOUSTIC FIELD

The present chapter analyzes the interaction of a rise bubble and a fall particle in water in weak acoustic field. Earlier this problem was investigated by D. A. Lyubimov, T. P. Lyubimova and L. S. Klimenko [130]. They considered the case of large amplitude of acoustic pressures within approximation, where the influence of bubble's natural oscillation is supposed to be insignificant. The present chapter looks at small amplitudes of acoustic pressures. For these acoustic pressures the approach developed by D. V. Lyubimov, T. P. Lyubimov an L. S. Klimenko concluded that the influence of sound on the bubble and particle motion was negligibly small. The present study puts forwards an approach, where bubble's natural oscillations are taken into account. This reveals the increase of particle and bubble collision radius for sound frequencies equaling the natural frequencies of bubble, even in the case of small acoustic pressures.

4.1. Problem Statement

The influence of sound on collision is analyzed in long-wave approximation, and all characteristics of a wave are thought to depend on time only.

The motion of pulsating bubble with constant velocity in ideal fluid is described by a system of equations

$$\rho\frac{\partial\vec{\mathrm{v}}}{\partial t}+\rho(\vec{\mathrm{v}}\cdot\nabla)\vec{\mathrm{v}}=-\nabla p \tag{4.1}$$

$$\nabla\cdot\vec{\mathrm{v}}=0 \tag{4.2}$$

with the boundary conditions

$$r=R:\ \vec{\mathrm{v}}\cdot\vec{n}=\frac{\partial R}{\partial t}+\vec{U}(t)\cdot\vec{n}, \tag{4.3}$$

$$r\to\infty:\ \vec{\mathrm{v}}\to\vec{V}_s,\ p\to p_s+p_a, \tag{4.4}$$

where $\vec{\mathrm{v}}$ is the fluid velocity, $\vec{U}(t)$ is the bubble velocity, p is the pressures, R is the bubble radius, p_s is the sound pressure, p_a is the atmospheric pressure, $\vec{n}$ is the normal vector to bubble surface, $r=\sqrt{(x-x_b)^2+(y-y_b)^2+(z-z_b)^2}$, (x_b,y_b,z_b) are the coordinates of bubble mass center.

Transforming into the frame of reference connected with the center of bubble mass

$$\vec{\mathrm{v}}\to\vec{\mathrm{v}}'+\vec{U}(t),$$

$$d\vec{x}\to d\vec{x}'+\vec{U}(t)dt,$$

$$\vec{x}\to\vec{x}'+\vec{x}_b,$$

let us transform the problem (4.1)-(4.4) into

$$\rho\frac{\partial\vec{\mathrm{v}}}{\partial t}+\rho\frac{\partial\vec{U}(t)}{\partial t}+\rho(\vec{\mathrm{v}}\cdot\nabla')\vec{\mathrm{v}}=-\nabla p \tag{4.5}$$

$$\nabla\cdot\vec{\mathrm{v}}=0 \tag{4.6}$$

$$r=R:\ \vec{\mathrm{v}}'\cdot\vec{n}=\frac{\partial R}{\partial t}, \tag{4.7}$$

$$r\to\infty:\ \vec{\mathrm{v}}'\to\vec{V}_s-\vec{U}\ . \tag{4.8}$$

Value $\vec{V}_s$ for acoustic pressure $p=10^3$ Pa is about 0,001 m/s, while $\vec{U}\sim 0.1$ m/s, that is why the contribution of $\vec{V}_s$ may be neglected.

Table 1. The term evaluation in the equation for pressure at the bubble's surface

$R\frac{\partial^2 R}{\partial t^2}$	$\frac{3}{2}\left(\frac{\partial R}{\partial t}\right)^2$	$\frac{3}{2}U\frac{\partial R}{\partial t}\cos\theta$	$\frac{R}{2}\frac{\partial U}{\partial t}\cos\theta$	$\frac{9}{8}U^2\cos^2\theta$	$\frac{5}{8}U^2$
~10 m^2/s^2	~10 m^2/s^2	~0,1 m^2/s^2	~0,1 m^2/s^2	~0,01 m^2/s^2	~0,01 m^2/s^2

Assuming that $\vec{U}(t)$ is directed along OZ axis and neglecting $\vec{V}_s$, we get the problem solution (4.5)-(4.8) as follows

$$V_x = \frac{3R^3}{2r^3}\frac{xz}{r^2}U + \frac{R^2}{r^2}\frac{\partial R}{\partial t}\frac{x}{r} \tag{4.9}$$

$$V_y = \frac{3R^3}{2r^3}\frac{zy}{r^2}U + \frac{R^2}{r^2}\frac{\partial R}{\partial t}\frac{y}{r} \tag{4.10}$$

$$V_z = -U - \frac{1}{2}\frac{R^3}{r^3}U + \frac{3}{2}U\frac{R^3}{r^5}z^2 + \frac{R^2 z}{r^3}\frac{\partial R}{\partial t} \tag{4.11}$$

$$p = p_s + p_a + \rho\frac{R^2}{r}\frac{\partial^2 R}{\partial t^2} - \rho\frac{R^4}{2r^4}\left(\frac{\partial R}{\partial t}\right)^2 + \frac{2\rho R}{r}\left(\frac{\partial R}{\partial t}\right)^2 + \frac{5}{2}\rho\frac{R^2 U}{r^3}z\frac{\partial R}{\partial t} +$$
$$- \rho\frac{R^5}{r^6}zU\frac{\partial R}{\partial t} + \frac{\rho z R^3}{2r^3}\frac{\partial}{\partial t}U - \frac{3}{8}\frac{\rho U^2 R^6 z^2}{r^8} - \frac{1}{8}\frac{\rho U^2 R^6}{r^6} - \frac{\rho}{2}\frac{U^2 R^3}{r^3} + \frac{3}{2}\frac{\rho U^2 R^3 z^2}{r^5}$$

Pressure at the bubble surface in a spherical system of coordinates is

$$\frac{p-(p_s+p_a)}{\rho} = R\frac{\partial^2 R}{\partial t^2} + \frac{3}{2}\left(\frac{\partial R}{\partial t}\right)^2 + \frac{3}{2}U\frac{\partial R}{\partial t}\cos\theta + \\ + \frac{R}{2}\frac{\partial U}{\partial t}\cos\theta + \frac{9}{8}U^2\cos^2\theta - \frac{5}{8}U^2, \tag{4.12}$$

where θ is a zenith angle. In the problem under analysis a bubble has a size of about 1 mm, sound frequency is about 4.000-7.000 Hz, the velocity of its rise is about 10 cm/s. This helps to evaluate the values in (4.12), which is given in Table 1. Here we can conclude that terms with bubble velocity U is at least 100 times less than that term with no velocity. This allows to neglect the terms with U. As result the pressure at the bubble boundary is as follows

$$p = p_s + p_a + \rho\left[R\frac{\partial^2 R}{\partial t^2} + \frac{3}{2}\left(\frac{\partial R}{\partial t}\right)^2\right]. \tag{4.13}$$

On the other side the pressure inside a bubble is defined by an expression

$$p = p_v + p_g - \frac{2\sigma}{R}, \tag{4.14}$$

where p_v is the pressure of saturated steams (for water at $t = 20^o$ $p_v = 2350$ Pa), p_g is the partial pressure of gas, σ is the coefficient of surface tension (for water at $t = 20^o$, $\sigma = 7.35\cdot 10^{-2}$ N/m). Let us assume that bubble pulsations are adiabatic, then

$$p_g R^{3\gamma} = p_{g0} R_0^{3\gamma}, \tag{4.15}$$

or

$$p = p_{g0}\left(\frac{R_0}{R}\right)^{3\gamma}, \tag{4.16}$$

By substituting (4.14) and (4.16) in (4.13), we get the Rayleigh–Plesset equation for an ideal fluid:

$$p_{\text{v}} + p_{g0}\left(\frac{R_0}{R}\right)^{3\gamma} - \frac{2\sigma}{R} = p_s + p_a + \rho\left[R\frac{\partial^2 R}{\partial t^2} + \frac{3}{2}\left(\frac{\partial R}{\partial t}\right)^2\right]. \tag{4.17}$$

Characteristic values for contribution of different terms in (4.17):

$$\frac{2\sigma}{\rho R} \sim 0.1 \text{ m}^2/\text{s}^2,\ \frac{p_{g0}}{\rho}\left(\frac{R_0}{R}\right)^{3\gamma} \sim 100 \text{ m}^2/\text{s}^2,\ \frac{p_a}{\rho} \sim 100 \text{ m}^2/\text{s}^2,\ \frac{p_{\text{v}}}{\rho} \sim 1 \text{ m}^2/\text{s}^2. \tag{4.18}$$

From (4.18) it follows that the summand characterizing the contribution of the surface forces may be neglected. As a result we get the equation

$$p_{\text{v}} + p_{g0}\left(\frac{R_0}{R}\right)^{3\gamma} - p_a = p_s + \rho\left[R\frac{\partial^2 R}{\partial t^2} + \frac{3}{2}\left(\frac{\partial R}{\partial t}\right)^2\right]. \tag{4.19}$$

The problem of particle fall and bubble rise also includes the gravity and viscous friction forces, which are not taken into account in the problem (4.5)-(4.8). Let us show that within our approximation the influence of gravity and viscosity on the bubble vibrations should be neglected. With no gravitational forces the equation (4.17) for the viscous fluid [143] is as follows

$$\frac{p_a}{\rho} + R\frac{\partial^2 R}{\partial t^2} + \frac{3}{2}\left(\frac{\partial R}{\partial t}\right)^2 - \frac{p_{g0}}{\rho}\left(\frac{R_0}{R}\right)^{3\gamma} + \frac{2\sigma}{\rho R} + \frac{4\eta}{\rho R}\dot{R} = \frac{p_{\text{v}} - p_s}{\rho}. \tag{4.20}$$

where η is the dynamic viscosity. The equation (4.20) differs from the equation (4.17) by the summand $\frac{4\eta}{\rho R}\dot{R}$, which characterizes the influence of viscous friction force on the bubble pulsation. The specific value of this term for the waters is ~ 0.001 m^2/s^2. Here we may conclude that we should neglect the contribution of the viscous forces into the bubble pulsation.

Gravitational forces result in additional pressures $\rho g R\cos\theta$. As a result (4.19) should have a summand with the specific value of $gR \sim 0.01$ m^2/s^2. This term may be neglected.

Consequently, within the used approximation the equation (4.19) should not change with viscous and gravitational forces.

With the gas density in a bubble 1000 times less than the fluid density we use the equation [144] to simulate translational motion of a bubble:

$$-\frac{2}{3}\pi\rho\frac{\partial}{\partial t}R^3 U + F_H(t) + F_d + F_A = 0, \tag{4.21}$$

where the Archimedes force $\vec{F}_A$ is calculated by the formula:

$$\vec{F}_A = \frac{4}{3}\pi R^3 \rho\vec{g}, \tag{4.22}$$

the force of viscous friction by the formula [144]:

$$\vec{F}_d = -\frac{C_D}{2}\rho\pi R^2\left|\vec{U}\right|\vec{U}$$

The coefficient C_D is calculated by the formula:

$$C_D = \frac{52.66\,\text{Re}^{2.05} - 46.53\cdot\text{Re}^{1.1} - 2324}{\text{Re}}, \tag{4.23}$$

where $\text{Re}(t) = 2RU/\nu$, ν are the kinematic viscosity of water. The equation (4.23) approximates experimentally obtained in [145] dependence of viscosity coefficient C_D on the Reynolds number for a bubble rise in distilled water [146] (comparison with the experimental curve is shown in Fig. 4.1).

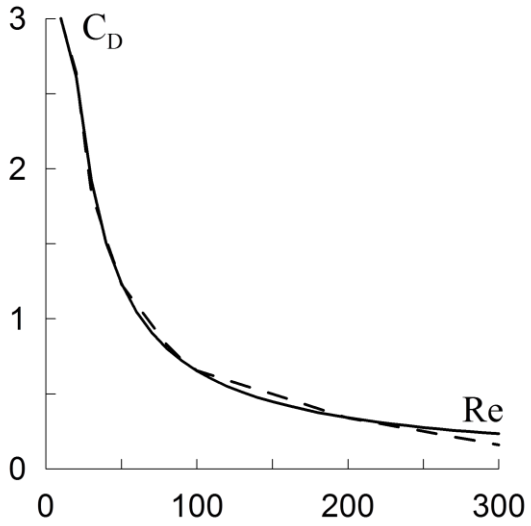

Fig. 4.1. Dependence of viscosity coefficient on the Reynolds number developed by the formula (4.23) and by the experimental data from [146, p.171].

The historical force is calculated by the formula [147, 148]:

$$F_H(t) = -6\pi\eta \int_0^t \left\{ \left[\pi\nu \int_\tau^t \frac{dt'}{R(t')^2} \right]^{1/(2\alpha)} + \frac{1}{G(\tau)} \left[\frac{\pi}{16} \left(\frac{\mathrm{Re}(\tau)}{f_H(\mathrm{Re}(\tau))} \right)^3 \times \right. \right. \\ \left. \left. \times \left(\nu \int_\tau^t \frac{dt'}{R(t')^2} \right)^2 \right]^{1/\alpha} \right\}^{-\alpha} \frac{d}{d\tau} (\mathrm{R}(\tau)\vec{U}) d\tau, \tag{4.24}$$

where $f_H(\mathrm{Re}) = 0.75 + 0.105\,\mathrm{Re}$, $\mathrm{Re}(t) = 2R\vec{U}/\nu$, $\alpha = 2$, $G(\tau) = 1$.

Dependence of bubble location on time calculated with the formula for the historic force (4.24) was compared with the experiment results in [148] and the numerical simulation results were found to correspond to the experiment results very well.

In the applications connected with the flotation the particle size of about 30 times less than the bubble and the influence of the particle on the fluid flow arisen due to the bubble presence may be considered to be small to negligible. This allows to use the Basset-Boussinesq-Oseen equation [149] to describe the particle motion:

$$m_p \left(\frac{d\vec{U}_p}{dt} + \frac{d\vec{U}}{dt} \right) = 3\pi d_p \eta (\vec{\mathrm{u}}_L - \vec{U}_p) + \frac{1}{6}\pi d_p^3 (\rho_p - \rho)\vec{g} - \frac{\pi}{6} d_p^3 \nabla p + \\ + \frac{\pi}{12} d_p^3 \rho \frac{d}{dt} (\vec{\mathrm{u}}_L - \vec{U}_p) - \frac{3}{2} d_p^2 \sqrt{\pi\eta\rho} \int_0^t \frac{d(\vec{U}_p - \vec{\mathrm{u}}_L)}{d\tau} \frac{d\tau}{\sqrt{(t-\tau)}}. \tag{4.25}$$

where d_p is the particle diameter, $\vec{\mathrm{u}}_L$ is the velocity of fluid at a point in the particle center, if there is no particle, $\vec{U}_p$ is the particle velocity, m_p is the particle mass. Fluid may be considered to be ideal in all area except the area behind the bubble [130], since $\vec{\mathrm{u}}_L$ velocity may be calculated by the formulas (4.9)-(4.11). In the equation (4.25) we use the Stokes force as viscous forces, because the Reynolds

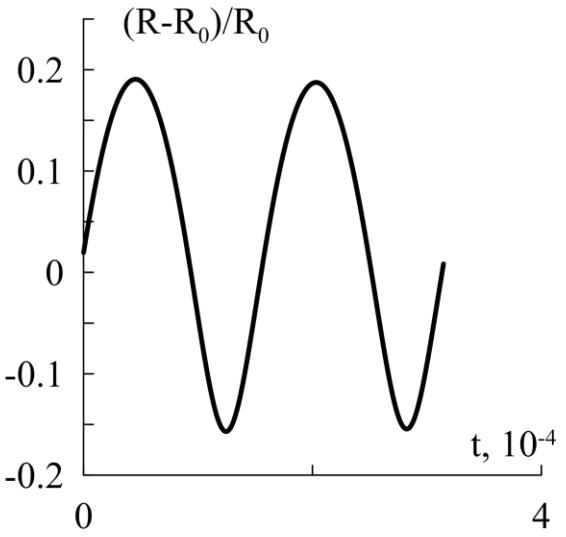

Fig. 4.2. The change in bubble radius ($R_0 = 500$ mkm) with time under the influence of sound with frequency 40500 rad/s and acoustic pressure 1000 Pa

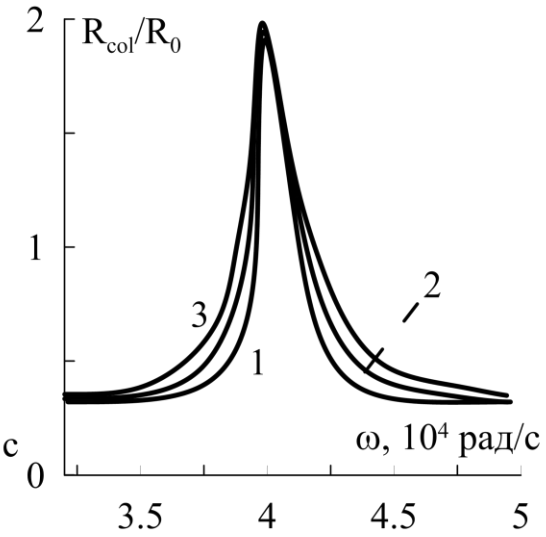

Fig. 4.3. Dependence of the particle (radius is 20 mkm and density is 2000 kg/m^2) collision radius with the bubble of 500 mkm radius on the sound frequency ω for the acoustic pressure in 1000 Pa (1), 1500 Pa (2), 2000 Pa (3).

numbers for the particles are about 0.01. The value $m_p \frac{d\vec{U}}{dt}$ is inertial force, which occurred due to the fact that the frame of reference is connected with the bubble.

Thus, in simulating the particle fall and bubble rise in acoustic field the bubble motion is described by the equation (4.21), particle motion - by the equation (4.25), where the fluid velocity is determined by the expressions (4.9)-(4.11).

4.2. Influence of sound on the collision radius

In most cases the weak intensity sound does not influence the trajectory of particle and bubble motion. However, for the resonance when the sound frequency equals the natural frequency of the bubble the sound influence may become noticeable.

To evaluate the value of the resonance frequency let us present the bubble radius as a sum of constant and variable components:

$$R = R_0 + R_1(t). \tag{4.26}$$

By substituting (4.26) in the equation of the bubble pulsations (4.19) and neglecting the term quadratic in $R_1(t)$ we get

$$\frac{\partial^2 R_1}{\partial t^2} + \frac{3 p_{g0} \gamma}{\rho R_0^2} R_1 = \frac{p_v - p_a - p_s}{\rho R_0}. \tag{4.27}$$

where acoustic pressure p_s changes as $A\cos\omega t$. From (4.27) we may get the expression for the resonance frequency of a bubble in the form [143]

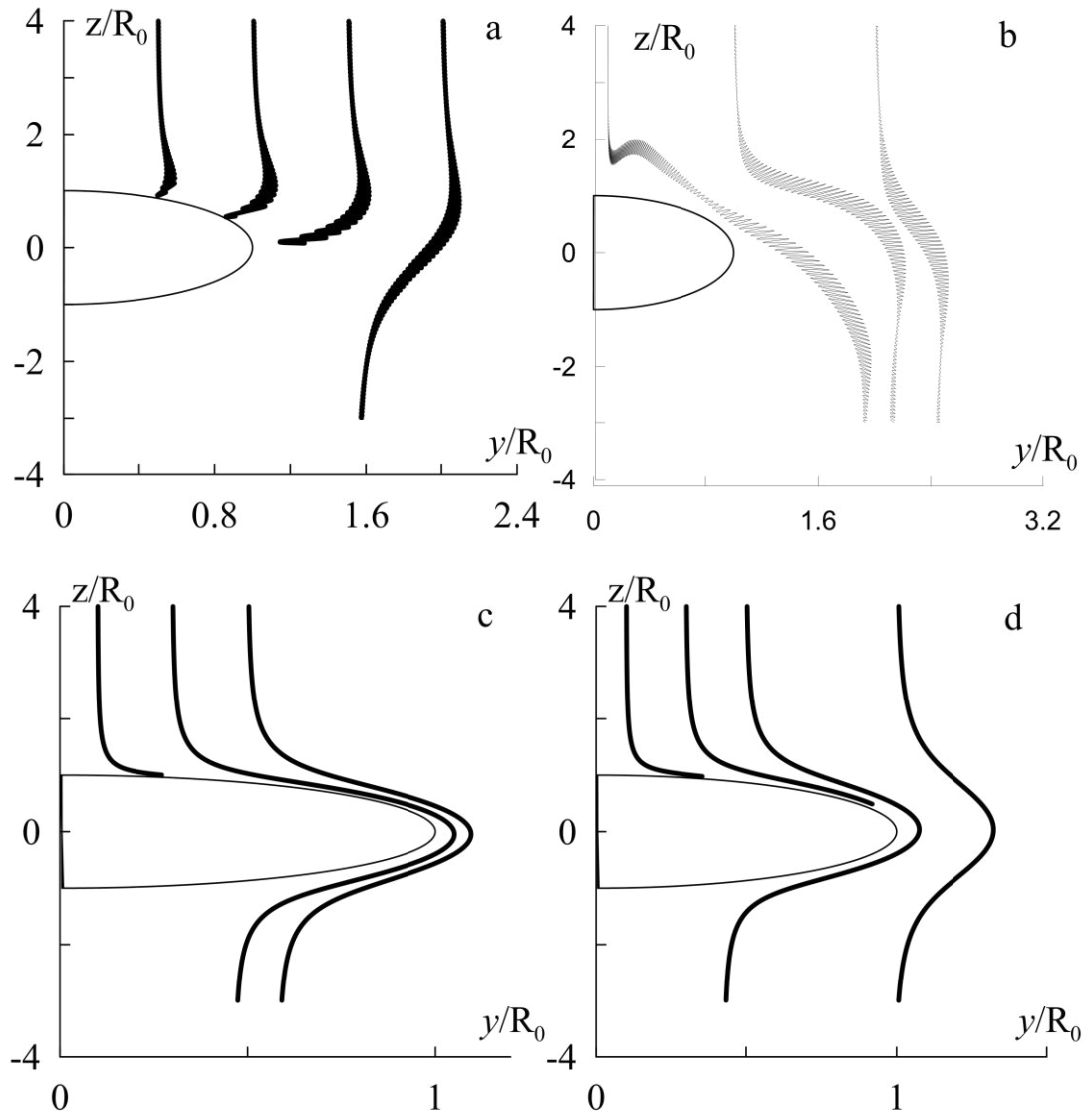

Fig. 4.4. Trajectories of the particle motion (20 mkm radius, 2000 kg/m^2 density (a,c) , 200 kg/m^2 density (b,d)) near the bubble in acoustic field with the frequency $\omega = 40000$ rad/s and acoustic pressure 1000 Pa (a,b) and with no sound (c,d).

$$\omega_r = \sqrt{\frac{3p_{g0}\gamma}{\rho R_0^2}}\,. \tag{4.28}$$

For the bubble with the radius of $R_0 = 500$ mkm the resonance frequency (4.28) equals approximately 40500 rad/s.

Amplitude of bubble pulsation found from (4.27) equals $AR_0/(3\gamma p_{g0})$. For the acoustic wave with the amplitude of acoustic pressure $A = 1000$ Pa the amplitude of the constrained pulsations of bubble is $0.002R_0$. For the impact of the sound with resonance frequency (4.28) the amplitude of the constrained pulsation increases in about hundred times up to $0.17R_0$ (Fig.4.2). As a result the field of fluid velocities caused by the bubble motion significantly changes resulting in the change in particle trajectory (Fig.4.4). Consequently, for the particles with the density more that water density the particle collision radius significantly increases (Fig.4.3).

Fig. 4.4 shows that the particles with the density more than the water density (4.4a, 4.4c) are attracted by the particle due to the sound influence, while the particles with the density less than water density (4.4b, 4.4d) repulse from the bubble.

Fig. 4.5 shows that in most cases with sound the radius of heavy particle collision is more than the radius of light particle collision. The change in particle density influences the most on the particle

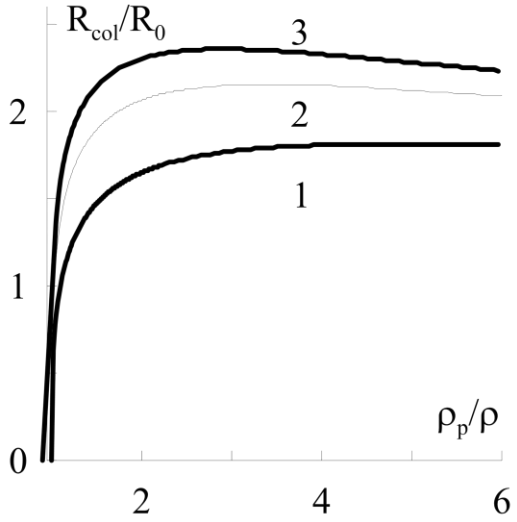

Fig. 4.5. Dependence of particle collision radius with a bubble with radius of 500 mkm on particle density in acoustic field with $\omega = 40000$ rad/s frequency and 1500 Pa acoustic pressure. Radius of particle is 100 mkm (3), 70 mkm (2), 40 mkm (1)

collision radius at the densities less than the doubled water density. For the heavy particles with $\rho > 3000$ kg/m^2 density collision radius may decrease with the density increase.

Thus, when the sound frequency equals natural bubble pulsation frequency, the collision radius has a resonance peak. For all other values of the frequencies the influence of the sound on the collision radius, in case of the weak acoustic fields, are small to be negligible. The natural frequencies depend on the bubble size, which means that with sound influence the possibility for the bubbles with a particular radius to trap particles increases.

The increase of acoustic pressure results in the increase of collision radius. With the acoustic pressures of about 1000 Pa the collision radius increases 5 times due to the sound influence with the frequency equaled the natural frequency of bubble. The approach of D.V.Lyubimov, T.P.Lyubimov, L.S. Klimenko gives the same collision radius increase due to the sound influence only for 100-1000 times higher acoustic pressures.

CONCLUSION

Peristaltic fluid flow in a channel with specified pressure wave at the boundary for random velocities of wave and wave numbers have been studied. The dependencies of flow rate on problem parameters have been specified. It was found that there is maximum value of flow rate, which may be reached by changing the problem parameters.

The influence of transverse vibrations on peristaltic flow with specified pressure wave at the boundary has been examined. The most influence of vibrations has been found, when the pressure wave frequency equals the vibration frequency.

The influence of the transverse wall pulsations on fluid transfer under the pressure drop and gravity for incompressible fluid in case of finite pulsation frequencies has been studied. It has been found that with the finite pulsation frequencies in comparison with the extreme cases of small frequencies studied earlier by other scientists the pulsations decrease the flow rate.

The influence of compressibility on the fluid flow in a vertical channel under gravity with transverse wall pulsations has been studied. It has been found that the compressibility causes time-independent non-homogeneity of density in a channel.

The influence of low intensity sound on the particle and floating bubble interaction has been examined. It has been found that the bubble and particle collision radius reaches its maximum at the sound frequency equal natural frequency of bubble.

References

1. Shapiro A.H. Jaffrine M.Y., Weinberg S.L. Peristaltic pumping with long wavelength at low Reynolds number // J.Fluid Mech. — 1969. — Vol. 37. — P. 799-825.

2. Jaffrine M.Y. Inertia and streamline curvature effects on peristaltic pumping // Int.J.Eng.Sci. — 1971. — Vol. 11. — P. 681-699.

3. Weinberg S.L. Eckstein E.C. Shapiro A.H., An experimental study of peristaltic pumping // J.Fluid Mech. — 1971. — Vol. 49. — P. 461-479.

4. Lyne W.H. Unsteady viscous flow over a wavy wall // J. Fluid Mech. — 1971. — Vol. 50. — P. 33-48.

5. Kaneko A. Honji H. Double structures of steady streaming in the oscillatory viscous flow over a wavy wall // J. Fluid Mech. — 1978. — Vol. 93. — P. 727-736.

6. Russel G.K. Structure and particle transport in second-order Stokes flow // Phys. Rev. E. — 1999. — Vol. 61. — P. 6606-6620.

7. Lykoudis P.S. Roos R. The fluid mechanics of the ureter from lubrication point of view // J. Fluid Mech. — 1970. — Vol. 43. — P. 661-674.

8. Fung Y.C. Peristaltic pumping: a bioengineering model // Urodynamics: Hydrodynamics of the Ureter and Renal Pelvis / book auth. Boyarsky S. — New York : Academic Press, 1971.

9. Jimenez-Lozano J. Sen M. Peristaltic flow with application to ureteral biomechanics. A Dissertation. — Notre Dame, USA, 2009.

10. Mekheimer Kh.S. Al-Arabi T. H. Nonlinear peristaltic transport of MHD flow through a porous medium // International Journal of Mathematics and Mathematical Sciences. — 2003. — Vol. 2003, N. 26. — P. 1663-1682.

11. Mekheimer Kh.S. Peristaltic Flow of a Magneto-Micropolar Fluid: Effect of Induced Magnetic Field // Journal of Applied Mathematic. — 2008. — Vol. 2008. — P. 1-23.

12. Kim H.L. Labay P., Boyarsky S., Glen G.F. An experimental model of ureteral colic // J.Urol. — 1970. — Vol. 104. — P. 380-391.

13. Elshehawey E.F. Wahed A. F., El-Sebaei Effects of Poiseuille flow on peristaltic transport // IJMMS. — 2001. — Vol. 26, N. 6. — P. 341–352.

14. Mekheimer Kh.S. Shehawey E. F. El, Elaw A. M. Peristaltic Motion of a Particle-Fluid Suspension in a Planar Channel // International Journal of Theoretical Physics. — 1998. — Vol. 37, N.11. — P. 2895-2920.

15. Jimenez-Lozano J. Sen M., Corona E. Analysis of peristaltic two-phase flow with application to ureteral biomechanics // Acta Mech. — 2011. — Vol. 219. — P. 91-109.

16. Misra J.C. Maiti S. Peristaltic transport of rheological fluid: model for movement of food bolus through esophagus // Appl. Math. Mech. — 2012. — Vol. 33,N. 3. — P. 315–332.

17. Tripathi D. Peristaltic Hemodynamic Flow of Couple-Stress Fluids Through a Porous Medium with Slip Effect // Transp Porous Med. — 2012. — Vol. 92. — P. 559–572.

18. Vijayaraj K. Krishnaiah G., Ravikumar M.M. Peristaltic pumping of a fluid of variable in a non-uniform tube with permeable wall // Journal of Theoretical and Applied Information Technology. — 2009. — Vol. 2009. — P. 82-91.

19. Suryanarayana-Reddy M. Sankar-Shekar-Raju G., Subba-Reddy M.V., Jayalakshmi K. Peristaltic MHD flow of a Bingham Fluid through a Porous Medium in a Channel // African Journal of Scientific Research. — 2011. — Vol. 3, N. 1. — P. 179-203.

20. Eldesoky I.M. Mousa A.A. Peristaltic Pumping of Fluid in Cylindrical Tube and its Applications in the Field of Aerospace // 13th International Conference on aerospace sciences & aviation technology. — 2009. — Vol. 13. — P. 26–28.

21. Wang Y Hayat T., Hutter K. Peristaltic flow of a Johnson-Segalman fluid through a deformable tube // Theor. Comput. Fluid Dyn. — 2007. — Vol. 21. — P. 369–380.

22. Elshehawey E.F. El-Dabe N. T. , El-Desoky I. M. Slip effects on the peristaltic flow of a non-Newtonian Maxwellian fluid // Acta Mechanica. — 2006. — Vol. 186. — P. 141-159.

23. Mekheimer Kh.S. Non-linear peristaltic transport of magnetohydrodynamic flow in an inclined planar channel // Arabian Journal for Science and Engineering A. — 2003. — Vol. 28, N. 2. — P. 183-201.

24. Muthu P. Rathish-Kumar B.V., Chandra P. Peristaltic motion of micropolar fluid in circular cylindrical tubes: Effect of wall properties // Applied Mathematical Modelling. — 2008. — Vol. 32. — P. 2019–2033.

25. Aarts A.C.T. Ooms G. Net flow of compressible viscous liquids induced by travelling waves in porousmedia // Journal of Engineering Mathematics. — 1998. — Vol. 34. — P. 435-450.

26. Shun-Fa Hwang Yu-Shiuan Shiu Fabrication and Characterization of Two-Chamber and Three-Chamber Peristaltic Micropumps // International journal of precision engineering and manufacturing. — 2010. — Vol. 11, N. 4. — P. 613-618.

27. Misra J.C. Pandey S.K. Peristaltic flow of a multilayered power-law fluid through a cylindrical tube // International Journal of Engineering Science. — 2001. — T. 39. — C. 387-402.

28. Misra J.C. Maiti S. Peristaltic Pumping of Blood Through Small Vessels of Varying Cross-section // J. Appl. Mech. — 2012. — Vol.79, N.6. — 061003.

29. Srinivasacharya D. Mishra M., Ramachandra-Rao A. Peristaltic pumping of a micropolar fluid in a tube // Acta Mechanica. — 2003. — Vol. 161. — P. 165–178.

30. Rachid H. Ouazzani M.T. The Effect of a Pulsatile Flow on the Peristaltic Output: Case of a Newtonian Fluid // Adv. Studies Theor. Phys. — 2008. — Vol. 2, N. 6. — P. 291 – 307.

31. Carew E.O. Pedley T.J. An active membrane model for peristaltic pumping. Part 1. Periodic activation waves in an infinite tube // Trans. ASME: J.Biomech. Eng. — 1997. — Vol. 119, N. 1. — P. 66-76.

32. Takagi D. GFD Proceedings Volume of WHOI // Nonlinear peristaltic waves: a bitter pill to swallow. — 2009. — P. 2-25.

33. Takagi D. Balmforth N. J. Peristaltic pumping of rigid objects in an elastic tube // J. Fluid Mech. — 2011. — Vol. 672. — P. 219–244.

34. Pandey S.K. Chaube M.K. Study of wall properties on peristaltic transport of a couple stress fluid // Meccanica. — 2011. — Vol. 46. — P. 1319–1330.

35. Davies C. Carpenter P.W. Instabilities in a plane channel flow between compliant walls // J. Fluid Mech. — 1997. — Vol. 352. — P. 205–243.

36. Hayat T. Javed M., Ali N. MHD Peristaltic Transport of a Jeffery Fluid in a Channel With Compliant Walls and Porous Space // Transp Porous Med. — 2008. — Vol. 74. — P. 259–274.

37. Hayat T. Javed M. Exact solution to peristaltic transport of power-law fluid in asymmetric channel with compliant walls // Appl. Math. Mech.. — 2010. — T. 31, №10. — C. 1231–1240.

38. Ramana-Kumari A.V. Radhakrishnamacharya G. Effect of slip on heat transfer to peristaltic transport // ARPN Journal of Engineering and Applied Sciences. — 2011. — Vol. 6, N. 7. — P. 118-131.

39. Sankad G.C. Radhakrishnamacharya G. Influence of wall properties on the peristaltic motion of a Hershel-Bulkley fluid in a channel // ARPN Journal of Engineering and Applied Sciences. — 2009. — Vol. 4, N.10. — P. 27-35.

40. Srinivasacharya D. Radhakrishnamacharya G., Srinivasulu C.H. The Effects of Wall Properties on Peristaltic Transport of a Dusty Fluid // Turkish J. Eng. Env. Sci. — 2008. — Vol. 32. — P. 357 – 365.

41. Prasad K.M. Radhakrishnamacharya G. Effect of Peripheral Layer on Peristaltic Transport of a Micropolar Fluid // Nonlinear Analysis: Modelling and Control. — 2009. — Vol. 14, N.1. — P. 103–113.

42. Muthu P. Rathish-Kumar B.V., Chandra P. On the influence of wall properties in the peristaltic motion of micropolar fluid // ANZIAM J. — 2003. — Vol. 45. — P. 245–260.

43. Vahidi B. Fatouraee N., Imanparast A.A Mathematical Simulation of the Ureter: Effects of the Model Parameters on Ureteral Pressure/Flow Relations // Journal of Biomechanical Engineering. — 2011. — Vol. 133, N.3. — P. 14-21.

44. Tripathi D. Chaube M.K., Gupta P.K. Stokes flow of micro-polar fluids by peristaltic pumping through tube with slip boundary condition // Appl. Math. Mech. — 2011. — Vol. 32, N.12. — P. 1587–1598.

45. Akbar N.S. Nadeem S., Hayat T., Hendi A.A. Peristaltic flow of a nanofluid with slip effects // Meccanica. — 2012. — Vol. 47, N.5. — P. 1283-1294.

46. Tripathi D. Gupta P.K., Das S. Influence of slip condition on peristaltic transport of a viscoelastic fluid with fractional Burger's model // Thermal Science. — 2011. — Vol. 15, N.2. — P. 501-515.

47. Kalidas D. Slip effects on heat transfer and peristaltic pumping of a Johnson–Segalman fluid in an inclined asymmetric channel // Arab J. — 2012. — Vol. 1, N.2. — P. 159-174.

48. Srinivas S. Kothandapani M. The influence of heat and mass transfer on MHD peristaltic flow through a porous space with compliant walls // Appl. Math. Comput. — 2009. — Vol. 213. — P. 197–208.

49. Srinivas S. Gayathri R., Kothandapani M. The influence of slip conditions, wall properties and heat transfer on MHD peristaltic transport // Comput. Phys. Commun. — 2009. — Vol. 180. — P. 2115–2122.

50. Ebaid A. Effects of magnetic field and wall slip conditions on the peristaltic transport of a Newtonian fluid in an asymmetric channel // Phys. Lett. A. — 2008. — Vol. 2008. — P. 4493–4499.

51. Hayat T. Qureshi M.U., Ali N. The influence of slip on the peristaltic motion of a third order fluid in an asymmetric channel // Phys. Lett. A.. — 2008. — Vol. 372. — P. 2653–2664.

52. Elshehawey E.F. Husseny S. Z. A. Effects of porous boundaries on peristaltic transport through a porous medium // Acta Mechanica. — 2000. — T. 143. — C. 165-177.

53. Akbar N.S. Nadeem S., Hayat T., Hendi A.A. Peristaltc flow of a nanofluid in a non-uniform tube // Heat Mass Transfer. — 2012. — Vol. 48. — P. 451–459.

54. Nadeem S. Akbar N.S., Ali M. Endoscopic effects on the peristaltic flow of an Eyring–Powell fluid // Meccanica. — 2012. — Vol. 47. — P. 687–697.

55. Nadeem S. Akbar N.S. Peristaltic flow of Walter's B fluid in a uniform inclined tube // J. Biorheol. — 2010. — Vol. 24. — P. 22-28.

56. Nadeem S. Akbar N.S. Effects of induced magnetic field on peristaltic flow of Johnson-Segalman fluid in a vertical symmetric channel // Appl. Math. Mech. — 2010. — Vol. 31, N.8. — P. 969–978.

57. Rami-Reddy G. Venkataramana S. Peristaltic transport of a conducting fluid through a porous medium in an asymmetric vertical channel // Adv. Appl. Sci. Res. — 2011. — Vol. 2, N.5. — P. 240-248.

58. Vasudev C. Rajeswara-Rao U., Subba-Reddy M.V., Prabhakara-Rao G. MHD peristaltic flow of a Newtonian fluid through a porous medium in an asymmetric vertical channel with heat transfer // International Journal of Science and Advanced Technology. — 2011. — Vol. 1, N.9. — P. 170-176.

59. Nadeem S. Akbar N.S. Magnetohydrodynamic peristaltic flow of a hyperbolic tangent fluid in a vertical asymmetric channel with heat transfer // Acta Mech. Sin.. — 2011. — Vol. 27, N.2. — P. 237–250.

60. Rami-Reddy G. Satya-Narayana P. V., Venkataramana S. Peristaltic Transport of a Conducting Fluid in an Inclined Asymmetric Channel // Applied Mathematical Sciences. — 2010. — Vol. 4, N.35. — P. 1729–1741.

61. Mishra M. Ramachandra-Rao A. Peristaltic transport of a Newtonian fluid in an asymmetric channel // Zeitschrift Angewandte Mathematik Physik. — 2003. — Vol. 54. — P. 532-550.

62. Medhavi A. Singh U. K. Peristaltic Induced Flow of a Particulate Suspension in a Non-uniform Tube // e -Journal of Science & Technology . — 2011. — T. 2, №6. — C. 77-93.

63. Misra J.C. Maiti S., Shit G.C. Peristaltic Transport of a Physiological Fluid in an Asymmetric Porous Channel in the Presence of an External Magnetic Field // Journal of Mechanics in Medicine and Biology. — 2008. — Vol. 8, N.4. — P. 507-525.

64. Radhakrishnamacharya G. Sharma R. Motion of a Self-Propelling Micro-Organism in a Channel Under Peristalsis: Effects of Viscosity Variation // Nonlinear Analysis: Modelling and Control. — 2007. — Vol. 12, N.3. — P. 409–418.

65. Medhavi A. Singh D., Yadav A. S., Gautam S.R. Peristaltic Induced Flow of a Two-Layered Suspension in Non-Uniform Channel // AAM: Intern. J. — 2011. — Vol. 6, N.2. — P. 462-481.

66. Medhavi A. Peristaltic pumping of a particulate suspension in a catheterized tube // e-Journal of Science & Technology. — 2010. — Vol. 7. — P. 77-93.

67. Hsu Y.C. Le N.B. Equivalent electrical network for performance characterization of piezoelectric peristaltic micropump // Microfluid Nanofluid. — 2009. — Vol. 7, N.2. — P. 237–248.

68. Alemayehu H. Radhakrishnamacharya G. The Effects of Peristalsis on Dispersion of a Micropolar Fluid in the Presence of Magnetic Field // World Academy of Science, Engineering and Technology. — 2011. — Vol. 75. — P. 1042-1048.

69. El-Dabe N. T. Abou-Zeid M. Y. The Wall Properties Effect on Peristaltic Transport of Micropolar Non-Newtonian Fluid with Heat and Mass Transfer // Hindawi Publishing Corporation Mathematical Problems in Engineering. — 2010. — Vol. 2010. — P. 1-40.

70. Nadeem S. Akbar N.S., Hayat T., Hendi A. A. Peristaltic flow of Walter's B fluid in endoscope // Appl. Math. Mech. — 2011. — Vol. 32, N.6. — P. 689–700.

71. Vasudev C. Rajeswara-Rao U., Subba-Reddy M.V., Prabhakara-Rao G. Effects of Heat Transfer on the Peristaltic Flow of Jeffrey Fluid through a Porous Medium in a Vertical Annulus // J. Basic. Appl. Sci. Res. — 2011. — Vol. 1, N.7. — P. 751-758.

72. Elshehawey E.F. El-Dabe N.T.M., Ghaly A.Y., Sayed H.M. Effects of Chemical Reaction, Heat, and Mass Transfer on Non-Newtonian Fluid Flow Through Porous Medium in a Vertical Peristaltic Tube // Transp Porous Med. — 2011. — Vol. 89. — P. 185–212.

73. Nadeem S. Akbar N.S. Influence of heat and mass transfer on a peristaltic motion of a Jeffrey-six constant fluid in an annulus // Heat Mass Transfer. — 2010. — Vol. 46. — P. 485–493.

74. Mekheimer Kh.S. Peristaltic transport of a Newtonian fluid through a uniform and non-uniform annulus // Arab. J. Sci. Eng. — 2005. — Vol. 30. — P. 69-83.

75. Firsov N.N. Stiureva G.M., Kostin G.M. Nekotorye reologicheskie effekty funktcionirovaniia pochki v norme i patologii // Biomekhanika. Tr. Rizh. NIIITiO. — Riga, 1975. — V. 13. — P. 184-188.

76. Roitman E.V. Dementeva I.I., Kolpakov P.E. Viazkost mochi kak otcenka gomeostaza kardiokhirurgicheskikh bolnykh v rannem posleoperatcionnom periode // Klin. lab. diagnostika.— 1995. — V. 4. — P. 29-31.

77. Hayat T. Wang Y., Hutter K., Asghar S., Siddiqui A. M. Peristaltic transport of an Oldroyd-B fluid in a planar channel // Mathematical Problems in Engineering. — 2004. — Vol. 2004, 4. — P. 347-376.

78. Elshehawey E.F. Sobh A. M. F. Peristaltic viscoelastic fluid motion in a tube // International Journal of Mathematics and Mathematical Sciences. — 2001. — Vol. 26, N.1. — P. 21-34.

79. Chrispell J.C. Fauci L.J. Peristaltic pumping of solid particles immersed in a viscoelastic fluid // Mathematical Modelling of Natural Phenomena. — 2011. — Vol. 6, N.5. — P. 67-83.

80. Mohamed H.H. Effect of relaxation and retardation time on peristaltic transport of the Oldroydian viscoelastic fluid // Journal of Applied Mechanics and Technical Physics. — 2005. — Vol. 46, N.6. — P. 842–850.

81. Medhavi A. Peristaltic Pumping of a Non-Newtonian Fluid // Appl. Appl. Math. — 2008. — Vol. 3, N.1. — P. 137 – 148.

82. Radhakrishnamacharya G. Flow of Herschel-Bulkley fluid through an inclined tube of non-uniform cross-section with multiple stenoses // Arc. of Mech. — 2008. — Vol. 60, N.2. — P. 161-172.

83. Misra J.C. Pandey S.K. Peristaltic Transport of blood in small vessels- study of a mathematical model // Computers and Mathematics with Applications. — 2002. — Vol. 43. — P. 1183 – 1119.

84. Mernone A.V. Mazumdar J.N., Lucas S.K. A mathematical study of peristaltic transport of a Casson fluid // Mathematical and Computer Modelling. — 2002. — Vol. 35, N.7. — P. 895-912.

85. Blair G.W.S. Spanner D.C. An Introduction to Biorheology. — Oxford and New York : Elsevier Biorheology Scient. Pub. Co, 1974.

86. Srivastava V.P. Saxena M. A two-fluid model of non-Newtonian blood flow induced by peristaltic waves // Rheol Acta. — 1995. — Vol. 34. — P. 406-414.

87. Charm S.E. Kurland G.S. Viscometry of human blood for shear rates of 0-100, 000 sec // Nature. — 1965. — Vol. 206. — P. 617-629.

88. Charm S.E. Kurland G.S. Blood Flow and Microcirculation. — New York : John Wiley, 1974.

89. Srivastava V.P. A Theoretical Model for Blood Flow in Small Vessels // An International Journal AAM. — 2007. — Vol. 2, N.1. — P. 51 – 65.

90. Maiti S. Misra J.C. Peristaltic Transport of a Couple Stress Fluid: Some Applications to Hemodynamics // Journal of Mechanics in Medicine and Biolog. — 2012. — Vol. 12, N.1. — P. 1-21.

91. Kavitha A. Hemadri Reddy R., Sreenadh S., Saravana R. Peristaltic flow of a Williamson fluid in an asymmetric channel throughn porous medium // International journal of innovative technology & creative engineering. — 2011. — Vol. 1, N.1. — P. 48-53.

92. Tripathi D. Ali N., Hayat T., Chaube M. K., Hendi A. A. Peristaltic flow of MHD Jeffrey fluid through finite length cylindrical tube // Appl. Math. Mech. — 2011. — Vol. 32, N.10. — P. 1231–1244.

93. Tsiklauri D. Beresnev I. Non-Newtonian effects in the peristaltic flow of a Maxwell fluid // Physical review E. . — 2011. — Vol. 64. — P. 1-5.

94. Nadeem S. Akbar N.S. Peristaltic Flow of a Maxwell Model Through Porous Boundaries in a Porous Medium // Transp Porous Med.. — 2011. — Vol. 86. — P. 895–909.

95. Hayat T. Ali N., Asghar S. An analysis of peristaltic transport for flow of a Jeffrey fluid // Acta Mechanica. — 2007. — Vol. 193. — P. 101-112.

96. Wang Y. Hayat T., Ali N., Oberlack M. Magnetohydrodynamic peristaltic motion of a Sisko fluid in a symmetric or asymmetric channel // Physica A. — 2008. — Vol. 387. — P. 347–362.

97. Ellahi R. Riaz A., Nadeem S., Ali M. Peristaltic flow of Carreau fluid in a rectangular duct through a porous medium // Mathematical Problems in Engineering. — 2012. — Vol. 2012. — P. 2-33.

98. Hayat T. Mahomed F. M., Asghar S. Peristaltic Flow of a Magnetohydrodynamic Johnson–Segalman Fluid // Nonlinear Dynamics. — 2005. — Vol. 40. — P. 375–385.

99. Ceniceros H.D. Fisher J.E. Peristaltic pumping of a viscoelastic fluid at high occlusion ratios and large Weissenberg numbers // Journal of Non-Newtonian Fluid Mechanics.. — 2012. — Vol. 172. — P. 31-34.

100. Krishna S.V.H.N. Kumari P, Kumar Y.V.K.R., Murthya M.V.R., Sreenadh S. Peristaltic Motion of a Fourth – Grade Fluid through a Porous Medium under Effect of a Magnetic Field in an Inclined Channel // J. Basic. Appl. Sci. Res. — 2011. — Vol. 1, N.9. — P. 1052-1064.

101. Hemadri Reddy R. Kavitha A., Sreenadh S., Hariprabakaran P. Effect of thickness of the porous material on the peristaltic pumping when the tube wall is provided with non-erodible porous lining // Advances in Applied Science Research. — 2011. — Vol. 2, N.2. — P. 1-16.

102. Elshehawey E.F. Gharsseldien Z.M. Peristaltic transport of three-layered flow with variable viscosity // Applied Mathematics and Computation. — 2004. — Vol. 153. — P. 417–432.

103. Nadeem S. Akbar N.S. Peristaltic flow of a couple stress fluid under the effect of induced magnetic field in an asymmetric channel // Arch Appl Mech.. — 2011. — Vol. 81. — P. 97–109.

104. Subba-Reddy M. V. Perumal S.V., Nagendra N. Proceedings of the 37th National & 4th International Conference on Fluid Mechanics and Fluid Power. IIT Madras. India // Hydromagnetic flow of generalized Newtonian fluid through a vertical tube with peristalsis. — 2010. — P. 1-9.

105. Abd-Alla A.M. Yahya G.A., Mahmoud S.R., Alosaimi H.S. Effect of the rotation, magnetic field and initial stress on peristaltic motion of micropolar fluid // Meccanica. — 2012. — Vol. 47, N.6. — P. 1455-1465.

106. Abd-Alla A.M. Yahya G.A., Al Osaimi H .S. Peristaltic transport of micropolar fluid in a tubes under influence of magnetic field and rotation // International Journal of Engineering & Technology. — 2011. — Vol. 11, N.1. — P. 22-39.

107. Tsiklauri D. Beresnev I. Non-Newtonian effects in the peristaltic flow of a Maxwell fluid // Phys Rev E Stat Nonlin Soft Matter Phys. — 2001. — Vol. 64. — P. 1-7.

108. Provost A.M. Schwarz W.H. A theoretical study of viscous effects in peristaltic pumping // J. Fluid. Mech. — 1994. — Vol. 279. — P. 177–195.

109. Weinberg S.L. Eckstein E.C., Shapiro A.H. Peristaltic pumping in circular tubes: A numerical study of fluid transport and its efficiency // J. Fluid Mech. — 1982. — Vol. 12, N.2. — P. 439-465.

110. Longuet-Higgins M.S. Peristaltic pumping in water waves // J. Fluid Mech. — 1983. — Vol. 137. — P. 393-407.

111. Shugan I. Fluid mass transfer in a channel with vibrating elastic walls // Physics of Vibrations. — 1999. — Vol. 7, N.2. — P. 107-117.

112. Liakhov G.V. Shugan I.V. Energeticheskaia effektivnost mekhanizma uskoreniia massoperenosa zhidkosti v kanale // JETP Letters. — 2002. — V. 28, №7. — P. 57-61.

113. Arinchin N.I., Borisevich G.F. Micropumping activity of the extended skeletal muscles, Minsk: Nauka I Technika (1986), 112p. [in Russian].

114. Zwick K.J. Ayyaswamy P.S. Cohen I.M. Oscillatory enhancement of the squeezing flow of yield stress fluids: A novel experimental result // J. Fluid Mech. — 1997. — Vol. 339. — P. 77-87.

115. Kazantcev V. F. Dvizhenie gazovykh puzyrkov pod deistviem sil Berknisa, voznikaiushchikh v akkusticheskom pole // Rep. AC USSR. — 1959. —V.129. №1. — P. 64-67.

116. Kuznetcov G.N., SHCHekin I.E. Vzaimodeistvie pulsiruiushchikh puzyrkov v viazkoi zhidkosti //Akkust. zhurn. — 1972. — V.18. №4. — P.565-570.

117. Mettin R., Ohl C.-D., Lauterborn W. Particle approach to structure formation in acoustic cavitation // Proc. NATO ASI Sonochemistry and Sonoluminescence. — 1999. — pp. 139–144.

118. Doinikov A. A. Translational motion of two interacting bubbles in a strong acoustic field // Phys. Rev. E. — 2001. — v.64, №2. — 026301.

119. Nikolaos A., Gaki A., Doinikov A., Tsamopoulos J.A. Secondary Bjerknes forces between two bubbles and the phenomenon of acoustic streamers// Journal of Fluid Mechanics. —2004. — pp 313-347.

120. Davletshin A.I. Matematicheskoe modelirovanie vzaimodeistviia gazovykh puzyrkov v zhidkosti v akusticheskom pole. Avtoreferat dissertatcii na soiskanie uchenoi stepeni kandidata fiziko-matematicheskikh nauk, Novosibirsk, 2010.

121. Aganin A. A., Davletshin A. I., Toporkov D. IU. Vzaimodeistvie gazovykh puzyrkov v zhidkosti s uchetom ikh maloi nesferichnosti. Matematicheskie metody i modeli:teoriia, prilozheniia i rol v obrazovanii. Sbornik nauchnykh trudov. Ulianovsk, 2009. 3-8 pp.

122. Mednikov E.P. Akusticheskaia koaguliatciia i osazhdenie aerozolei. - M. AS USSR,1963 – 264 p.

123. Song L. Theoretical development of acoustic agglomeration of aerosol particles. J. Acoust. Soc. Am. Volume 85, Issue S1, 1989,pp. S135-S135.

124. Hoffmann T.L., Koopmann G.H. (1996), Visualization of acoustic particle interaction and agglomeration: Theory and Experiments, J. Acoust. Soc. Am., 99, 4, pp:2130-2141.

125. Chou K. H. , Lee P. S. and Shaw D. T. Aerosol agglomeration in high-intensity acoustic fields. Journal of Colloid and Interface Science, Volume 83, Issue 2, October 1981, Pages 335-353.

126. Scattering of spatially inhomogeneous sound waves by a spherical particle. Kobelev Yu.A. Acoustical Physics. 2009. T. 55. № 1. C. 17-26.

127. Hay T.A. A Model of the Interaction of Bubbles and Solid Particles under Acoustic Excitation. Dissertation for the Degree of Doctor of Philosophy. The University of Texas at Austin, 2008, 193 p.

128. Hay T. A., Hamilton M. F., Ilinskii Y. A., Zabolotskaya E. A.. Model of coupled pulsation and translation of a gas bubble and rigid particle. J. Acoust Soc Am. 2009 March; 125(3): 1331–1339.

129. Yu. A. Ilinskii, M. F. Hamilton, and E. A. Zabolotskaya. Bubble interaction dynamics in Lagrangian and Hamiltonian mechanics. J. Acoust. Soc. Am., 121:786–795, 2007.

130. Klimenko L.S. Generatciia techeniia i povedenie chastitcy okolo puzyrka v kolebliushcheisia zhidkosti // Dissertatciia na soiskanie stepeni kandidata fiziko-matematicheskikh nauk. Perm.2011.

131. Nozdrachev A.D. Fiziologiia vegetativnoi nervnoi sistemy. — Leningrad: Meditcina,1983.

132. Pustylnikov L.D. On Ulam Problem // Theor. Math. Phys. — 1983. — Vol. 57. — P. 1035-1038.

133. Chirikov B.V. A universal instability of many-dimensional oscillator systems // Physics Reports. — 1979. — Vol. 52, N.5. — P. 263-379.

134. Luck J.M. Mehta A. Bouncing ball with a finite restitution // Physical review E. — 1993. — Vol. 48, N.5. — P. 3988–3997.

114. Zwick K.J. Ayyaswamy P.S. Cohen I.M. Oscillatory enhancement of the squeezing flow of yield stress fluids: A novel experimental result // J. Fluid Mech. — 1997. — Vol. 339. — P. 77-87.

135. Antunes J. Piteau Ph. A nonlinear analytical model for the squeeze-film dynamics of parallel plates subjected to axial flow // International Journal of Mechanical Sciences. — 2010. — Vol. 52. — 1491–1504.

136. Aristov S.N. Knyazev D.V. Viscous Fluid Flow between Moving Parallel Plates // Fluid Dynamics. — 2012. — Vol. 47, N.4. — P. 476–482.

137. Ishizawa S. The unsteady laminar flow between two parallel disks with arbitrary varying gap width // Bull. JSME. — 1966. — Vol. 9, N.35. — P. 533–550.

138. Wang C.Y. Watson L.T. Squeezing of a viscous fluid between elliptic plates // Appl. Sc. L. Res. — 1979. — Vol. 35. — P. 195-207.

139. Secomb T.W. Flow in a Channel with Pulsating Walls // J. Fluid Mech. — 1978. — Vol. 88, N.2. — P. 273–288.

140. Hall P. Papageorgiou D.T. The onset of chaos in a class of Navier–Stokes solutions // J. Fluid Mech. — 1999. —Vol. 393. — P. 59–87.

141. Filippov L.O. Matinin A.S. Lekhatinov CH.A. Povyshenie kinetiki flotatcii v mnogozonnoi flotatcionnoi mashine tipa reaktor-separator pod vliianiem impulsnykh vozdeistvii v protochnom rezhime // Gornyi zhurnal. — 2012. — T. 9. — C.102-106.

142. Aristov S.N. Kniazev D.V., Polianin A.D. Tochnye resheniia uravnenii Nave–Stoksa s lineinoi zavisimostiu komponent skorosti ot dvukh prostranstvennykh peremennykh // Teor. osnovy khimicheskoi tekhnologii. — 2009. — T. 43, №5. — C. 547–566.

143. Рождественский В.В. Кавитация // Ленинград: Издательство "Судостроение", 1977. – 247 с.

144. Takemura F., Magnaudet J. The history force on a rapidly shrinking bubble rising at finite Reynolds number // Phys. Fluids. – 2004. – V.16. – 3247.

145. Gaudin A.M. Flotation, 2nd ed //New York: McGraw-Hill - 1957. – 573 c.

146. Clift R., Grace J.R., Weber M.E. Bubbles, drops and particles // New York: Academic Press. – 1978. – 380 c.

147. Mei R. Flow due to an oscillating sphere and an expression for unsteady drag on the sphere at finite Reynolds number // J. Fluid Mech. – 1994. – V.270. – pp.133-174.

148. Takemura F., Magnaudet J. The history force on a rapidly shrinking bubble rising at finite Reynolds number // Phys. Fluids. – 2004. - V.16. – 3247.

149. Maxey M.R., Riley J.J. Equation of motion for a small rigid sphere in a nonuniform flow // Phys. Fluids . – 1983. – V. 26, 4 – pp. 883 – 889.

150. Anrep GV, Cerqua S, Samaan A. The effect of muscular contraction upon the blood flow in the skeletal muscle, in the diaphragm and in the small intestine. Proc R Soc Lond B Biol Sci 1933;114:245–57.

151. Kwi-joo Lee, Igor Shugan and Kyoung-Hwa Kim. Fluid Mass Streaming in a Channel under Standing Wall Vibrations // Journal of the Korean Physical Society, Vol. 45, No. 2, August 2004, pp. 399-403.

152. Tsangaris S. Longitudinal dispersion in a duct with moving walls // Zeitschrift für angewandte Mathematik und Physik ZAMP.1986, Volume 37, Issue 6, pp 895-909.

153. Waters S. L. Solute uptake through the walls of a pulsating channel // J. Fluid Mech. 2001. Vol. 433. pp.193-208.

154. Aristov S.N. Knyazev D.V. Viscous Fluid Flow between Moving Parallel Plates // Fluid Dynamics. — 2012. — Vol. 47, N.4. — P. 476–482.

155. Ishizawa S. The unsteady laminar flow between two parallel disks with arbitrary varying gap width // Bull. JSME. — 1966. — Vol. 9, N.35. — P. 533–550.

156. Wang C.Y. Watson L.T. Squeezing of a viscous fluid between elliptic plates // Appl. Sc. L. Res. — 1979. — Vol. 35. — P. 195-207.

Appendix № 1 to paragraph 2.2.3. Program to find solution

This program was written for Maple 16. The solution for the longitudinal velocity is written in uq, for the transverse one - in vq, for pressure - in pq, for the deviation from average wall position – in xiq.

The number of terms in series

```
N:=7:

eq1:=c/lambda*diff(vx(t,x,y),t)+vx(t,x,y)/h*diff(vx(t,x,y),x)+vy(t,x,y)/lambda
*diff(vx(t,x,y),y)+1/h/rho*diff(p(t,x,y),x)-nu* (1/h**2 * diff(vx(t,x,y), x$2) +1 /lambda**2
*diff(vx(t,x,y),y$2));

eq2:= c/lambda*diff(vy(t,x,y),t)+vx(t,x,y)/h*diff(vy(t,x,y),x) +vy(t,x,y)/lambda* diff(vy(t,x,y)
,y)+1/lambda/rho*diff(p(t,x,y),y)-nu*(1/h**2*diff(vy(t,x,y),x$2)+ 1/lambda**2*diff(vy(t,x,y),y$2));

eq3:=diff(vx(t,x,y),x)/h+diff(vy(t,x,y),y)/lambda;

eq4:=expand(h/c**2*expand(subs(vx(t,x,y)=v(t,x,y)*c*h/lambda,vy(t,x,y) = u(t,x,y) *c,p(t,x,y)=nu
*rho *c/h**2*lambda*p1(t,x,y),eq1)));

eq5:=expand(h/c**2*expand(subs(vx(t,x,y)=v(t,x,y)*c*h/lambda,vy(t,x,y) =u(t,x,y) *c,p(t,x,y)=nu*
rho*c/h**2*lambda*p1(t,x,y),eq2)));

eq6:=expand(h/c**2*expand(subs(vx(t,x,y)=v(t,x,y)*c*h/lambda,vy(t,x,y)
=u(t,x,y)*c,p(t,x,y)=nu*rho*c/h**2*lambda*p1(t,x,y),eq3)));

eq7:=expand(expand(subs(nu=h*c/Re,h=delta*lambda,eq4))*delta);

eq8:=expand(subs(nu=h*c/Re,h=delta*lambda,eq5));

eq9:=expand(c/delta*expand(subs(nu=h*c/Re,h=delta*lambda,eq6)));

uq:=0:vq:=0:xiq:=0:pq:=0:

for i from 1 to N do

uq:=uq+u1[i](t,x,y)*delta**i:

vq:=vq+v1[i](t,x,y)*delta**i:

xiq:=xiq+xi1[i](t,y)*delta**i:

pq:=pq+p1[i](t,x,y)*delta**i

end do:

g(t-y):=A*Re*cos(t-y):

e1:=expand(subs(u(t,x,y)=uq,v(t,x,y)=vq,xi(t,y)=xiq,p1(t,x,y)=pq,eq7)):

e2:=expand(subs(u(t,x,y)=uq,v(t,x,y)=vq,xi(t,y)=xiq,p1(t,x,y)=pq,eq8)):
```

```
e3:=expand(subs(u(t,x,y)=uq,v(t,x,y)=vq,xi(t,y)=xiq,p1(t,x,y)=pq,eq9)):
e1:=convert(series(e1,delta=0,N),polynom):
e2:=convert(series(e2,delta=0,N),polynom):
e3:=convert(series(e3,delta=0,N),polynom):
Uplus:=uq:uqq:=uq:
for i from 1 to N do
uqq:=diff(uqq,x):
Uplus:=Uplus+uqq*a**i/i!:
end do:
Uplus:=convert(series(subs(a=xiq,Uplus),delta=0,N),polynom):
Uminus:=uq:uqq:=uq:
for i from 1 to N do
uqq:=diff(uqq,x):
Uminus:=Uminus+uqq*a**i/i!:
end do:
Uminus:=convert(series(subs(a=-xiq,Uminus),delta=0,N),polynom):
Vplus:=vq:uqq:=vq:
for i from 1 to N do
uqq:=diff(uqq,x):
Vplus:=Vplus+uqq*a**i/i!:
end do:
Vplus:=convert(series(subs(a=xiq,Vplus),delta=0,N),polynom):
Vminus:=vq:uqq:=vq:
for i from 1 to N do
uqq:=diff(uqq,x):
Vminus:=Vminus+uqq*a**i/i!:
end do:
Vminus:=convert(series(subs(a=-xiq,Vminus),delta=0,N),polynom):
```

```
pplus:=pq:uqq:=pq:

for i from 1 to N do

uqq:=diff(uqq,x):

pplus:=pplus+uqq*a**i/i!:

end do:

pplus:=convert(series(subs(a=xiq,pplus),delta=0,N),polynom)-delta*g(t-y):

pminus:=pq:uqq:=pq:

for i from 1 to N do

uqq:=diff(uqq,x):

pminus:=pminus+uqq*a**i/i!:

end do:

pminus:=convert(series(subs(a=-xiq,pminus),delta=0,N),polynom)-delta*g(t-y):

for i from 1 to (N-1) do

pq11:=solve(int(coeff(e1,delta**i),x)=0,p1[i](t,x,y))+C;

C1:=solve(subs({p1[i](t,x,y)=subs(x=1,pq11),x=1},coeff(pplus,delta**i)),C);

pq12:=subs(C=C1,pq11);

p1[i](t,x,y):=simplify(pq12);

uq11:=solve(int(int(coeff(e2,delta**i),x),x)+x*C+D1,u1[i](t,x,y));

C2:=solve({subs({u1[i](t,x,y)=subs(x=1,uq11),x=1},coeff(Uplus,delta**i)),subs({u1[i](t,x,y)=subs(x=
-1,uq11),x=-1},coeff(Uminus,delta**i))},{C,D1});

uq12:=subs(C2,uq11);

u1[i](t,x,y):=simplify(uq12);

vq11:=solve(int(coeff(e3,delta**i),x)+C,v1[i](t,x,y));

C3:=solve(subs({v1[i](t,x,y)=subs(x=1,vq11),x=1},coeff(Vplus,delta**i))+subs({v1[i](t,x,y)=subs(x=-
1,vq11),x=-1},coeff(Vminus,delta**i)),C);

vq12:=subs(C=C3,vq11);

v1[i](t,x,y):=simplify(vq12);

xi1[i](t,y):=simplify(int(subs({v1[i](t,x,y)=subs(x=1,vq12),x=1},coeff(Vplus,delta**i)),t))-
int(simplify(int(subs({v1[i](t,x,y)=subs(x=1,vq12),x=1},coeff(Vplus,delta**i)),t)),t=0..2*Pi)/2/Pi;
```

```
end do:
```

Appendix № 2 to paragraph 3.7. Coefficients in solution

Paragraph 4.5 gives the solution to the Navier-Stokes equation system for compressible fluid in approximation of small amplitude of wall vibrations. First-order longitudinal velocity is determined by the formula

$$\begin{aligned}\mathrm{u}_1 = {} & C_s^+ e^{\Omega' y}\sin(t+\Omega' y) + C_s^- e^{-\Omega' y}\sin(t-\Omega' y) + C_c^+ e^{\Omega' y}\cos(t+\Omega' y) + \\ & + C_c^- e^{-\Omega' y}\cos(t-\Omega' y) + U_s^- e^{-\delta y}\sin(t-yk) + U_c^- e^{-\delta y}\cos(t-yk) + \\ & + U_s^+ e^{\delta y}\sin(t+yk) + U_c^+ e^{\delta y}\cos(t+yk) + y\Big[U_{ys}^- e^{-\delta y}\sin(t-yk) + \\ & + U_{yc}^- e^{-\delta y}\cos(t-yk) + U_{ys}^+ e^{\delta y}\sin(t+yk) + U_{yc}^+ e^{\delta y}\cos(t+yk)\Big] \\ & - y^2 \Omega \mathrm{Fr}\sin t.\end{aligned}$$

transverse velocity by

$$\begin{aligned}\mathrm{v}_1 = {} & V_{1s}^- e^{-\delta y}\sin(t-yk) + V_{1c}^- e^{-\delta y}\cos(t-yk) \\ & + V_{1s}^+ e^{\delta y}\sin(t+yk) + V_{1c}^+ e^{\delta y}\cos(t+yk),\end{aligned}$$

and density by

$$\rho_1 = R_{1s}^- e^{-\delta y}\sin(t-yk) + R_{1c}^- \cos(t-yk) + R_{1s}^+ e^{\delta y}\sin(t+yk) + R_{1c}^+ e^{\delta y}\cos(t+yk).$$

Here the variables were introduced:

$$R_{1c}^+ = R_{1c}^- = \frac{\delta \sin k \cosh\delta - k\cos k \sinh\delta}{\cosh 2\delta - \cos 2k},$$

$$R_{1s}^+ = R_{1s}^- = -\frac{k \sin k \cosh\delta + \delta\cos k \sinh\delta}{\cosh 2\delta - \cos 2k},$$

$$V_{1c}^- = -V_{1c}^+ = -\frac{\cos k \sinh\delta}{\cosh 2\delta - \cos 2k},\ V_{1s}^- = -V_{1s}^+ = -\frac{\sin k \cosh\delta}{\cosh 2\delta - \cos 2k},$$

$$U_{yc}^- = -U_{yc}^+ = -4\Omega'^4 \mathrm{Fr}\frac{V_c^-(\delta^2 - k^2) + 2V_s^-(\Omega'^2 - k\delta)}{(\delta^2+k^2)^2 - 8\delta k\Omega'^2 + 4\Omega'^4},$$

$$U_{ys}^+ = -U_{ys}^- = 4\Omega'^4 \mathrm{Fr}\frac{V_{1s}^+(k^2 - \delta^2) + 2V_{1c}^+(\Omega'^2 - \delta k)}{(\delta^2+k^2)^2 - 8\delta k\Omega'^2 + 4\Omega'^4},$$

$$\begin{aligned}U_c^+ = U_c^- = {} & (-2\delta^3 U_{yc}^+ + 2(U_{ys}^+ k - \Omega'^2 \mathrm{Fr} R_c^+)\delta^2 + (-2U_{yc}^+ k^2 - 4\Omega'^2 U_{ys}^+ + 4k\Omega'^2 \mathrm{Fr} R_s^+)\delta \\ & - 4\Omega'^4 \mathrm{Fr} R_s^+ + 4\Omega'^2 U_{yc}^+ k + 2k^3 U_{ys}^+ + 2k^2 \Omega'^2 \mathrm{Fr} R_c^+) / ((\delta^2+k^2)^2 - 8\delta k\Omega'^2 + 4\Omega'^4),\end{aligned}$$

$$\begin{aligned}U_s^+ = U_s^- = {} & (-2\delta^3 U_{ys}^+ - 2(U_{yc}^+ k + \Omega'^2 \mathrm{Fr} R_s^+)\delta^2 + (-2U_{ys}^+ k^2 + 4\Omega'^2 U_{yc}^+ - 4k\Omega'^2 \mathrm{Fr} R_c^+)\delta \\ & + 4\Omega'^4 \mathrm{Fr} R_c^+ + 4\Omega'^2 U_{ys}^+ k - 2k^3 U_{yc}^+ + 2k^2 \Omega'^2 \mathrm{Fr} R_s^+)) / ((\delta^2+k^2)^2 - 8\delta k\Omega'^2 + 4\Omega'^4),\end{aligned}$$

$$C_s^+ = C_s^- = \frac{e^{\Omega'-\delta}}{2e^{4\Omega'}\cos 4\Omega' - e^{8\Omega'} - 1} \times$$
$$\times\Big[\Big\{(-U_s^+ - U_{ys}^+)\cos(3\Omega'+k) + (U_{yc}^+ + U_c^+)\sin(3\Omega'+k)\Big\}e^{2(\Omega'+\delta)}$$
$$+\Big\{(U_{ys}^- - U_s^-)\cos(3\Omega'-k) - (-U_{yc}^- + U_c^-)\sin(3\Omega'-k)\Big\}e^{4\Omega'+2\delta}$$
$$+\Big\{(U_{ys}^+ + U_s^+)\cos(\Omega'-k) + (U_{yc}^+ + U_c^+)\sin(\Omega'-k)\Big\}e^{6\Omega'+2\delta}$$
$$-e^{2\Omega'}(U_{ys}^- + U_s^-)\cos(3\Omega'-k) + e^{2\Omega'}(U_c^- + U_{yc}^-)\sin(3\Omega'-k)$$
$$+(U_s^+ - U_{ys}^+)\cos(\Omega'-k) + e^{4\Omega'}(U_{ys}^+ - U_s^+)\cos(3\Omega'+k)$$
$$+(U_{yc}^+ - U_c^+)\sin(\Omega'-k) - e^{4\Omega'}(U_c^+ - U_{yc}^+)\sin(3\Omega'+k)$$
$$+2\mathrm{Fr}\Omega'^2(e^{2\Omega'+\delta} + e^{4\Omega'+\delta})\cos 3\Omega' - 2\mathrm{Fr}\Omega'^2 e^{6\Omega'+\delta}\cos\Omega'$$
$$+\Big\{(U_{ys}^- + U_s^-)e^{6\Omega'} + e^{2\delta}(U_s^- - U_{ys}^-)\Big\}\cos(\Omega'+k)$$
$$+\Big\{(U_c^- + U_{yc}^-)e^{6\Omega'} - e^{2\delta}(U_c^- - U_{yc}^-)\Big\}\sin(\Omega'+k) - 2\mathrm{Fr}\Omega'^2 e^{\delta}\cos\Omega'\Big]$$

$$C_c^+ = C_c^- = \frac{e^{\Omega'-\delta}}{2e^{4\Omega'}\cos 4\Omega' - e^{8\Omega'} - 1} \times$$
$$\times\Big[\Big\{(U_{yc}^+ + U_c^+)\cos(3\Omega'+k) + (U_{ys}^+ + U_s^+)\sin(3\Omega'+k)\Big\}e^{2(\Omega'+\delta)}$$
$$+\Big\{(U_c^- - U_{yc}^-)\cos(3\Omega'-k) - (U_s^- - U_{ys}^-)\sin(3\Omega'-k)\Big\}e^{4\Omega'+2\delta}$$
$$+\Big\{(-U_{yc}^+ - U_c^+)\cos(\Omega'-k) + (U_{ys}^+ + U_s^+)\sin(\Omega'-k)\Big\}e^{6\Omega'+2\delta}$$
$$+e^{2\Omega'}(U_c^- + U_{yc}^-)\cos(3\Omega'-k) + e^{2\Omega'}(U_{ys}^- + U_s^-)\sin(3\Omega'-k)$$
$$+(U_{yc}^+ - U_c^+)\cos(\Omega'-k) + e^{4\Omega'}(U_c^+ - U_{yc}^+)\cos(3\Omega'+k)$$
$$+(U_{ys}^+ - U_s^+)\sin(\Omega'-k) + e^{4\Omega'}(U_{ys}^+ - U_s^+)\sin(3\Omega'+k)$$
$$-2\mathrm{Fr}\Omega'^2 e^{2\Omega'+\delta}\sin 3\Omega' + 2\mathrm{Fr}\Omega'^2 e^{4\Omega'+\delta}\sin 3\Omega' - 2\mathrm{Fr}\Omega'^2 e^{6\Omega'+\delta}\sin\Omega'$$
$$+\Big\{-(U_{yc}^- + U_c^-)e^{6\Omega'} - e^{2\delta}(U_c^- - U_{yc}^-)\Big\}\cos(\Omega'+k) +$$
$$+\Big\{(U_{ys}^- + U_s^-)e^{6\Omega'} - e^{2\delta}(U_s^- - U_{ys}^-)\Big\}\sin(\Omega'+k) + 2\mathrm{Fr}\Omega'^2 e^{\delta}\sin\Omega'\Big]$$